



Search for same-charge top-quark pair production in pp collisions at $\sqrt{s} = 13$ TeV with the ATLAS detector

The ATLAS Collaboration

A search for the production of top-quark pairs with the same electric charge (tt or $\bar{t}\bar{t}$) is presented. The analysis uses proton–proton collision data at $\sqrt{s} = 13$ TeV, recorded by the ATLAS detector at the Large Hadron Collider, corresponding to an integrated luminosity of 140 fb^{-1} . Events with two same-charge leptons and at least two b -tagged jets are selected. Neural networks are employed to define two selections sensitive to additional couplings beyond the Standard Model that would enhance the production rate of same-sign top-quark pairs. No significant signal is observed, leading to an upper limit on the total production cross-section of same-sign top-quark pairs of 1.6 fb at 95 % confidence level. Corresponding limits on the three Wilson coefficients associated with the $O_{tu}^{(1)}$, $O_{Qu}^{(1)}$, and $O_{Qu}^{(8)}$ operators in the Standard Model Effective Field Theory framework are derived.

Contents

1	Introduction	2
2	ATLAS detector	4
3	Data and simulated events	5
3.1	Signal simulation	5
3.2	Simulation of background events	7
4	Event reconstruction and object identification	8
5	Analysis workflow	10
5.1	Definition of signal enhanced regions via NNs	12
5.2	Definition of background-enriched regions	14
6	Systematic uncertainties	15
6.1	Experimental uncertainties	16
6.2	Modeling uncertainties	16
6.3	Non-prompt-lepton background modeling uncertainties	17
7	Results	18
8	Conclusion	25

1 Introduction

The search for exclusive production of top-quark pairs with the same electric charge (same-sign, SS)¹ is driven by the potential to uncover phenomena beyond the Standard Model (BSM) of particle physics. In the Standard Model (SM), SS top-quark pair production is forbidden at leading order (LO) in perturbation theory. This process can only occur at the lowest perturbative order through the exchange of two W bosons, as shown in Figure 1(a). The cross-section for this process is calculated to be approximately $\sigma(pp \rightarrow tt)_{SM} \simeq 4 \cdot 10^{-15}$ pb for proton–proton collisions at $\sqrt{s} = 13$ TeV [1], which is not detectable at the Large Hadron Collider (LHC). The observation of this process at the LHC would therefore imply the existence of BSM physics processes.

Model-independent searches for BSM processes at high energies can be conducted using the Standard Model Effective Field Theory (SMEFT). In this approach, the SM is assumed to be a LO and low-energy approximation of a more fundamental theory, with a new-physics energy scale Λ substantially larger than the SM electroweak (EW) scale.

In this paper, a search for SS top-quark pair production is presented. The process is described, using the SMEFT framework, as a pointlike interaction involving four up-type fermions as shown in Figure 1(b). Among the complete set of dimension-6 EFT operators expressed in the Warsaw basis [2], only five can be

¹ For simplicity, throughout this paper charge conjugation is implicitly assumed, therefore “same-sign top-quark pairs” refers to both tt and $\bar{t}\bar{t}$.

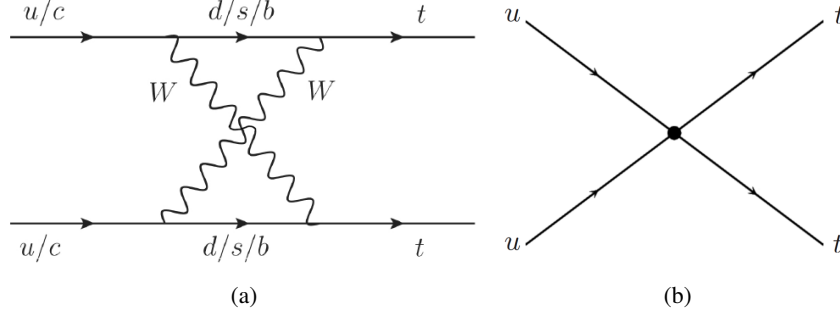


Figure 1: Lowest-order Feynman diagrams for same-sign top-quark pair production (a) in the SM and (b) as a pointlike effective-field-theory (EFT) four-fermion interaction.

responsible for the production of this SS top-quark signal [3] with a flavor universality assumption. The following notation is used for the operators following the conventions of Ref. [4]:

$$\begin{aligned}
O_{tu}^{(1)} &= [\bar{t}_R \gamma^\mu u_R] [\bar{t}_R \gamma_\mu u_R], \\
O_{Qq}^{(1)} &= [\bar{Q}_L \gamma^\mu q_L] [\bar{Q}_L \gamma_\mu q_L], \\
O_{Qq}^{(3)} &= [\bar{Q}_L \gamma^\mu \sigma^a q_L] [\bar{Q}_L \gamma_\mu \sigma^a q_L], \\
O_{Qu}^{(1)} &= [\bar{Q}_L \gamma^\mu q_L] [\bar{t}_R \gamma_\mu u_R], \\
O_{Qu}^{(8)} &= [\bar{Q}_L \gamma^\mu T^A q_L] [\bar{t}_R \gamma_\mu T^A u_R].
\end{aligned}$$

In these expressions, Q_L and t_R are the left-handed doublet and right-handed singlet of the third quark generation, q_L and u_R are related to the first two generations, and σ^a and T^A are the generators of $SU(2)_L$ and $SU(3)_C$, respectively. Only $O_{tu}^{(1)}$, $O_{Qu}^{(1)}$, and $O_{Qu}^{(8)}$ are considered, since $O_{Qq}^{(1)}$ and $O_{Qq}^{(3)}$ are already constrained by B_d mixing and dijet production measurements [5]. The effective Lagrangian related to these operators is expressed as:

$$\mathcal{L}_{D=6}^{qq \rightarrow tt} = \frac{1}{\Lambda^2} \left(c_{tu}^{(1)} O_{tu}^{(1)} + c_{Qu}^{(1)} O_{Qu}^{(1)} + c_{Qu}^{(8)} O_{Qu}^{(8)} \right) + h.c. \quad (1)$$

where $c_{tu}^{(1)}$, $c_{Qu}^{(1)}$ and $c_{Qu}^{(8)}$ are the Wilson coefficients (WCs) related to the EFT operators.

Searches for new physics processes containing two SS leptons have only small background contributions from known SM processes, such as diboson production including vector boson scattering $W^\pm W^\pm$, and are dominated by $t\bar{t}W$, $t\bar{t}Z$ and $t\bar{t}H$ production in the multilepton final state, where one or more leptons are undetected.

Both the ATLAS and CMS collaborations have searched for anomalous production of events containing pairs of SS leptons at the LHC, using proton–proton (pp) collision data at $\sqrt{s} = 7, 8$ and 13 TeV [6–11].

A previous ATLAS analysis [8] with 20 fb⁻¹ of pp collision data at $\sqrt{s} = 8$ TeV set 95% confidence level (CL) upper limits on $\sigma(pp \rightarrow tt)$ at 62, 51 and 38 fb assuming a contact interaction for left–left, left–right and right–right chirality of the SS top quarks, respectively. This corresponds to limits on the WCs of $|c|/\Lambda^2 < 0.053, 0.137$ and 0.042 TeV^{-2} [8]. A 95% CL limit on the tt production cross-section at $\sqrt{s} = 13$ TeV of $\sigma(pp \rightarrow tt) < 89 \text{ fb}$ is set by the ATLAS Collaboration using 36 fb⁻¹ of pp collision data, assuming a BSM flavor-changing neutral current mediator with a mass of 1 TeV [10].

In this paper, a dedicated analysis is designed to specifically target the search for SS top-quark pair production with a minimized model dependence.

2 ATLAS detector

The ATLAS detector [12] at the LHC covers nearly the entire solid angle around the collision point.² It consists of an inner tracking detector surrounded by a thin superconducting solenoid, electromagnetic and hadron calorimeters, and a muon spectrometer incorporating three large superconducting air-core toroidal magnets.

The inner-detector system (ID) is immersed in a 2 T axial magnetic field and provides charged-particle tracking in the range of $|\eta| < 2.5$. The high-granularity silicon pixel detector covers the vertex region and typically provides four measurements per track, the first hit normally being in the insertable B-layer. It is followed by the silicon microstrip tracker, which usually provides eight measurements per track. These silicon detectors are complemented by the transition radiation tracker (TRT), which enables radially extended track reconstruction up to $|\eta| = 2.0$. The TRT also provides electron identification information based on the fraction of hits (typically 30 in total) above a higher energy-deposit threshold corresponding to transition radiation.

The calorimeter system covers the pseudorapidity range $|\eta| < 4.9$. In the region $|\eta| < 3.2$, electromagnetic calorimetry is provided by barrel and endcap high-granularity lead/liquid-argon (LAr) calorimeters, with an additional thin LAr presampler covering $|\eta| < 1.8$ to correct for energy loss in material upstream of the calorimeters. Hadron calorimetry is provided by the steel/scintillator-tile calorimeter, segmented into three barrel structures with $|\eta| < 1.7$, and two copper/LAr hadron endcap calorimeters. The solid angle coverage is completed with forward copper/LAr and tungsten/LAr calorimeter modules optimized for electromagnetic and hadronic energy measurements respectively.

The muon spectrometer (MS) comprises separate trigger and high-precision tracking chambers measuring the deflection of muons in a magnetic field generated by the superconducting air-core toroidal magnets. The field integral of the toroids ranges between 2.0 and 6.0 T m across most of the detector. Three layers of precision chambers, each consisting of layers of monitored drift tubes, cover the region $|\eta| < 2.7$, complemented by cathode-strip chambers in the forward region, where the background is highest. The muon trigger system covers the range $|\eta| < 2.4$ with resistive-plate chambers in the barrel, and thin-gap chambers in the endcap regions.

Interesting events are selected by the first-level trigger system implemented in custom hardware, followed by selections made by algorithms implemented in software in the high-level trigger [13]. The first-level trigger accepts events from the 40 MHz bunch crossings at a rate below 100 kHz, which the high-level trigger further reduces in order to record events to disk at an average rate of about 1 kHz.

An extensive software suite [14] is used in data simulation, in the reconstruction and analysis of real and simulated data, in detector operations, and in the trigger and data acquisition systems of the experiment.

² ATLAS uses a right-handed coordinate system with its origin at the nominal interaction point (IP) in the centre of the detector and the z -axis along the beam pipe. The x -axis points from the IP to the centre of the LHC ring, and the y -axis points upwards. Polar coordinates (r, ϕ) are used in the transverse plane, ϕ being the azimuthal angle around the z -axis. The pseudorapidity is defined in terms of the polar angle θ as $\eta = -\ln \tan(\theta/2)$ and is equal to the rapidity $y = \frac{1}{2} \ln \left(\frac{E+p_z c}{E-p_z c} \right)$ in the relativistic limit. Angular distance is measured in units of $\Delta R \equiv \sqrt{(\Delta y)^2 + (\Delta \phi)^2}$.

3 Data and simulated events

This analysis uses pp collision data at $\sqrt{s} = 13$ TeV collected with the ATLAS detector between 2015 and 2018. After the application of data-quality requirements [15], the data sample corresponds to an integrated luminosity of 140 fb^{-1} [16]. Only events recorded under stable beam conditions and for which all detector subsystems were known to be in a good operating condition are used.

Monte Carlo (MC) simulated events were produced to study signal and background processes. The simulated events were processed through either a full simulation of the ATLAS detector using GEANT4 [17, 18], or a fast simulation, in which the simulation of the calorimeter response is replaced by a parameterization of the shower shapes [19]. Both types of simulated events were processed through the same reconstruction software used for the pp collision data.

Additional inelastic pp collisions from the same and neighboring bunch crossings (pileup) are modeled using events from minimum-bias interactions simulated with PYTHIA 8.186 [20] using the NNPDF2.3LO set of parton distribution functions (PDFs) [21] and the A3 set of tunable parameters [22], referred to as “tune”. They were overlaid onto the simulated hard-scatter events according to the luminosity profile of the recorded data. The number of pp interactions per bunch crossing in the data used here ranges from about 8 to 70, with an average of 34.

Unless otherwise specified, events generated with MADGRAPH5_AMC@NLO [23] or POWHEG BOX [24–26] were interfaced to PYTHIA 8 [27] and used the A14 tune [28] with the NNPDF2.3LO PDF set to model the parton shower (PS), underlying event (UE) and hadronization. Events interfaced to HERWIG 7 [29, 30] used the MMHT2014LO PDF set [31] and the corresponding tune provided by HERWIG, H7.2-Default or H7-UE-MMHT. Events simulated with SHERPA [32] used the PS and hadronization model and the tune provided by the SHERPA authors. All simulated events, except those produced with the SHERPA event generator, used EVTGEN [33] to model the decays of heavy-flavor hadrons. The mass of the top quark and the Higgs boson were set to 172.5 GeV and 125 GeV, respectively.

Samples of simulated MC events were produced for the different signal and background processes. The generators used for the matrix element (ME) and PS simulation and the PDF configurations of all samples are summarized in Table 1, with the samples used to estimate the systematic uncertainties that are described in Section 6.2 given in parentheses.

3.1 Signal simulation

SS top-quark signal samples were simulated using MADGRAPH5_AMC@NLO v2.9.3 together with the SMEFTSIM3.0 Feynrules package [34–36], using the m_W electroweak input scheme. Only the three operators $O_{tu}^{(1)}$, $O_{Qu}^{(1)}$, and $O_{Qu}^{(8)}$ were considered. Flavor universality was imposed, so that the WCs for $uutt$, $uqtt$, and $cqtt$ vertices were bound to the same value. The ME calculation for the signal processes was performed at LO in quantum chromodynamics (QCD) without additional jets using the NNPDF30LO [37] PDF set.³ Top quarks were decayed into a W boson and a b -quark, and the W bosons subsequently decayed into a charged lepton and a neutrino of the same flavor.

A nominal sample was produced, in which the WCs were set to $c_{tu}^{(1)} = 0.04$, $c_{Qu}^{(1)} = 0.1$ and $c_{Qu}^{(8)} = 0.1$. This set of WC values corresponds to cross-sections of $\sigma(pp \rightarrow tt) = 97.6 \text{ fb}$ and $\sigma(pp \rightarrow \bar{t}\bar{t}) = 2.4 \text{ fb}$,

³ The ME calculation is at LO and the jet multiplicity could hence be mismodeled. This was tested by applying scale variations to the jet multiplicity distribution and it was found to have a negligible impact on the results.

respectively. The SS top-quark signal is highly charge-asymmetric leading to a cross-section which is approximately 40 times larger for tt production compared to $t\bar{t}$ production. Instead of generating multiple signal samples associated with different assumptions on WCs, the MADGRAPH5_AMC@NLO reweighting tool [38] was exploited to obtain the necessary set of signal predictions from the nominal sample. An event weight for a different set of WCs is obtained as:

$$W_{\text{new}} = \frac{|M_{\text{new}}|^2}{|M_{\text{orig}}|^2} W_{\text{orig}} \quad (2)$$

where W_{orig} is the original event weight and M_{new} , M_{orig} are the re-computed and original MEs, respectively. The chosen ranges for the WCs, $c_{tu}^{(1)} = [0.01, 0.05]$, $c_{Qu}^{(1)} = [0.05, 0.15]$, and $c_{Qu}^{(8)} = [0.10, 0.30]$, imply values for the SS top pair production cross-section in the dileptonic decay channel ranging from 1 fb to 100 fb, approximately, assuming a new-physics scale $\Lambda = 1$ TeV.

Table 1: The samples used for event generation of signal and background processes. Those used to estimate the systematic uncertainties are shown in parentheses. The production of an electroweak boson is denoted by V (W or Z/γ^*). The parton density function (PDF) shown in the table is the one used for the matrix element (ME). The tune is the set of tuned parameters of the parton-shower (PS) generator.

Process	Generator	ME order	PS	PDF (ME)	Tune
$tt/\bar{t}\bar{t}$ EFT signal	MADGRAPH5_AMC@NLO	LO	PYTHIA 8	NNPDF3.0LO	A14
$t\bar{t}W$	SHERPA 2.2.10 (MADGRAPH5_AMC@NLO) (POWHEG BOX) (POWHEG BOX)	NLO (NLO) (NLO) (NLO)	SHERPA (PYTHIA 8) (PYTHIA 8) (HERWIG 7.2)	NNPDF3.0NNLO (NNPDF3.0NNLO) (NNPDF2.3LO) (NNPDF3.0NNLO)	SHERPA default (A14) (A14) (H7.2-Default)
$t\bar{t}Z/\gamma^*$	MADGRAPH5_AMC@NLO (MADGRAPH5_AMC@NLO) (MADGRAPH5_AMC@NLO)	NLO (NLO) (NLO)	PYTHIA 8 (HERWIG 7.2) (PYTHIA 8)	NNPDF3.0NNLO (NNPDF3.0NNLO) (NNPDF3.0NNLO)	A14 (H7.2-Default) (A14 Var3c)
$t\bar{t}ll$	MADGRAPH5_AMC@NLO	NLO	PYTHIA 8	NNPDF3.0NNLO	A14
$t\bar{t}H$	POWHEG BOX (POWHEG BOX) (MADGRAPH5_AMC@NLO)	NLO (NLO) (NLO)	PYTHIA 8 (HERWIG 7.04) (PYTHIA 8)	NNPDF3.0NNLO (NNPDF3.0NNLO) (NNPDF3.0NNLO)	A14 (H7UE-MMHT) (A14)
$VV, qqVV, VVV$	SHERPA 2.2.2	NLO	SHERPA	NNPDF3.0NNLO	SHERPA default
Four top	MADGRAPH5_AMC@NLO	NLO	PYTHIA 8	NNPDF3.1NNLO	A14
$t\bar{t}$	POWHEG BOX	NLO	PYTHIA 8	NNPDF3.0NNLO	A14
s -, t -channel, Wt single top	POWHEG BOX	NLO	PYTHIA 8	NNPDF3.0NNLO	A14
$Z \rightarrow l^+l^-$ (Mat Conv)	POWHEG BOX	NLO	PYTHIA 8	CT10NNLO	AZNLO
$Z \rightarrow l^+l^-+(\gamma^*)$	POWHEG BOX	NLO	PYTHIA 8	CT10NNLO	AZNLO
$Z \rightarrow l^+l^-$	SHERPA 2.2.1	NLO	SHERPA	NNPDF3.0NNLO	SHERPA default
W +jets	SHERPA 2.2.1	NLO	SHERPA	NNPDF3.0NNLO	SHERPA default
$V\gamma$	SHERPA 2.2.8	NLO	SHERPA	NNPDF3.0NNLO	SHERPA default
$t(Z/\gamma^*), t\bar{t}, t\bar{t}WH$	MADGRAPH5_AMC@NLO	LO	PYTHIA 8	NNPDF2.3LO	A14
$t\bar{t}W^+W^-, t\bar{t}ZZ, t\bar{t}HH$	MADGRAPH5_AMC@NLO	LO	PYTHIA 8	NNPDF2.3LO	A14
$tW(Z/\gamma^*), tWH, tHqb$	MADGRAPH5_AMC@NLO	NLO	PYTHIA 8	NNPDF3.0NNLO	A14
VH	POWHEG BOX	NLO	PYTHIA 8	NNPDF3.0NNLO	A14

3.2 Simulation of background events

SM processes such as the production of $t\bar{t}W$, $t\bar{t}Z$, $t\bar{t}\gamma$, $t\bar{t}H$, $t\bar{t}t\bar{t}$, WW +jets, WZ +jets and ZZ +jets can have two leptons of the same electric charge in the final state and mimic the signal signature.

The $t\bar{t}W$ production is expected to constitute the largest fraction of the background in the signal-dominated regions. It was simulated using SHERPA 2.2.10. Both the factorization and renormalization scales, μ_F and μ_R , were set to $H_T/2$, where H_T is the sum of the transverse masses $m_T = \sqrt{m^2 + p_T^2}$ of all particles generated in the ME calculation. The sample was simulated at next-to-leading order (NLO) in QCD accuracy for MEs for up to one and LO accuracy for up to two additional jets. The additional partons were matched and merged with the SHERPA PS based on Catani–Seymour dipole factorization [39, 40], using the MEPS@NLO prescription [41–44] with a CKKW merging scale of 30 GeV. The virtual QCD corrections for MEs at NLO accuracy were provided by the OPENLOOPS 2 library [45–47]. Samples were simulated using the NNPDF3.0_{NNLO} [37] PDF set. The LO EW contributions were obtained from a dedicated sample simulated with SHERPA 2.2.10 and were combined with the NLO QCD sample described above. Three alternative $t\bar{t}W$ samples are used in the estimation of systematic uncertainties and are listed in Table 1. The events were normalized using a cross-section of 722 fb as calculated in Ref. [48].

The production of $t\bar{t}Z/\gamma^*$ events was modeled using the MADGRAPH5_AMC@NLO generator. The functional forms of μ_F and μ_R were set to $0.5 \times \sum_i \sqrt{m_i^2 + p_{T,i}^2}$, where the sum runs over all the particles generated in the ME calculation. The cross-sections were calculated at NLO QCD and NLO EW accuracy using MADGRAPH5_AMC@NLO as reported in Ref. [49]. The cross-section of $t\bar{t}Z$ ($\ell\bar{\ell}$) with an off-shell Z boson, denoted by $t\bar{t}\ell\bar{\ell}$, was scaled by an off-shell correction estimated at one-loop level in α_s . Two alternative $t\bar{t}Z/\gamma^*$ samples were simulated at NLO QCD with the MADGRAPH5_AMC@NLO generator and interfaced either to PYTHIA 8 or HERWIG 7.2.

The production of $t\bar{t}H$ events was modeled using the POWHEG BOX v2 [24, 50–53] generator. The functional form of μ_F and μ_R was set to $\sqrt[3]{m_T(t) \cdot m_T(\bar{t}) \cdot m_T(H)}$. The cross-section was calculated at NLO accuracy as reported in Ref. [49]. Two alternative $t\bar{t}H$ samples were simulated, one with the MADGRAPH5_AMC@NLO generator interfaced to PYTHIA 8 and one with the POWHEG BOX generator interfaced to HERWIG 7.2.

Diboson final states (VV) were simulated with the SHERPA 2.2.2 generator using the NNPDF3.0_{NNLO} [37] PDF set, taking off-shell effects into account. MEs at NLO (LO) accuracy in QCD were used for up to one (three) additional parton emission(s). Loop-induced processes were simulated at LO for up to one additional parton emission. The calculations were matched and merged with the SHERPA parton shower based on Catani–Seymour dipole factorization using the MEPS@NLO prescription. The virtual QCD corrections were provided by the OPENLOOPS library.

The $t\bar{t}$ production was simulated with POWHEG BOX v2 and normalized to the cross-section prediction at next-to-next-to-leading order (NNLO) in QCD including the resummation of next-to-next-to-leading logarithmic (NNLL) soft-gluon terms calculated using TOP++ 2.0 [54–60]. The h_{damp} parameter that controls the transverse momentum of the first gluon emission beyond the Born configuration in POWHEG BOX was set to $1.5 m_{\text{top}}$ [61].

The associated production of single top quarks with W bosons (tW) was modeled with the POWHEG BOX v2 generator at NLO in QCD. The diagram-removal scheme [62] was used to remove interference and overlap with $t\bar{t}$ production. The inclusive cross-section was corrected to the theory prediction calculated at NLO in QCD with NNLL soft-gluon corrections [63]. Single top-quark production in the s -channel and t -channel was modeled with the POWHEG BOX v2 generator at NLO in QCD using the five- and four-flavor scheme,

respectively. The inclusive cross-section for the single-top t -channel process was corrected to the theory prediction calculated at NLO in QCD with HATHOR 2.1 [64, 65].

The contribution from material photon conversions (Mat Conv) and internal photon conversion (Int Conv) were estimated by using $Z \rightarrow \ell^+ \ell^-$ events, simulated with the POWHEG BOX generator at NLO in QCD using the CT10_{NLO} PDF set interfaced to PYTHIA 8 using the AZNLO tune [66].

The production of $t\bar{t}\bar{t}$ events was simulated with the MADGRAPH5_AMC@NLO generator using the NNPDF3.1_{NLO} PDF set and was interfaced to PYTHIA 8. Several rare processes were also considered in the background estimate: tZ , VH , $t\bar{t}WW$, $t\bar{t}HH$, $t\bar{t}WH$, $t\bar{t}ZZ$, tWZ , tWH , $tHqb$, ttt , and VVV production. All processes involving at least one top quark were simulated with MADGRAPH5_AMC@NLO, while VVV events were simulated with SHERPA 2.2.2 and VH was simulated with POWHEG BOX v2.

The simulated events were normalized to the cross-sections computed at the highest order available in perturbation theory. Corrections were applied to the simulated events so that the selection efficiencies, energy scales and energy resolutions of reconstructed objects match those determined from data control samples.

4 Event reconstruction and object identification

Events of interest for this analysis are those compatible with the production of two top quarks with the same electric charge. The dilepton final state studied here is characterized by the presence of two SS leptons, two b -hadrons and missing transverse momentum from the two undetected neutrinos.

Interaction vertices are reconstructed from at least two tracks with transverse momentum (p_T) larger than 500 MeV. The primary vertex of the event is defined as the one with the largest $\sum_{\text{tracks}} p_T^2$ value [67]. Events were selected using a combination of single-lepton and dilepton triggers. Single-electron triggers required a minimum p_T threshold of 24 (26) GeV in the 2015 (2016–2018) data-taking period. Single-muon triggers had a lowest p_T threshold of 20 (26) GeV in 2015 (2016–2018). The dielectron triggers required two electrons with minimum p_T thresholds ranging from 12 GeV in 2015 to 24 GeV in 2017–2018, whereas the dimuon triggers used asymmetric p_T thresholds for the leading (subleading) muons: 18 (8) GeV in 2015 and 22 (8) GeV in 2016–2018. Finally, the electron+muon trigger required events to have an electron candidate with a 17 GeV threshold and a muon candidate with a 14 GeV threshold for all periods.

Electron candidates are reconstructed from energy clusters in the electromagnetic calorimeter matched to a track in the ID [68]. They are required to satisfy $p_T > 10$ GeV and $|\eta_{\text{cluster}}| < 2.47$, excluding the pseudorapidity region corresponding to the transition between the barrel and endcap calorimeters ($1.37 < |\eta_{\text{cluster}}| < 1.52$). Loose and tight electron identification working points (WPs) are used [68].

Muon candidates are reconstructed by combining tracks in the ID with tracks in the MS [69]. They are required to satisfy $p_T > 10$ GeV and $|\eta| < 2.5$. Loose and medium muon identification WPs are used [69].

Only lepton candidates with ID tracks originating from the primary vertex of the interaction are considered. Electron (muon) candidates are required to have a transverse impact parameter, d_0 , satisfying $|d_0/\sigma(d_0)| < 5$ (3), where $\sigma(d_0)$ is the measured uncertainty in d_0 , and a longitudinal impact parameter, z_0 , satisfying $|z_0 \sin \theta| < 0.5$ mm (0.5 mm), where θ is the polar angle of the track.

Table 2: Summary of the definitions of the loose inclusive (L_{inc}), medium inclusive (M_{inc}), medium (M), and tight (T) leptons.

Lepton	e				μ			
Category	L_{inc}	M_{inc}	M	T	L_{inc}	M_{inc}	M	T
Isolation	Yes				Yes			
Non-prompt lepton BDT WP	No	<i>Tight</i>	<i>Tight-not-VeryTight</i>	<i>VeryTight</i>	No	<i>Tight</i>	<i>Tight-not-VeryTight</i>	<i>VeryTight</i>
Identification	Loose	Tight			Medium			
Electron charge-misassignment veto	No	Yes			Not applicable			
Electron conversion candidate veto	No	Yes			Not applicable			
$ d_0 /\sigma_{d_0}$	< 5				< 3			
$ z_0 \sin \theta $	< 0.5 mm							

To reject objects mistakenly identified as prompt leptons, namely misidentified jets and leptons from heavy-flavor hadron decays or photon conversions, lepton candidates are also required to fulfill track and calorimeter-based isolation criteria [69, 70]. Additionally, a boosted decision tree (BDT) discriminant, developed for Ref. [71], referred to as the non-prompt lepton BDT, is employed to reject non-prompt leptons. These leptons mainly originate from the decay of c - and b -hadrons that can be identified by their track isolation and origin in displaced vertices, due to the decay of long-lifetime hadrons. Two working points, named *Tight* and *VeryTight*, are defined based on the BDT output score. The *Tight* WP selects prompt leptons with an efficiency for muons (barrel/endcap electrons) that satisfy the calorimeter- and track-based isolation criteria of about 60% (60/70%) for $p_T \sim 20$ GeV and reaches a plateau of 95% (95/90%) at $p_T \sim 40$ (40/65) GeV. The prompt lepton efficiency of the *VeryTight* WP for muons (barrel/endcap electrons) that satisfy the calorimeter- and track-based isolation criteria is about 55% (55/60%) for $p_T \sim 20$ GeV and reaches a plateau of 90% (85/83%) at $p_T \sim 40$ (40/65) GeV. The corresponding rejection factor against muons (electrons) from the decay of b -hadrons ranges from 33 to 50 (20 to 50) for the *Tight* WP, and from 50 to 100 (33 to 66) for the *VeryTight* WP, depending on p_T and $|\eta|$, after resolving ambiguities between overlapping reconstructed objects.

To reject background electrons due to a wrong charge assignment, a BDT based on calorimeter and track reconstruction parameters is used, obtaining an efficiency of approximately 96% in the barrel region and 81% in the endcaps, with corresponding rejection factors of 19 and 40 in the two regions, respectively. Electrons originating in the detector material or from photon conversions are suppressed by rejecting candidates that are associated with a displaced vertex at radial distance from the interaction point (IP) $r > 20$ mm and an invariant mass of their combination with their closest opposite-charge tracks smaller than 100 MeV. The definitions of the lepton categories used in the analysis to define signal or control regions are summarized in Table 2 and comprise loose inclusive (L_{inc}), medium inclusive (M_{inc}), medium (M), and tight (T) leptons.⁴

Jets are reconstructed from collections of tracks in the ID and energy deposit clusters in the calorimeters, combined using a particle-flow (PFlow) algorithm [72]. Jet candidates built from PFlow objects using the anti- k_t algorithm [73, 74] with a radius parameter of $R = 0.4$ are calibrated using simulation with corrections obtained from in situ techniques in data [75]. Jets are required to satisfy $p_T > 25$ GeV and $|\eta| < 2.5$. A jet-vertex tagger (JVT) [76] algorithm is applied to jets with $p_T < 60$ GeV and $|\eta| < 2.4$ to reduce pileup. Jets containing b -hadrons are identified (b -tagged) via the DL1r algorithm [77] that

⁴ The M and T WPs are mutually exclusive while the M_{inc} WP is the disjoint union of M and T .

makes use of the impact parameters of tracks and the displaced vertices reconstructed in the ID, combined with discriminating variables constructed with a recurrent neural network (NN) [77], which exploits the spatial and kinematic correlations between tracks originating from the same b -hadron. Two b -tagging WPs, corresponding to average b -tagging efficiencies of 60% and 77%, are used. The two WPs correspond to a light-jet⁵ rejection factor of about 200 or 2500, and a charm-jet (c -jet) rejection factor of about 6 or 40, as determined for jets with $p_T > 20$ GeV and $|\eta| < 2.5$ in simulated $t\bar{t}$ events [77].

To prevent leptons and jets being reconstructed multiple times as different objects in the event, a sequential overlap removal procedure is applied to L_{inc} leptons to remove such reconstruction ambiguities. If two electrons are within $\Delta R = 0.1$, only the one with the higher p_T is considered. If an electron and a muon are within $\Delta R = 0.1$, the muon is removed if it is only reconstructed from an ID track and the associated calorimeter deposit is consistent with a minimum ionizing particle, otherwise the electron is removed. If an electron and a jet are within $\Delta R < 0.2$ of each other, the jet is removed if it is not b -tagged (70% WP) or if it has $p_T > 200$ GeV, otherwise the electron is removed. Jets that are not b -tagged and contain less than three tracks with $p_T > 500$ MeV and are within $\Delta R < 0.4$ from muons are rejected, otherwise, the muon is rejected. For each lepton satisfying all previous criteria a variable-size cone of $\Delta R < 0.04 + 10 \text{ GeV}/p_{T,\text{lep}}$ and up to a maximum $\Delta R = 0.4$ is defined. If a selected jet that survived the previous steps is found within this cone, the lepton is rejected.

The missing transverse momentum, E_T^{miss} , is defined as the magnitude of the vector sum of the p_T of all selected and calibrated leptons and jets, plus a term to account for the momentum of soft particles that are not associated with any of the selected objects [76]. This soft term is calculated from ID tracks matched to the selected primary vertex, enhancing its resilience to contamination from pileup interactions.

5 Analysis workflow

In this search for SS top-pair production only the decay topology where both W bosons decay leptonically is considered. Events are divided into non-overlapping phase-space regions. Four signal regions (SRs), nine control regions (CRs), and four validation regions (VRs), enriched in either signal or background events, are defined based on the predictions from the simulation of signal and background events in the ATLAS detector.

Signal event candidates are pre-selected by requiring the presence of precisely two leptons, $\ell = e, \mu$, of the same electric charge and with $p_T > 20$ GeV. At least two jets are required in the event. For the suppression of background contributions, either both leptons are classified as M_{inc} and at least two jets satisfy the 77% efficiency b -tagging WP, or both leptons are classified as T and only one jet has to satisfy the 77% WP. The dominant background processes in the SRs are the production of $t\bar{t}W$, $t\bar{t}Z$ and $t\bar{t}H$. The $t\bar{t}W$ and $t\bar{t}Z$ normalizations are constrained by a likelihood fit to data described in Section 7. The $t\bar{t}H$ is normalized as described in Section 3.

The pre-selected events are classified using deep neural networks to create two separate regions enriched in events from the different EFT operators. A split by total lepton charge is applied to further divide the events into $++$ and $--$ regions, in order to be sensitive to the different rates and kinematic properties of $t\bar{t}$ and $t\bar{t}$ events⁶. The SRs and VRs are defined by splitting the pre-selected events based on the azimuthal angle

⁵ Light jet refers to a jet not containing a b - or c -hadron.

⁶ Although the analysis is sensitive to both charge configurations, for the EFT interpretation in which the cross-section is highly asymmetric, the analysis gets most of its sensitivity from the $t\bar{t}$ channel.

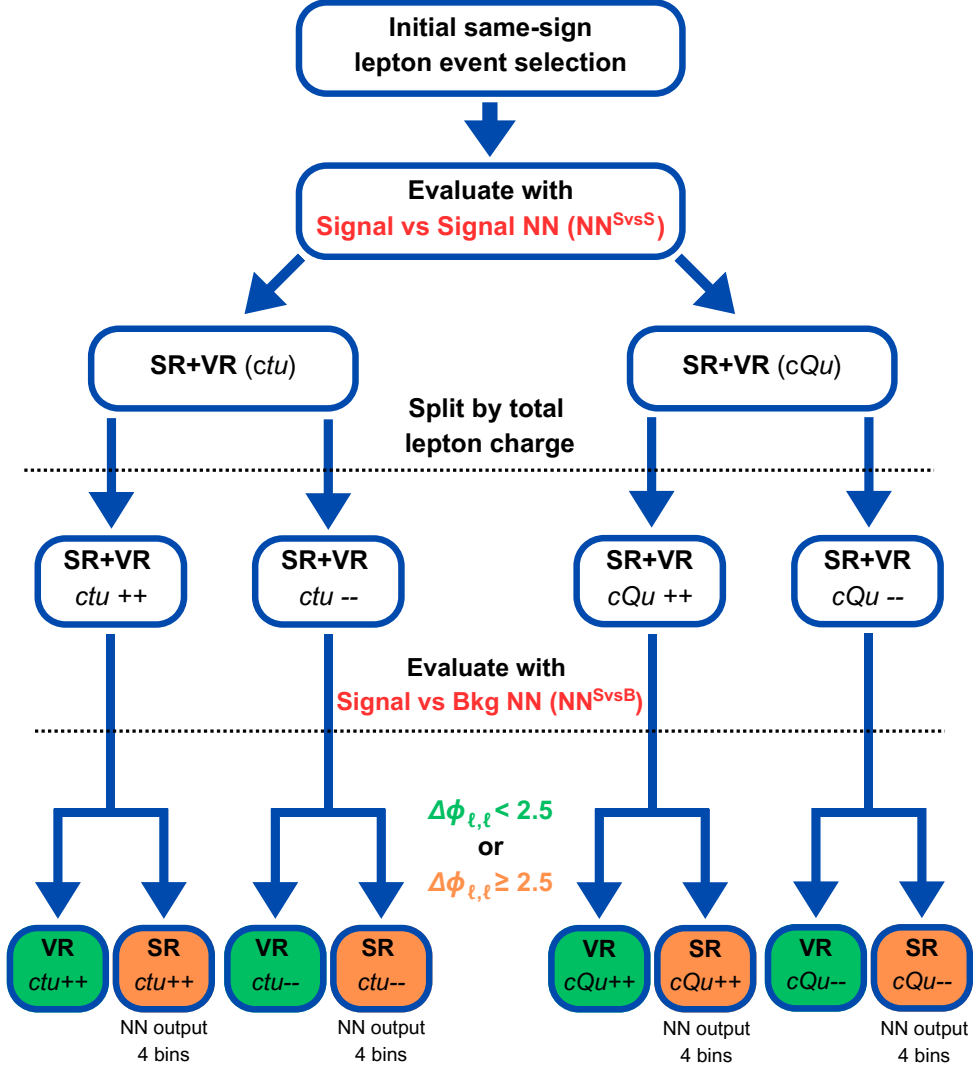


Figure 2: Flowchart representation of the definition of signal regions (SRs) and validation regions (VRs). The first step is the selection of signal-like events. This is followed by the discrimination using a first set of deep neural networks, trained to separate signal events from the different EFT operators. The output of the NNs is used to define the SRs for $c_{tu}^{(1)}$ and c_{Qu} . Afterwards, the regions are split by total lepton charge into $++$ and $--$ regions. A second set of NNs is used to separate the signal from background contributions. As a last step, the regions are split based on the $\Delta\phi_{\ell,\ell}$ variable to define the final SRs and VRs. The output of this NN^{SvsB} is split into four bins per signal region.

between the two charged leptons, $\Delta\phi_{\ell,\ell}$. Figure 2 shows the definition of the SRs and VRs. In Figure 3 the distribution of the sum of the p_T of the leptons (H_T^{lep}) and the distribution of the invariant mass of the two leptons ($m_{\ell\ell}$) is shown for the merged region (SRs+VRs) split by charge. A second set of NNs, called NN^{SvsB}, is used in the SRs to discriminate signal from background events. The output of NN^{SvsB} is split into four bins per region, which are used in a maximum-likelihood fit to data. The nine CRs are specifically designed to constrain different sources of background. The fit is performed simultaneously in all SRs and CRs to extract the signal strength and several background normalization factors. The VRs are

used to validate the background modeling and are not used in the fit.

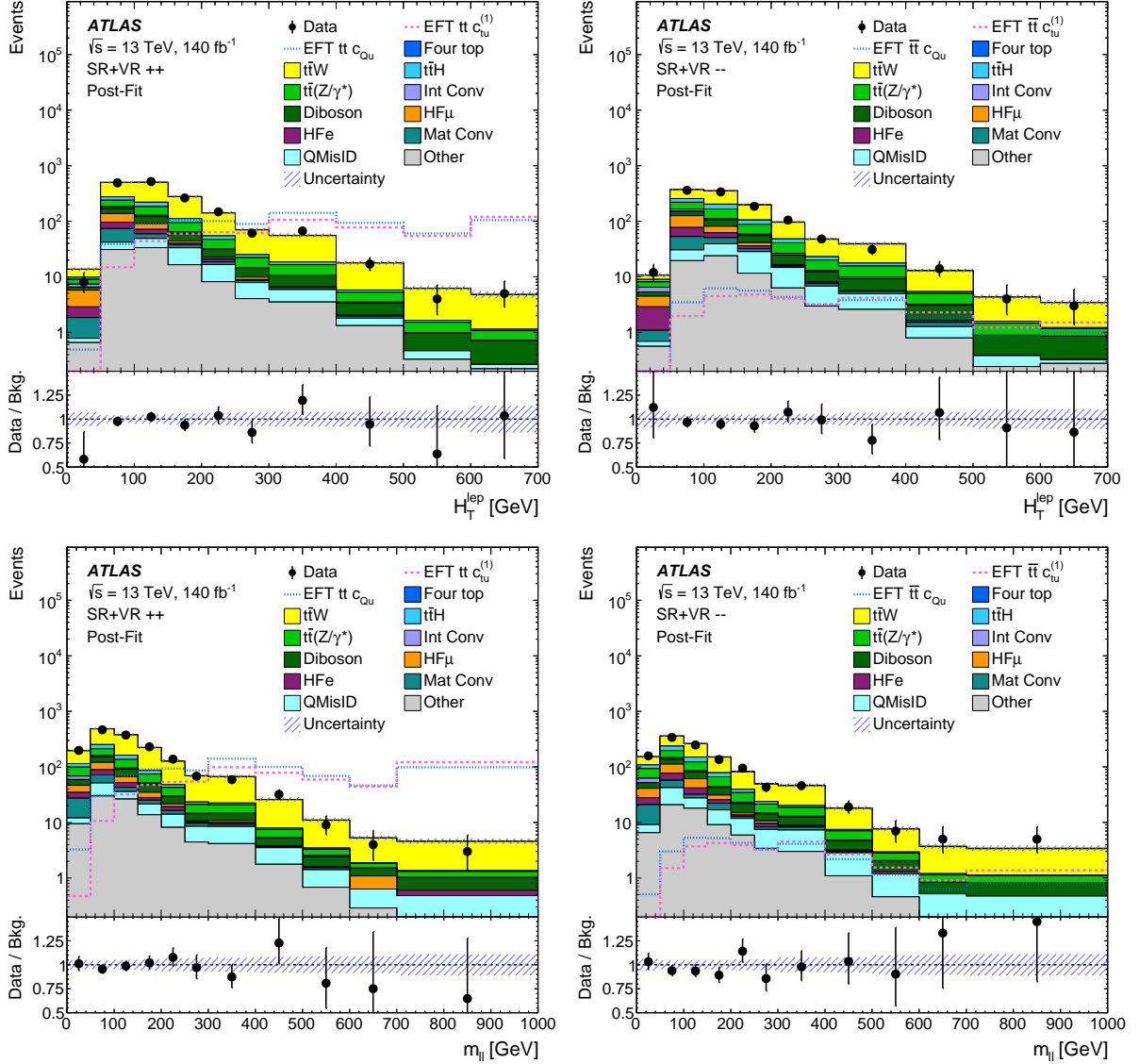


Figure 3: Comparison between data and the background expectation of the H_T^{lep} and $m_{\ell\ell}$ distributions in the merged regions (SRs+VRs) split by lepton charge, shown after the background-only likelihood fit. Two signal samples using the Wilson coefficient values of $c_{tu}^{(1)} = 0.04$, $c_{Qu}^{(1)} = 0.0$, $c_{Qu}^{(8)} = 0.0$ and $c_{tu}^{(1)} = 0.0$, $c_{Qu}^{(1)} = 0.1$, $c_{Qu}^{(8)} = 0.2$ are shown as a dotted line and a dashed line, respectively. They are normalized to their respective predicted cross-sections. The ratio of the data to the total post-fit background is shown in the lower panel. The combined statistical and systematic uncertainty in the MC simulation is indicated by the hatched band, while the vertical error bars represent the statistical uncertainty in the data.

5.1 Definition of signal enhanced regions via NNs

The two sets of NNs are trained based on the KERAS library [78] with TENSORFLOW as a backend [79] and the ADAM optimiser [80]. Both sets of NNs have the same architecture, with one input layer, five hidden

layers consisting of 128, 64, 32, 16, and 8 nodes and a single node in the output layer. The networks are trained with MC simulated samples. To make use of all the generated events, the samples are split into two orthogonal subsets and a cross-training procedure is adopted in which each subset is alternatively used for training and testing.

The operator $O_{tu}^{(1)}$ and the two operators $O_{Qu}^{(1)}$, $O_{Qu}^{(8)}$ have different kinematic properties due the different chirality of the operators. The kinematic properties of the two O_{Qu} operators are very similar and therefore are combined into a single signal category. A set of NNs, referred to as NN^{SvsS} , are trained to discriminate between SS top-quark pairs generated by the different EFT operators. Signal events in the nominal $t\bar{t}$ and $\bar{t}t$ samples are weighted first according to the EFT benchmark $c_{tu}^{(1)} = 0.04$, $c_{Qu}^{(1)} = 0$, $c_{Qu}^{(8)} = 0$ and then according to $c_{tu}^{(1)} = 0$, $c_{Qu}^{(1)} = 0.1$, $c_{Qu}^{(8)} = 0.2$ ⁷. These two weighted samples are used to train and test the NN^{SvsS} . The classification is based on nine kinematic quantities: the angular variables $\Delta\phi_{\ell,\ell}$, $\Delta R_{\ell,\ell}$, $\Delta\eta_{\ell,\ell}$ between the two leptons, the invariant mass of the two-lepton system, the scalar sum of the p_T of all jets, the scalar sum of the p_T of all leptons, the p_T of the leading jet, E_T^{miss} and the transverse mass of the combined lepton and E_T^{miss} system. The NN^{SvsS} output distributions for the simulated signal and background events from MC simulations before the fit are shown in Figure 4. Lower or higher values correspond to $O_{tu}^{(1)}$ - or O_{Qu} -like events, respectively. Two orthogonal regions are defined by requiring $NN^{SvsS} \leq 0.538$ and $NN^{SvsS} > 0.538$. This value corresponds to a classification efficiency of 65% for both categories. The efficiency times acceptance values for signal events that enter the SR_{tu} and SR_{Qu} regions are 26.8% and 12.4% for signal events that originate from the $O_{tu}^{(1)}$ operator, and 15.8% and 19.5% for signal events that originate from the O_{Qu} operators.

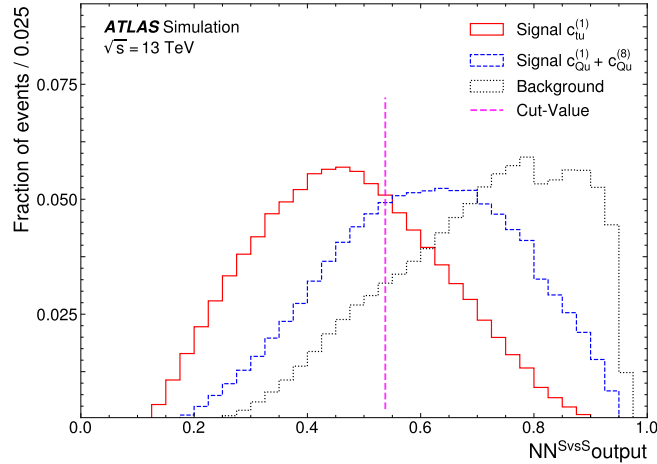


Figure 4: NN output variable for NN^{SvsS} used to classify the data into $c_{tu}^{(1)}$ - and c_{Qu} -like regions. The distribution for signal $c_{tu}^{(1)}$ was generated with $c_{tu}^{(1)} = 0.04$ with the other Wilson coefficients being set to zero, while the other signal distribution was produced with $c_{tu}^{(1)} = 0$, $c_{Qu}^{(1)} = 0.1$ and $c_{Qu}^{(8)} = 0.2$. The background distribution shown is the sum of all background processes from MC simulations before the likelihood fit. The value chosen to separate the signal events is shown by the vertical dashed line. An efficiency of 65% is obtained for the correct classification of c_{Qu} events and of $c_{tu}^{(1)}$ events.

A second set of NNs, referred to as NN^{SvsB} , are used to discriminate the SS top-quark signal from

⁷ The value of $c_{Qu}^{(8)} = 0.2$ is used instead of $c_{Qu}^{(8)} = 0.1$ to enhance the discriminating power relative to the $c_{tu}^{(1)} = 0.04$ sample.

background events. The discrimination is based on six kinematic quantities: the sum of the p_T of the leptons, the b -tagging score of the leading and sub-leading p_T jets, the p_T of the leading jet, the transverse mass of the leptons and the E_T^{miss} system, and the number of jets in the event. The distributions of these quantities show significant differences between the signal regions SR_{Qu} and SR_{tu} and for tt and $t\bar{t}$ events, therefore NN^{SvsB} is trained separately for each of the four signal regions defined by the EFT operators and the charge of the two leptons: SR_{tu}^{++} , SR_{tu}^{--} , SR_{Qu}^{++} and SR_{Qu}^{--} .⁸ Although $\Delta\phi_{\ell,\ell}$ and $\Delta R_{\ell,\ell}$ also show significant differences between signal and background, these quantities are not used in the training of NN^{SvsB} . Instead, the value of $\Delta\phi_{\ell,\ell}$ is used after the NN^{SvsB} classification to define the validation regions ($\Delta\phi_{\ell,\ell} < 2.5$) with negligible signal contamination and to enhance the purity of the signal regions ($\Delta\phi_{\ell,\ell} \geq 2.5$).

5.2 Definition of background-enriched regions

The background contributions from different physics processes are modeled using MC simulations, data-driven techniques, or a combination of both.

The $t\bar{t}W$ production is the dominant background in the SRs. Its contribution is modeled using MC events, as described in Section 3. Dedicated analyses of $t\bar{t}W$ production have measured larger cross-sections [81] than predicted in theoretical calculations [48]. It is therefore crucial for this search to constrain the $t\bar{t}W$ normalization in data. This is done using the NN^{SvsB} distributions in the SRs, which are enriched in $t\bar{t}W$ events especially in the first bins where the SS top-quark pair contribution is negligible.

The normalization of the other backgrounds are either taken from simulation, highest order perturbation theory calculations or determined in dedicated CRs. In these CRs the different background contributions are enhanced through specific event selections that differ from those used to define the SRs.

Irreducible backgrounds are those which can produce two prompt SS leptons, and include $t\bar{t}V$, $t\bar{t}H$, tZ , VV and $t\bar{t}t\bar{t}$ production, with V being a vector boson, W or Z , and rare processes. The rare processes are combined with the tZ process in the category *Other* in the following. Their shape estimation relies on good modeling of these processes in the MC simulation.

The CRs defined for $t\bar{t}Z$ and VV share some common selection requirements. Events with three charged leptons in the final state, an opposite-sign (OS) pair with the same flavor plus an additional lepton are selected. The invariant mass of the OS pair is required to be within 10 GeV of the Z boson mass. The transverse momentum of the OS pair and of the SS pair are required to be $p_T(\text{OS}) > 10$ GeV and $p_T(\text{SS}) > 20$ GeV, respectively. Furthermore both SS leptons must be classified as M_{inc} while the other lepton is required to be classified as L_{inc} . At least four jets are required in the $t\bar{t}Z$ CR, while events with exactly two or three jets are selected for the VV CR. Finally, in both CRs, at least one jet is required to be b -tagged according to the 60% WP or at least two jets are required to be b -tagged according to the 77% WP.

Reducible backgrounds contain at least one charge misidentified lepton or one fake or non-prompt lepton. These backgrounds mainly come from $t\bar{t}$ and V +jets production and are estimated by using data-driven procedures. Their contributions depend on the lepton reconstruction, so they are estimated separately for electrons and muons.

⁸ Charge splitting of the signal samples is not applied in NN^{SvsB} training because it is found to be ineffective.

Seven CRs enriched in non-prompt lepton events are defined. Among these, five are used to estimate non-prompt leptons coming from the decay of b , c , and light hadrons, referred to as heavy-flavor CRs, two for electrons (HFe) and three for muons (HF μ). In the heavy-flavor CRs, events with at least two jets and two SS leptons with $p_T > 20$ GeV are selected. Separate CRs are defined depending on the flavor of the sub-leading lepton. Additionally, separate CRs are defined depending on the lepton classification according to the categories used in the analysis: namely the TM , MT and TT combinations. This results in three CRs for each lepton flavor, namely HFe TM , HF μ TM , HF μ MT , HFe TT and HF μ TT . The CR for HFe MT is not used as some differences between the data and MC, which could be of statistical origin, are observed in this region and as removing this CR from the fit has no impact on the expected result. To suppress the contribution from $t\bar{t}W$ production in these regions, only events with exactly one b -tagged jet (77% WP) are selected and in the TM and MT regions, the transverse mass of the lepton and E_T^{miss} system is required to be $m_{T,\ell E_T^{\text{miss}}} < 250$ GeV. The p_T distribution of the sub-leading lepton is used to extract the two normalization factors for e and μ , by leaving them free in the fit to data.

Two CRs are defined to estimate the contributions to the background from leptons originating from photon conversions $\gamma/\gamma^* \rightarrow e^+e^-$ in the detector material (CR Mat Conv) or in the vicinity of the interaction point (CR Int Conv). Three-lepton events, where two leptons are of the same sign and have $p_T > 20$ GeV and one lepton is of opposite sign with $p_T > 10$ GeV are selected. Both SS leptons must be classified as M_{inc} while the OS lepton must satisfy the L_{inc} criteria. Events with b -tagged jets (77% WP) are rejected. Events in which the invariant mass of the OS same-flavor leptons is within 10 GeV of the Z boson mass are removed. Furthermore, the invariant mass of the three-lepton system must satisfy $|m_{\ell\ell\ell} - m_Z| < 10$ GeV, and $E_T^{\text{miss}} < 50$ GeV. The two CRs require different selections on the invariant mass of the electron candidates and its closest track evaluated at the primary vertex, $m_{\text{trk-trk,PV}}$, and conversion vertices, $m_{\text{trk-trk,CV}}$. Specifically, material conversions candidates are required to have a conversion vertex found with a radial distance from the IP $r > 20$ mm and $0 < m_{\text{trk-trk,CV}} < 100$ MeV, while interaction conversion candidates have to be rejected as material conversion candidates and have $0 < m_{\text{trk-trk,PV}} < 100$ MeV.

An additional source of background is identified from electron charge misidentification (QMisID), mainly in $t\bar{t}$ events.⁹ This background is estimated with a data-driven method using $Z \rightarrow ee$ events and is negligible in the four 3ℓ CRs. A likelihood-based method is used to measure the rate of reconstructed SS and OS electron pairs in specific control regions, while the non- Z backgrounds are subtracted via a sideband method utilizing events outside the Z boson mass window. The QMisID is then extracted from the ratio of SS to OS electron pairs in different p_T and η bins and varies from 10^{-5} for low- p_T electrons up to $4 \cdot 10^{-4}$ for high- p_T electrons. The QMisID backgrounds are then estimated by applying these rates to data events that satisfy the requirements for the 2ℓ regions, except that the two leptons are required to have opposite charges.

6 Systematic uncertainties

The signal and background event yields in signal, validation and control regions are affected by uncertainties due to the imperfect modeling of the physics processes and of the detector response. The systematic uncertainties are divided into two categories. The first category includes experimental uncertainties in the reconstruction of the final-state objects: leptons, jets, b -tagged jets and E_T^{miss} . The second category are modeling uncertainties, which are related to the choice of the MC generator, the PS and hadronization models, the choice of μ_F and μ_R , and the uncertainties in the PDFs.

⁹ The muon charge misidentification rate is estimated to be of the order of 10^{-5} and has a negligible impact.

All systematic uncertainties are incorporated in the likelihood function used to extract the yields of signal and backgrounds. Nuisance parameters (NPs) are associated with each source of systematic uncertainty considered in the analysis. The nominal values and ± 1 standard deviation (σ) variations of each NP are provided by dedicated studies. The maximum-likelihood fit used to determine the signal and background yields also provides the values and uncertainties of all NPs.

6.1 Experimental uncertainties

The uncertainty in the integrated luminosity is 0.83% [16], obtained using the LUCID-2 detector [82] for the primary luminosity measurements, complemented by measurements using the inner detector and the calorimeters. The MC samples are reweighted to reproduce the pileup distribution observed in the data. The corresponding pileup uncertainty is evaluated by varying these reweighting factors within their uncertainties, derived to cover the differences between the predicted and measured inelastic cross-section values [83].

Scale factors are applied to simulated events to account for differences between simulation and data in the efficiencies of electrons and muons when applying reconstruction, identification, trigger and isolation criteria. These scale factors and their systematic uncertainties are evaluated for electrons and muons as a function of transverse energy (or p_T) and η using tag-and-probe methods on e^+e^- and $\mu^+\mu^-$ decays in Z and J/ψ events [68, 69, 84]. The lepton energy/momentum scale and resolution and their corresponding uncertainties are also obtained from leptonic Z decays [68, 85].

The jet energy scale (JES) is calibrated using test-beam data, simulation, and in situ techniques [75]. The corresponding uncertainty has 30 uncorrelated components, including effects due to pileup modeling, jet flavor composition and response, differences between jets from b -quarks and those from gluons or light quarks and effects of jets not fully contained in the calorimeter. The uncertainty in the jet energy resolution (JER) is evaluated via thirteen orthogonal components as a function of jet p_T and η [75].

The uncertainty in the efficiency originating from the JVT requirement is obtained using $Z(\rightarrow \mu^+\mu^-)+$ jets events [86]. The uncertainty in E_T^{miss} due to possible miscalibration of its soft-track component is derived from data–simulation comparisons of the p_T balance between the hard and soft E_T^{miss} components [76].

The uncertainties related to the b -tagging efficiency of true b -jets and the mistagging rates of light-quark and c -jets is also considered. The b -tagging efficiency is measured in dileptonic $t\bar{t}$ events as a function of the jet p_T . Differences between data and simulation are corrected using scale factors. The uncertainty in these scale factors consists of 45 orthogonal components [87]. The rate of mistagging c -jets as b -jets is measured in semileptonic $t\bar{t}$ events, where one W boson can decay to a c -quark and a down-type quark [88]. The mistagging rate of c -jets is calculated as a function of the jet p_T and has an overall uncertainty between 3% and 17%, broken down into 20 orthogonal components. The misidentification rate of light-quark jets is evaluated based on techniques described in Ref. [89]. The resulting uncertainties in the scale factors are also decomposed into 20 orthogonal components.

6.2 Modeling uncertainties

For QCD $t\bar{t}W$, $t\bar{t}Z$, diboson, HFe , $HF\mu$, material photon conversions and internal photon conversions, the normalization is allowed to float freely in the fit. No normalization uncertainty is hence applied to $t\bar{t}$, single-top-quark, Z +jets and W +jets production, as all of these processes exclusively contribute

to non-prompt lepton backgrounds. For all other processes, dedicated normalization uncertainties are included as NPs in the fit. For the additional contributions to $t\bar{t}W$ from NLO electroweak diagrams a 20% normalization uncertainty is applied [90], as only QCD $t\bar{t}W$ events are considered in the free normalization parameter. The $t\bar{t}\bar{t}$, $t\bar{t}H$, and tZ processes are assigned uncertainties of 20% [91], 11% [49], and 20% [92], respectively. An additional 50% normalization uncertainty is assigned to EW $t\bar{t}W$, $t\bar{t}Z$, $t\bar{t}H$ and $t\bar{t}$ events containing additional heavy-flavor jets, following Ref. [93]. For the QmisID process a normalization uncertainty of 20% is applied. All other minor processes are assigned a conservative 50% normalization uncertainty.

For the dominant backgrounds, additional modeling uncertainties are considered, which use the alternative samples listed in parentheses in Table 1. The comparison between different generator setups include acceptance effects, migration between event categories and effects on the kinematic distributions. The impact of the generator choice is used as a systematic uncertainty for $t\bar{t}W$ and $t\bar{t}H$. For $t\bar{t}W$ production this uncertainty is evaluated by comparing the nominal SHERPA 2.2.10 sample with alternative samples generated with MADGRAPH5_AMC@NLO interfaced to PYTHIA 8. For $t\bar{t}H$ the nominal POWHEG BOX sample is compared with the alternative MADGRAPH5_AMC@NLO sample interfaced to PYTHIA 8. Uncertainties in the PS and hadronization modeling are assigned to the $t\bar{t}W$, $t\bar{t}H$ and $t\bar{t}Z$ processes. For $t\bar{t}H$ and $t\bar{t}Z$, the uncertainties are derived by comparing the nominal samples with alternative samples for which the individual ME generators were interfaced to HERWIG 7 instead of PYTHIA 8. For $t\bar{t}W$ production, two alternative samples were generated. The matrix element of both samples was generated with POWHEG BOX interfaced to PYTHIA 8 for one sample and to HERWIG 7 for the other. The relative differences between the two samples are determined for all bins in the analysis and applied to the nominal SHERPA 2.2.10 $t\bar{t}W$ sample.

Uncertainties related to the choice of μ_F and μ_R for the ME calculations are also taken into account for the $t\bar{t}H$, $t\bar{t}W$, $t\bar{t}Z$, and VV processes by varying their values by factors of 0.5 and 2.0 independently. For $t\bar{t}W$, separate scale uncertainties are derived for the QCD and EW components. For the signal samples, the effect of varying μ_R and μ_F is evaluated at generator level. Its effect on the jet multiplicity distribution is propagated via a reweighting procedure to the NN-output distributions in the SRs, resulting in a shape uncertainty of 2%–25% depending on the signal region and NN-output bin.

Uncertainties in initial-state radiation are taken into account by varying α_s^{ISR} according to the Var3c variation of the A14 tune [28] for $t\bar{t}Z$ events. For $t\bar{t}W$, two additional PDF uncertainties are taken into account. The first uncertainty is defined by comparing the nominal PDF with $\alpha_s = 0.118$ to variations with $\alpha_s = 0.117$ and $\alpha_s = 0.119$. The second uncertainty is based on the comparisons of the nominal PDF set NNPDF3.0_{NLO} to the alternative PDF sets CT14_{NNLO} [94] and MMHT2014_{NNLO68CL} [31].

6.3 Non-prompt-lepton background modeling uncertainties

Non-prompt lepton background estimates are affected by uncertainties due to an imperfect modeling of the variables used in the non-prompt lepton BDT. Systematic uncertainties, based on the residual disagreement observed between data and MC, are included as 34 NPs that can affect the shape of the distributions but not their normalization. Additional uncertainties, accounting for differences between the efficiencies of the non-prompt lepton BDT working points when using an alternative simulation, are considered. This uncertainty is estimated for the *Tight-not-VeryTight* and *VeryTight* WPs, respectively, by comparing the efficiencies in the nominal POWHEG+PYTHIA 8 $t\bar{t}$ simulation with an alternative $t\bar{t}$ simulation

(POWHEG+HERWIG 7.1.3 or SHERPA 2.2.10) as a function of the lepton p_T . As a consequence a normalization uncertainty of 20% is applied to both HF e and HF μ in the SRs.

Additional uncertainties are introduced to cover possible discrepancies between data and MC in the estimated rate of electron conversions. These uncertainties are derived by comparing the conversion rates in data and MC in dedicated 2ℓ validation regions, which require two *Tight* SS leptons where one of them is required to be a conversion candidate. Interaction and material conversion extrapolation uncertainties of 50% and 10%, respectively, are assigned to the conversion rates in the SRs.

A systematic uncertainty is assigned to the QmisID background process. The uncertainty is assessed by combining four different sources of uncertainty: the differences between misidentified electrons and positrons, the variation of rates within the m_Z window, the difference between the measured rates with the likelihood method and those obtained by matching reconstructed to generated $Z \rightarrow e^+e^-$ simulated events, and the statistical uncertainty from the likelihood method. The uncertainty increases as a function of the electron p_T and decreases with $|\eta|$ and ranges between 10% and 60%.

7 Results

A maximum-likelihood fit is performed in the four SRs and the nine CRs to simultaneously determine the signal strength of the SS top-quark pair production and the background normalization factors defined in Section 6.2. For the four SRs the NN^{SvsB} distributions are used as discriminants, while simpler discriminants are used in the CRs. The number of b -tagged jets is used for the $t\bar{t}Z$ and diboson CRs, the transverse momentum of the sub-leading lepton is used for the HF e TM and HF μ TM CRs, and for the remaining HF CRs and photon conversion CR the total number of events per region is used.

The likelihood function $\mathcal{L}(\mu, \vec{\lambda}, \vec{\theta})$, defined as the product of Poisson probability terms for all bins, depends on the signal strength parameter μ , the normalization factors for several backgrounds $\vec{\lambda}$, and a set of NPs $\vec{\theta}$, each one linked to a source of systematic uncertainty described in Section 6. Both μ and $\vec{\lambda}$ are allowed to vary freely in the likelihood fit. The NPs $\vec{\theta}$ can produce variations in the signal and background expectations and are subject to Gaussian constraints in the likelihood fit. Statistical uncertainties in each bin, due to the limited size of the experimental and simulated samples, are taken into account with dedicated parameters. The statistical analysis is performed using the RooFIT framework [95] with the statistical model built following the HistFactory format [96].

Figures 5 and 6 show the observed and expected number of events in the nine CRs and four SRs, respectively, after the likelihood fit under the signal-plus-background hypothesis. The corresponding post-fit yields are shown in Tables 3–5. They are consistent with the observed data within their uncertainties and align with the pre-fit yields. In the VRs good agreement between data and simulation is also observed post-fit.

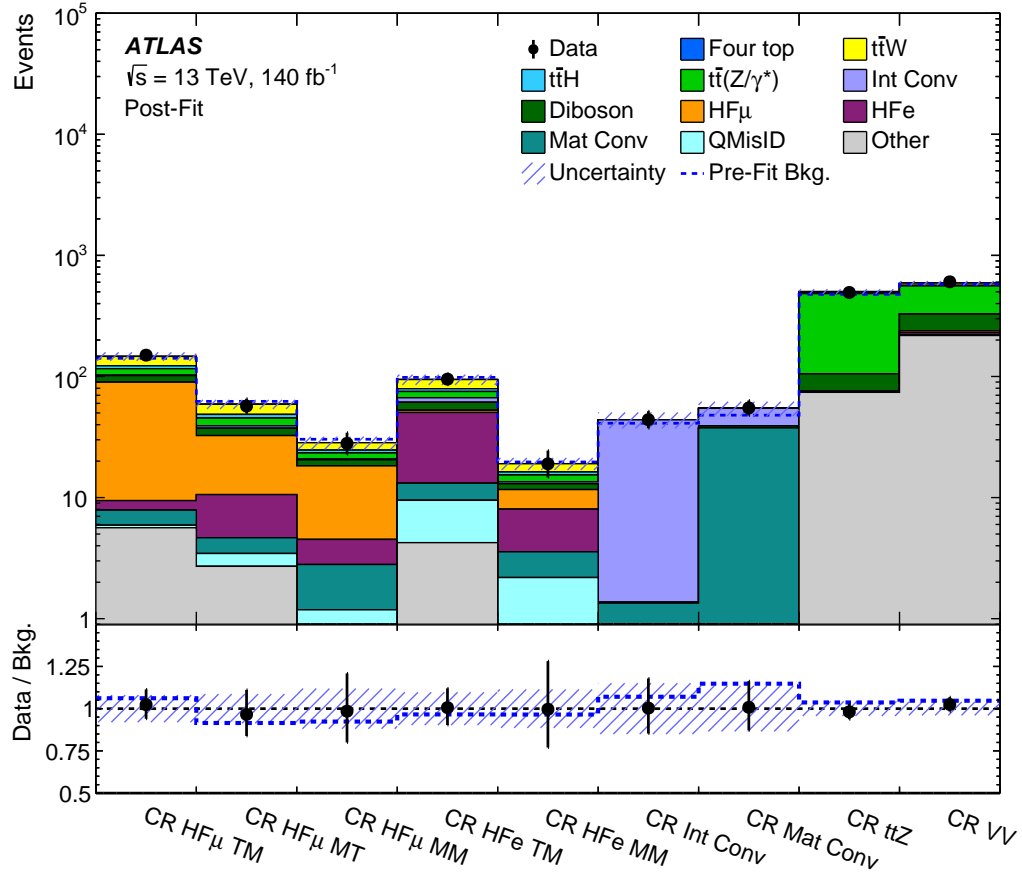


Figure 5: Comparison between the event yields in data and the background expectation after the likelihood fit for the nine control regions. The post-fit background expectations are shown as filled histograms, the combined pre-fit background expectations are shown as dashed lines. The ratio of the data to the total post-fit background is shown in the lower panel. The combined statistical and systematic uncertainty in the simulation is indicated by the hatched band, while the vertical error bars represent the statistical uncertainty in the data.

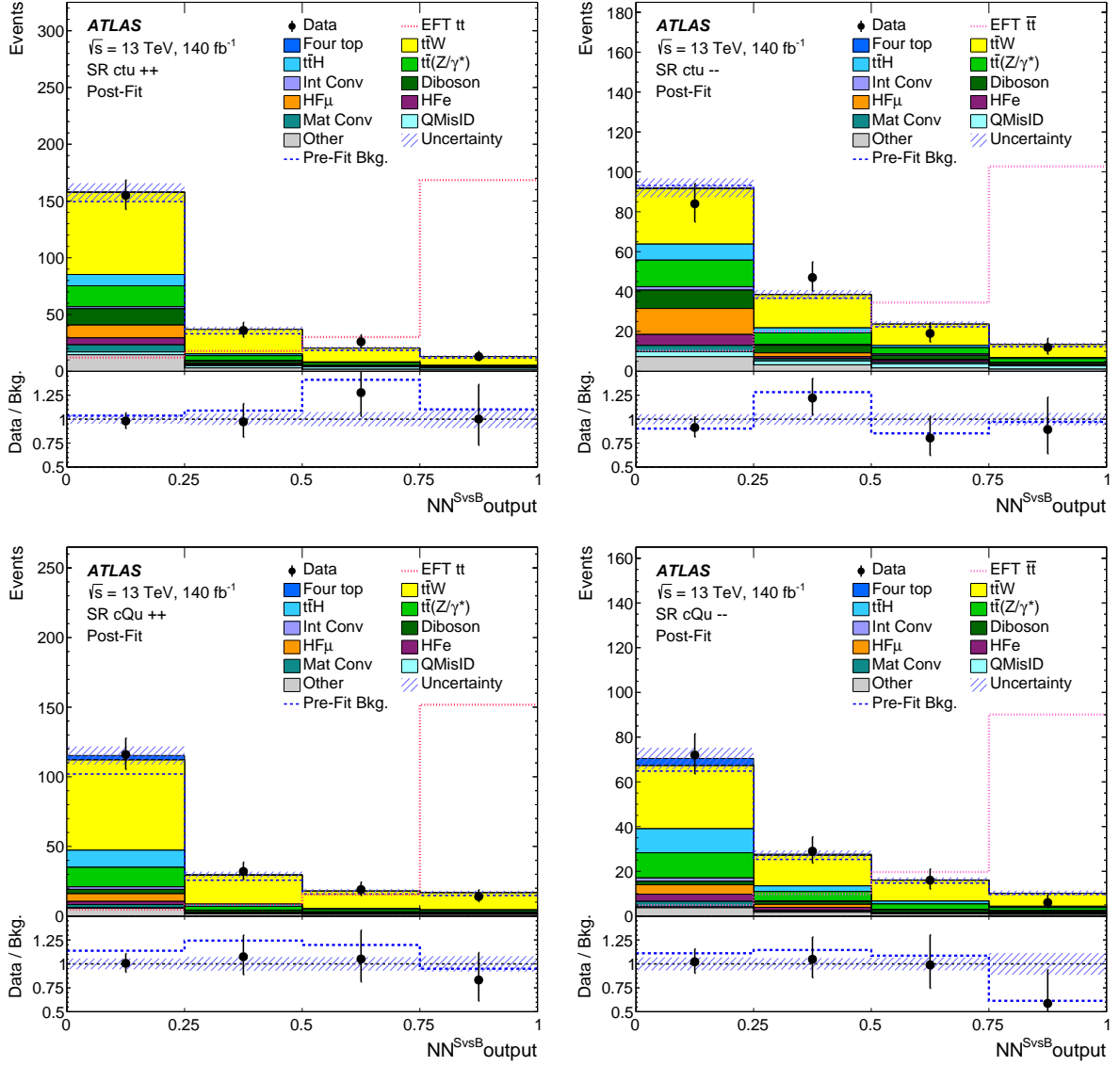


Figure 6: Distributions of the NN^{SvsB} output for data and the expected background after the likelihood fit in the four signal regions. The post-fit background expectations are shown as filled histograms, the combined pre-fit background expectations are shown as dashed lines. The signal distribution using the Wilson coefficient values $c_{tu}^{(1)} = 0.04$, $c_{Qu}^{(1)} = 0.1$, $c_{Qu}^{(8)} = 0.1$ is shown with a dotted line, normalized to the same number of events as the background. The ratio of the data to the total post-fit background is shown in the lower panel. The combined statistical and systematic uncertainty in MC simulation is indicated by the hatched band, while the vertical error bars represent the statistical uncertainty in the data.

Table 3: Summary of the observed and predicted number of events in the five 2ℓ control regions. The background prediction is shown after the combined likelihood fit to data under the signal-plus-background hypothesis across all control regions and signal regions. The uncertainties in the total yields are smaller than the sum in quadrature of the uncertainties in the individual contributions due to anti-correlations resulting from the likelihood fit.

Process	CR HF μ TM	CR HF μ MT	CR HF μ MM	CR HF e TM	CR HF e MM
$t\bar{t}W$	24.0 \pm 4.9	10.3 \pm 2.0	3.73 \pm 0.87	15.1 \pm 2.9	2.76 \pm 0.59
$t\bar{t}(Z/\gamma^*)$	13.6 \pm 2.1	6.20 \pm 0.97	2.59 \pm 0.47	8.4 \pm 1.7	1.90 \pm 0.32
$t\bar{t}H$	6.6 \pm 4.0	3.2 \pm 1.9	1.28 \pm 0.79	4.1 \pm 2.4	0.90 \pm 0.58
Four top	0.113 \pm 0.028	0.071 \pm 0.017	0.046 \pm 0.012	0.069 \pm 0.019	0.036 \pm 0.010
Diboson	11.9 \pm 6.1	4.9 \pm 2.5	2.2 \pm 1.1	8.6 \pm 4.4	1.35 \pm 0.72
HFe	1.6 \pm 1.1	5.9 \pm 2.9	1.71 \pm 0.97	37 \pm 12	4.5 \pm 1.6
HF μ	80 \pm 14	21.9 \pm 5.6	13.8 \pm 3.2	2.20 \pm 0.66	3.62 \pm 0.99
Mat Conv	2.0 \pm 7.1	1.20 \pm 0.56	1.62 \pm 0.51	3.7 \pm 2.1	1.38 \pm 0.43
Int Conv	0.68 \pm 0.41	1.7 \pm 1.0	0.30 \pm 0.18	5.5 \pm 3.2	0.48 \pm 0.30
QMisID	0.28 \pm 0.13	0.75 \pm 0.54	0.38 \pm 0.26	5.2 \pm 2.9	1.6 \pm 1.0
Other	5.6 \pm 1.5	2.71 \pm 0.66	0.81 \pm 0.21	4.2 \pm 1.0	0.63 \pm 0.16
Total Bkg.	147 \pm 12	59.0 \pm 5.1	28.4 \pm 3.4	94.4 \pm 9.2	19.1 \pm 2.2
Data	150	57	28	95	19

Table 4: Summary of the observed and predicted number of events in the four 3ℓ control regions. The background prediction is shown after the combined likelihood fit to data under the signal-plus-background hypothesis across all control regions and signal regions. The uncertainties in the total yields are smaller than the sum in quadrature of the uncertainties in the individual contributions due to anti-correlations resulting from the likelihood fit.

Process	CR Int Conv	CR Mat Conv	CR ttZ	CR VV
$t\bar{t}W$	–	–	8.4 \pm 1.8	24.5 \pm 4.7
$t\bar{t}(Z/\gamma^*)$	–	–	378 \pm 32	230 \pm 27
$t\bar{t}H$	–	–	10.0 \pm 6.3	6.3 \pm 4.0
Four top	–	–	1.61 \pm 0.32	0.092 \pm 0.020
Diboson	0.025 \pm 0.019	1.34 \pm 0.72	29 \pm 15	90 \pm 45
HFe	–	–	0.47 \pm 0.35	9.2 \pm 6.8
HF μ	–	–	1.04 \pm 0.35	7.5 \pm 1.8
Mat Conv	1.3 \pm 1.1	37.6 \pm 8.6	0.59 \pm 0.40	2.19 \pm 0.77
Int Conv	42.5 \pm 6.8	15.6 \pm 4.3	0.14 \pm 0.15	1.66 \pm 0.96
QMisID	–	–	0.22 \pm 0.17	0.83 \pm 0.41
Other	–	–	74 \pm 23	218 \pm 40
Total Bkg.	43.9 \pm 6.6	54.6 \pm 7.3	503 \pm 22	590 \pm 23
Data	44	55	494	605

Table 5: Summary of the observed and predicted number of events in the four signal regions. The background prediction is shown after the combined likelihood fit to data under the signal-plus-background hypothesis across all control regions and signal regions. The uncertainties in the total yields are smaller than the sum in quadrature of the uncertainties in the individual contributions due to anti-correlations resulting from the likelihood fit.

Process	SR_{ctu++}	SR_{ctu--}	SR_{cQu++}	SR_{cQu--}
$t\bar{t}W$	114 ± 15	62 ± 10	110 ± 15	56.9 ± 9.0
$t\bar{t}(Z/\gamma^*)$	25.5 ± 2.4	24.1 ± 2.6	19.5 ± 1.8	19.1 ± 1.8
$t\bar{t}H$	12.4 ± 7.5	12.3 ± 7.1	15.1 ± 9.6	15.1 ± 9.2
Four top	0.72 ± 0.15	0.69 ± 0.14	4.16 ± 0.83	4.07 ± 0.82
Diboson	18.1 ± 9.3	15.9 ± 8.1	6.3 ± 3.2	4.2 ± 2.1
HFe	6.5 ± 2.9	7.6 ± 3.0	3.0 ± 1.1	4.9 ± 2.5
HF μ	12.6 ± 2.7	15.7 ± 3.2	6.3 ± 1.8	5.7 ± 1.7
Mat Conv	7.6 ± 2.5	5.5 ± 1.6	2.73 ± 0.83	3.3 ± 1.2
Int Conv	2.7 ± 1.6	3.0 ± 1.7	2.1 ± 1.2	2.7 ± 1.6
QMisID	8.1 ± 2.2	8.1 ± 2.2	1.48 ± 0.39	1.48 ± 0.39
Other	20.3 ± 5.4	13.3 ± 3.9	9.3 ± 2.7	7.0 ± 2.6
Total Bkg.	228 ± 11	167.7 ± 7.9	180 ± 10	124.5 ± 6.3
Data	230	162	181	123

The fitted signal yield in each of the four SRs is found to be ≤ 0.001 events and is therefore rounded to zero. A negative signal yield is not allowed in the fit as the quadratic EFT parameterization only allows for positive cross-sections by definition. Since no significant signal is observed, upper limits on the three WCs are determined by running 1D- and 2D-likelihood scans. Expected limits are also derived using a hybrid-Asimov data sample [97], which combines real data distributions in all nine CRs and the first two bins of each SRs, with Asimov data for the remaining bins determined under the background-only assumption.

The results of Ref. [98] indicate that Wilks' Theorem is violated by quadratic EFT terms, which can lead to over- or undercoverage for the derived confidence intervals (CIs). It is carefully checked if this affects the results of this analysis by comparing the observed limits with limits that are derived from MC pseudo-data samples. No undercoverage is observed, while overcoverage is observed for WC values close to 0. The observed limits are slightly affected by overcoverage leading to at most 9% looser limits.

In the likelihood scans, the WCs are varied in the range of $[-0.01, 0.01]$ for $c_{tu}^{(1)}$, $[-0.03, 0.03]$ for $c_{Qu}^{(1)}$, and $[-0.06, 0.06]$ for $c_{Qu}^{(8)}$. All NPs, normalization factors, and the other two WCs are allowed to vary freely. The resulting observed (expected) limits at 95% CL in $(\text{TeV}/\Lambda)^2$ are $|c_{tu}^{(1)}| < 0.0068$ (0.0071), $|c_{Qu}^{(1)}| < 0.020$ (0.022) and $|c_{Qu}^{(8)}| < 0.041$ (0.046).

These observed (expected) WCs limits are translated into 95% CL cross-section limits on SS top-quark pair production by using the fitted EFT parameterization, varying only one WC at a time. For all three WCs the observed (expected) cross-section limit at 95% CL is 1.6 (2.0) fb.

In Table 6, the observed 95% CIs for the three WCs are shown for different sets of uncertainties, considering either only statistical uncertainties, or statistical and modeling uncertainties, or all uncertainties. The sensitivity of the analysis is limited by the available number of events. A degradation of the observed limits

of about 3% is observed when including all systematic uncertainties, with the largest degradation caused by the modeling uncertainties for $t\bar{t}W$. The dominant uncertainties are indeed modeling uncertainties related to the ME and the PS of $t\bar{t}W$ events.

In Figure 7, the observed CIs on the three WCs are compared with the previous best constraints from the ATLAS Run 1 analysis of events with b -tagged jets and a SS lepton pair [8]. For the comparison with the ATLAS Run 1 analysis, the 95% CL cross-section limits are converted to constraints on the WCs using the fitted EFT parameterization, as no specific WC limits were provided by the original analysis. The observed limits in this analysis are found to be an order of magnitude more stringent than the limits from the ATLAS Run 1 analysis.

In Figure 8, the observed lower limits on Λ for the WCs values 0.01, 1 and $4\pi^2$ are compared with the results of other analyses.

Two-dimensional-likelihood scans are performed for the three WCs, whose results are shown in Figure 9.

Table 6: Observed 95% CL confidence intervals on the three Wilson coefficients for different sets of uncertainties. The first, second and third rows show the limits obtained by considering, respectively: only the statistical uncertainties, both the statistical and modeling uncertainties, and all uncertainties. The new-physics scale is set to $\Lambda = 1\text{TeV}$.

Uncertainties	Wilson Coefficient CIs at 95% CL ($\times 10^{-2}$)		
	$c_{tu}^{(1)}$	$c_{Qu}^{(1)}$	$c_{Qu}^{(8)}$
Statistical uncertainty only	[-0.65, 0.65]	[-1.9, 1.9]	[-3.9, 3.9]
Statistical + modeling uncertainties	[-0.67, 0.67]	[-1.9, 1.9]	[-4.0, 4.0]
Total uncertainty	[-0.68, 0.68]	[-2.0, 2.0]	[-4.1, 4.1]

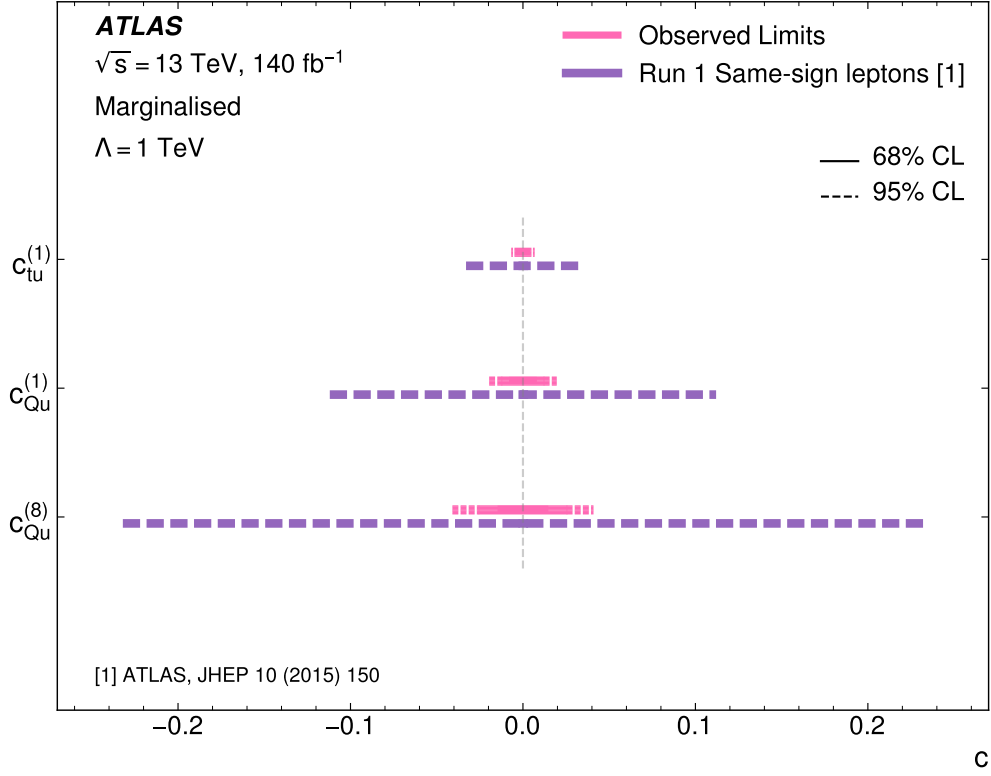


Figure 7: Comparison of the observed limits on the three WCs to the limit obtained by the ATLAS Run 1 analysis of events with b -tagged jets and a same-sign lepton pair [8]. The cross-section limits from that analysis are converted to the limits on the WCs by using the fitted EFT parametrization. The bounds on the WCs are shown at the 68% CL (solid) and/or 95% CL (dashed) levels. For the ATLAS Run 1 analysis only the bounds at 95% CL are available. The vertical bar represents the SM prediction. The new-physics scale is set to $\Lambda = 1\text{TeV}$.

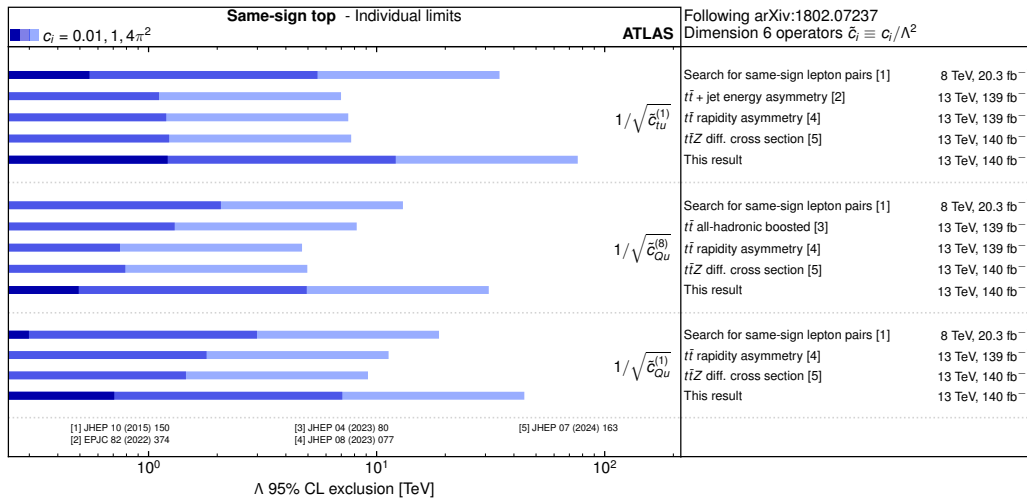


Figure 8: Observed lower limits at 95% confidence level on the scale of new physics Λ for Wilson coefficient values of 0.01, 1 and $4\pi^2$. The limits are compared with the results of other analyses.

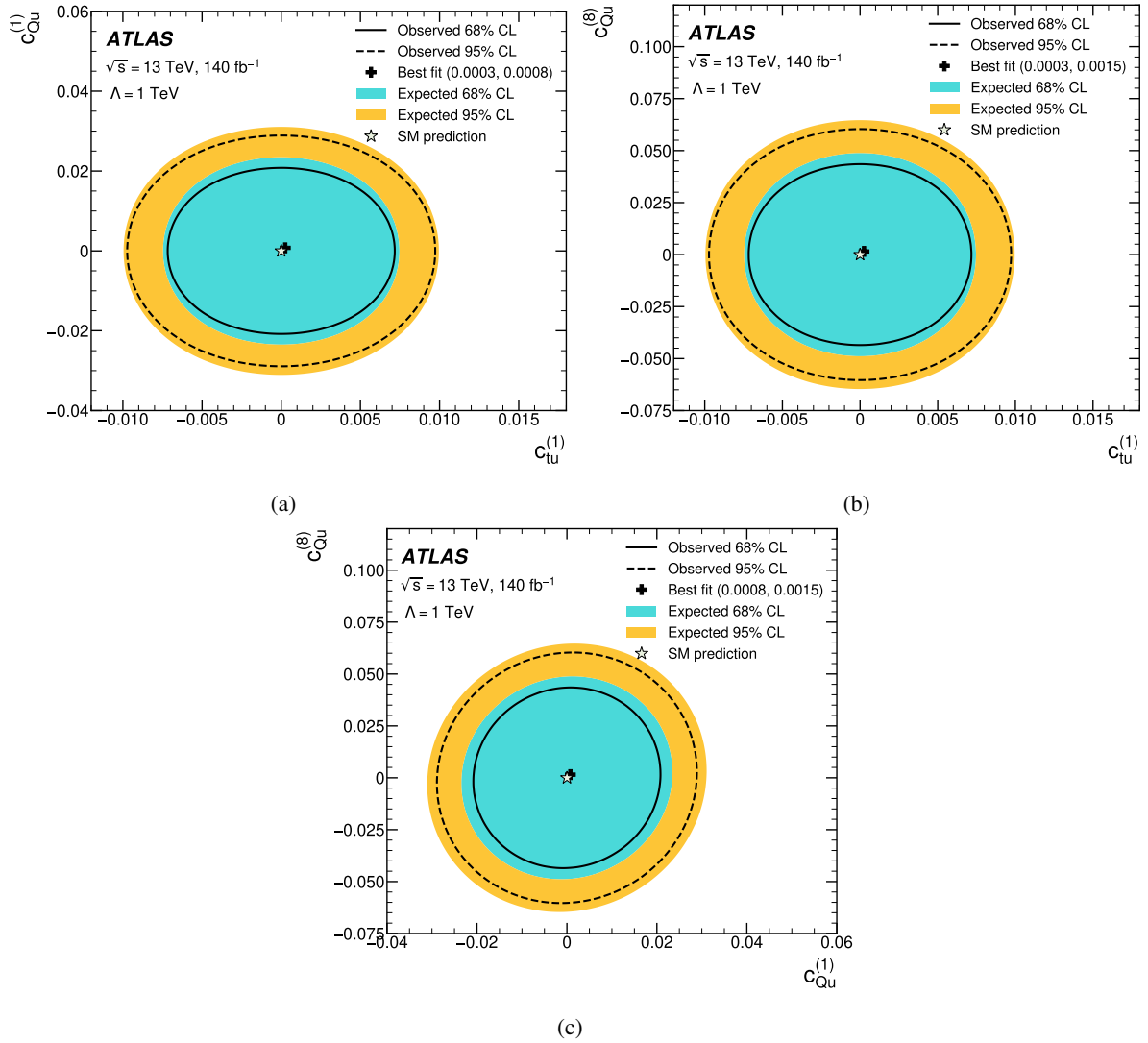


Figure 9: 2D likelihood scans for the different combinations of Wilson coefficients: (a) $c_{tu}^{(1)}$ versus $c_{Qu}^{(1)}$, (b) $c_{tu}^{(1)}$ versus $c_{Qu}^{(8)}$ and (c) $c_{Qu}^{(1)}$ versus $c_{Qu}^{(8)}$. The observed limits at 68% and 95% CL are represented by solid and dashed lines, respectively, while the expected limits are illustrated by the inner and outer shaded regions. The best fit value is marked with a cross. The SM prediction is marked with a star. The new-physics scale is set to $\Lambda = 1 \text{ TeV}$.

8 Conclusion

A search for the production of top-quark pairs with the same electric charge is reported. This search uses the full Run 2 data sample of $\sqrt{s} = 13 \text{ TeV}$ proton–proton collision data, with an integrated luminosity of 140 fb^{-1} , recorded from 2015 to 2018 with the ATLAS detector at the Large Hadron Collider. Standard model effective field theory is used to simulate the signal process, considering three Wilson coefficients associated with the $O_{tu}^{(1)}$, $O_{Qu}^{(1)}$, and $O_{Qu}^{(8)}$ operators with the new physics scale set to $\Lambda = 1 \text{ TeV}$. Neural networks are employed to define signal regions sensitive to these Wilson coefficients. The largest background processes are constrained using dedicated control regions. The results are in agreement with

the SM, with no significant signal detected. Upper limits at 95% CL are determined for the three WCs and on the production cross-section of same-sign top-quark pairs. The observed (expected) limits on the WCs are $|c_{tu}^{(1)}| < 0.0068$ (0.0071), $|c_{Qu}^{(1)}| < 0.020$ (0.022) and $|c_{Qu}^{(8)}| < 0.041$ (0.046) respectively. The observed (expected) upper limit on the total production cross-section of same-sign top-quark pairs $\sigma(pp \rightarrow tt)$ is 1.6 (2.0) fb at 95% CL. These are the most stringent limits on the WCs associated with the $O_{tu}^{(1)}$, $O_{Qu}^{(1)}$, and $O_{Qu}^{(8)}$ operators to date, improving previous limits by approximately a factor of 10.

Acknowledgements

We thank CERN for the very successful operation of the LHC and its injectors, as well as the support staff at CERN and at our institutions worldwide without whom ATLAS could not be operated efficiently.

The crucial computing support from all WLCG partners is acknowledged gratefully, in particular from CERN, the ATLAS Tier-1 facilities at TRIUMF/SFU (Canada), NDGF (Denmark, Norway, Sweden), CC-IN2P3 (France), KIT/GridKA (Germany), INFN-CNAF (Italy), NL-T1 (Netherlands), PIC (Spain), RAL (UK) and BNL (USA), the Tier-2 facilities worldwide and large non-WLCG resource providers. Major contributors of computing resources are listed in Ref. [99].

We gratefully acknowledge the support of ANPCyT, Argentina; YerPhI, Armenia; ARC, Australia; BMWFW and FWF, Austria; ANAS, Azerbaijan; CNPq and FAPESP, Brazil; NSERC, NRC and CFI, Canada; CERN; ANID, Chile; CAS, MOST and NSFC, China; Minciencias, Colombia; MEYS CR, Czech Republic; DNRF and DNSRC, Denmark; IN2P3-CNRS and CEA-DRF/IRFU, France; SRNSFG, Georgia; BMBF, HGF and MPG, Germany; GSRI, Greece; RGC and Hong Kong SAR, China; ISF and Benozziyo Center, Israel; INFN, Italy; MEXT and JSPS, Japan; CNRST, Morocco; NWO, Netherlands; RCN, Norway; MNiSW, Poland; FCT, Portugal; MNE/IFA, Romania; MSTDI, Serbia; MSSR, Slovakia; ARIS and MVZI, Slovenia; DSI/NRF, South Africa; MICIU/AEI, Spain; SRC and Wallenberg Foundation, Sweden; SERI, SNSF and Cantons of Bern and Geneva, Switzerland; NSTC, Taipei; TENMAK, Türkiye; STFC/UKRI, United Kingdom; DOE and NSF, United States of America.

Individual groups and members have received support from BCKDF, CANARIE, CRC and DRAC, Canada; CERN-CZ, FORTE and PRIMUS, Czech Republic; COST, ERC, ERDF, Horizon 2020, ICSC-NextGenerationEU and Marie Skłodowska-Curie Actions, European Union; Investissements d’Avenir Labex, Investissements d’Avenir Idex and ANR, France; DFG and AvH Foundation, Germany; Herakleitos, Thales and Aristeia programmes co-financed by EU-ESF and the Greek NSRF, Greece; BSF-NSF and MINERVA, Israel; NCN and NAWA, Poland; La Caixa Banking Foundation, CERCA Programme Generalitat de Catalunya and PROMETEO and GenT Programmes Generalitat Valenciana, Spain; Göran Gustafssons Stiftelse, Sweden; The Royal Society and Leverhulme Trust, United Kingdom.

In addition, individual members wish to acknowledge support from Armenia: Yerevan Physics Institute (FAPERJ); CERN: European Organization for Nuclear Research (CERN PJAS); Chile: Agencia Nacional de Investigación y Desarrollo (FONDECYT 1230812, FONDECYT 1230987, FONDECYT 1240864); China: Chinese Ministry of Science and Technology (MOST-2023YFA1605700), National Natural Science Foundation of China (NSFC - 12175119, NSFC 12275265, NSFC-12075060); Czech Republic: Czech Science Foundation (GACR - 24-11373S), Ministry of Education Youth and Sports (FORTE CZ.02.01.01/00/22_008/0004632), PRIMUS Research Programme (PRIMUS/21/SCI/017); EU: H2020 European Research Council (ERC - 101002463); European Union: European Research Council (ERC - 948254, ERC 101089007), European Union, Future Artificial Intelligence Research

(FAIR-NextGenerationEU PE00000013), Italian Center for High Performance Computing, Big Data and Quantum Computing (ICSC, NextGenerationEU); France: Agence Nationale de la Recherche (ANR-20-CE31-0013, ANR-21-CE31-0013, ANR-21-CE31-0022, ANR-22-EDIR-0002); Germany: Baden-Württemberg Stiftung (BW Stiftung-Postdoc Eliteprogramme), Deutsche Forschungsgemeinschaft (DFG - 469666862, DFG - CR 312/5-2); Italy: Istituto Nazionale di Fisica Nucleare (ICSC, NextGenerationEU), Ministero dell'Università e della Ricerca (PRIN - 20223N7F8K - PNRR M4.C2.1.1); Japan: Japan Society for the Promotion of Science (JSPS KAKENHI JP22H01227, JSPS KAKENHI JP22H04944, JSPS KAKENHI JP22KK0227, JSPS KAKENHI JP23KK0245); Netherlands: Netherlands Organisation for Scientific Research (NWO Veni 2020 - VI.Veni.202.179); Norway: Research Council of Norway (RCN-314472); Poland: Ministry of Science and Higher Education (IDUB AGH, POB8, D4 no 9722), Polish National Agency for Academic Exchange (PPN/PPO/2020/1/00002/U/00001), Polish National Science Centre (NCN 2021/42/E/ST2/00350, NCN OPUS nr 2022/47/B/ST2/03059, NCN UMO-2019/34/E/ST2/00393, UMO-2020/37/B/ST2/01043, UMO-2021/40/C/ST2/00187, UMO-2022/47/O/ST2/00148, UMO-2023/49/B/ST2/04085, UMO-2023/51/B/ST2/00920); Slovenia: Slovenian Research Agency (ARIS grant J1-3010); Spain: Generalitat Valenciana (Artemisa, FEDER, ID-IFEDER/2018/048), Ministry of Science and Innovation (MCIN & NextGenEU PCI2022-135018-2, MICIN & FEDER PID2021-125273NB, RYC2019-028510-I, RYC2020-030254-I, RYC2021-031273-I, RYC2022-038164-I); Sweden: Swedish Research Council (Swedish Research Council 2023-04654, VR 2018-00482, VR 2022-03845, VR 2022-04683, VR 2023-03403, VR grant 2021-03651), Knut and Alice Wallenberg Foundation (KAW 2018.0458, KAW 2019.0447, KAW 2022.0358); Switzerland: Swiss National Science Foundation (SNSF - PCEFP2_194658); United Kingdom: Leverhulme Trust (Leverhulme Trust RPG-2020-004), Royal Society (NIF-R1-231091); United States of America: U.S. Department of Energy (ECA DE-AC02-76SF00515), Neubauer Family Foundation.

References

- [1] V. Hirschi and O. Mattelaer, *Automated event generation for loop-induced processes*, 2015, arXiv: [1507.00020 \[hep-ph\]](#).
- [2] B. Grzadkowski, M. Iskrzyński, M. Misiak, and J. Rosiek, *Dimension-six terms in the Standard Model Lagrangian*, *JHEP* **10** (2010) 85, arXiv: [1008.4884 \[hep-ph\]](#).
- [3] C. Degrande, J.-M. Gérard, C. Grojean, F. Maltoni, and G. Servant, *An effective approach to same sign top pair production at the LHC and the forward–backward asymmetry at the Tevatron*, *Phys. Lett.* **703** (2011) 306, arXiv: [1104.1798 \[hep-ph\]](#).
- [4] I. Brivio et al., *O new physics, where art thou? A global search in the top sector*, *JHEP* **02** (2020) 131, arXiv: [1910.03606 \[hep-ph\]](#).
- [5] UFit Collaboration, *Model-independent constraints on Delta F=2 operators and the scale of New Physics*, *JHEP* **03** (2008) 049, arXiv: [0707.0636 \[hep-ph\]](#).
- [6] CMS Collaboration, *Search for same-sign top-quark pair production at $\sqrt{s} = 7$ TeV and limits on flavour changing neutral currents in the top sector*, *JHEP* **08** (2011) 005, arXiv: [1106.2142 \[hep-ex\]](#).
- [7] ATLAS Collaboration, *Search for same-sign top-quark production and fourth-generation down-type quarks in pp collisions at $\sqrt{s} = 7$ TeV with the ATLAS detector*, *JHEP* **04** (2012) 069, arXiv: [1202.5520 \[hep-ex\]](#).
- [8] ATLAS Collaboration, *Analysis of events with b-jets and a pair of leptons of the same charge in pp collisions at $\sqrt{s} = 8$ TeV with the ATLAS detector*, *JHEP* **10** (2015) 150, arXiv: [1504.04605 \[hep-ex\]](#).
- [9] CMS Collaboration, *Search for physics beyond the standard model in events with two leptons of same sign, missing transverse momentum, and jets in proton–proton collisions at $\sqrt{s} = 13$ TeV*, *Eur. Phys. J. C* **77** (2017) 578, arXiv: [1704.07323 \[hep-ex\]](#).
- [10] ATLAS Collaboration, *Search for new phenomena in events with same-charge leptons and b-jets in pp collisions at $\sqrt{s} = 13$ TeV with the ATLAS detector*, *JHEP* **12** (2018) 039, arXiv: [1807.11883 \[hep-ex\]](#).
- [11] CMS Collaboration, *Search for physics beyond the standard model in events with jets and two same-sign or at least three charged leptons in proton–proton collisions at $\sqrt{s} = 13$ TeV*, *Eur. Phys. J. C* **80** (2020) 752, arXiv: [2001.10086 \[hep-ex\]](#).
- [12] ATLAS Collaboration, *The ATLAS Experiment at the CERN Large Hadron Collider*, *JINST* **3** (2008) S08003.
- [13] ATLAS Collaboration, *Performance of the ATLAS trigger system in 2015*, *Eur. Phys. J. C* **77** (2017) 317, arXiv: [1611.09661 \[hep-ex\]](#).
- [14] ATLAS Collaboration, *Software and computing for Run 3 of the ATLAS experiment at the LHC*, (2024), arXiv: [2404.06335 \[hep-ex\]](#).
- [15] ATLAS Collaboration, *ATLAS data quality operations and performance for 2015–2018 data-taking*, *JINST* **15** (2020) P04003, arXiv: [1911.04632 \[physics.ins-det\]](#).

- [16] ATLAS Collaboration, *Luminosity determination in pp collisions at $\sqrt{s} = 13$ TeV using the ATLAS detector at the LHC*, *Eur. Phys. J. C* **83** (2023) 982, arXiv: 2212.09379 [hep-ex].
- [17] ATLAS Collaboration, *The ATLAS Simulation Infrastructure*, *Eur. Phys. J. C* **70** (2010) 823, arXiv: 1005.4568 [physics.ins-det].
- [18] S. Agostinelli et al., *GEANT4 – a simulation toolkit*, *Nucl. Instrum. Meth. A* **506** (2003) 250.
- [19] ATLAS Collaboration, *The new Fast Calorimeter Simulation in ATLAS*, ATL-SOFT-PUB-2018-002, 2018, URL: <https://cds.cern.ch/record/2630434>.
- [20] T. Sjöstrand, S. Mrenna, and P. Skands, *A brief introduction to PYTHIA 8.1*, *Comput. Phys. Commun.* **178** (2008) 852, arXiv: 0710.3820 [hep-ph].
- [21] NNPDF Collaboration, R. D. Ball, et al., *Parton distributions with LHC data*, *Nucl. Phys. B* **867** (2013) 244, arXiv: 1207.1303 [hep-ph].
- [22] ATLAS Collaboration, *The Pythia 8 A3 tune description of ATLAS minimum bias and inelastic measurements incorporating the Donnachie–Landshoff diffractive model*, ATL-PHYS-PUB-2016-017, 2016, URL: <https://cds.cern.ch/record/2206965>.
- [23] J. Alwall et al., *The automated computation of tree-level and next-to-leading order differential cross sections, and their matching to parton shower simulations*, *JHEP* **07** (2014) 079, arXiv: 1405.0301 [hep-ph].
- [24] S. Frixione, G. Ridolfi, and P. Nason, *A positive-weight next-to-leading-order Monte Carlo for heavy flavour hadroproduction*, *JHEP* **09** (2007) 126, arXiv: 0707.3088 [hep-ph].
- [25] E. Re, *Single-top Wt-channel production matched with parton showers using the POWHEG method*, *Eur. Phys. J. C* **71** (2011) 1547, arXiv: 1009.2450 [hep-ph].
- [26] S. Alioli, P. Nason, C. Oleari, and E. Re, *NLO single-top production matched with shower in POWHEG: s- and t-channel contributions*, *JHEP* **09** (2009) 111, arXiv: 0907.4076 [hep-ph].
- [27] T. Sjöstrand et al., *An introduction to PYTHIA 8.2*, *Comput. Phys. Commun.* **191** (2015) 159, arXiv: 1410.3012 [hep-ph].
- [28] ATLAS Collaboration, *ATLAS Pythia 8 tunes to 7 TeV data*, ATL-PHYS-PUB-2014-021, 2014, URL: <https://cds.cern.ch/record/1966419>.
- [29] M. Bähr et al., *Herwig++ physics and manual*, *Eur. Phys. J. C* **58** (2008) 639, arXiv: 0803.0883 [hep-ph].
- [30] J. Bellm et al., *Herwig 7.0/Herwig++ 3.0 release note*, *Eur. Phys. J. C* **76** (2016) 196, arXiv: 1512.01178 [hep-ph].
- [31] L. A. Harland-Lang, A. D. Martin, P. Motylinski, and R. S. Thorne, *Parton distributions in the LHC era: MMHT 2014 PDFs*, *Eur. Phys. J. C* **75** (2015) 204, arXiv: 1412.3989 [hep-ph].
- [32] E. Bothmann et al., *Event generation with Sherpa 2.2*, *SciPost Phys.* **7** (2019) 034, arXiv: 1905.09127 [hep-ph].
- [33] D. J. Lange, *The EvtGen particle decay simulation package*, *Nucl. Instrum. Meth. A* **462** (2001) 152.

- [34] I. Brivio, Y. Jiang, and M. Trott, *The SMEFTsim package, theory and tools*, [JHEP **12** \(2017\) 070](#), arXiv: [1709.06492 \[hep-ph\]](#).
- [35] I. Brivio, *SMEFTsim 3.0 — a practical guide*, [JHEP **04** \(2021\) 073](#), arXiv: [2012.11343 \[hep-ph\]](#).
- [36] A. Alloul, N. D. Christensen, C. Degrande, C. Duhr, and B. Fuks, *FeynRules 2.0 — A complete toolbox for tree-level phenomenology*, [Comput. Phys. Commun. **185** \(2014\) 2250](#), arXiv: [1310.1921 \[hep-ph\]](#).
- [37] NNPDF Collaboration, R. D. Ball, et al., *Parton distributions for the LHC run II*, [JHEP **04** \(2015\) 040](#), arXiv: [1410.8849 \[hep-ph\]](#).
- [38] O. Mattelaer, *On the maximal use of Monte Carlo samples: re-weighting events at NLO accuracy*, [Eur. Phys. J. C **76** \(2016\)](#), arXiv: [1607.00763 \[hep-ph\]](#).
- [39] T. Gleisberg and S. Höche, *Comix, a new matrix element generator*, [JHEP **12** \(2008\) 039](#), arXiv: [0808.3674 \[hep-ph\]](#).
- [40] S. Schumann and F. Krauss, *A parton shower algorithm based on Catani–Seymour dipole factorisation*, [JHEP **03** \(2008\) 038](#), arXiv: [0709.1027 \[hep-ph\]](#).
- [41] S. Höche, F. Krauss, M. Schönherr, and F. Siegert, *A critical appraisal of NLO+PS matching methods*, [JHEP **09** \(2012\) 049](#), arXiv: [1111.1220 \[hep-ph\]](#).
- [42] S. Höche, F. Krauss, M. Schönherr, and F. Siegert, *QCD matrix elements + parton showers. The NLO case*, [JHEP **04** \(2013\) 027](#), arXiv: [1207.5030 \[hep-ph\]](#).
- [43] S. Catani, F. Krauss, B. R. Webber, and R. Kuhn, *QCD Matrix Elements + Parton Showers*, [JHEP **11** \(2001\) 063](#), arXiv: [hep-ph/0109231](#).
- [44] S. Höche, F. Krauss, S. Schumann, and F. Siegert, *QCD matrix elements and truncated showers*, [JHEP **05** \(2009\) 053](#), arXiv: [0903.1219 \[hep-ph\]](#).
- [45] F. Buccioni et al., *OpenLoops 2*, [Eur. Phys. J. C **79** \(2019\) 866](#), arXiv: [1907.13071 \[hep-ph\]](#).
- [46] F. Cascioli, P. Maierhöfer, and S. Pozzorini, *Scattering Amplitudes with Open Loops*, [Phys. Rev. Lett. **108** \(2012\) 111601](#), arXiv: [1111.5206 \[hep-ph\]](#).
- [47] A. Denner, S. Dittmaier, and L. Hofer, *COLLIER: A fortran-based complex one-loop library in extended regularizations*, [Comput. Phys. Commun. **212** \(2017\) 220](#), arXiv: [1604.06792 \[hep-ph\]](#).
- [48] R. Frederix and I. Tsinikos, *On improving NLO merging for $t\bar{t}W$ production*, [JHEP **11** \(2021\) 029](#), arXiv: [2108.07826 \[hep-ph\]](#).
- [49] D. de Florian et al., *Handbook of LHC Higgs Cross Sections: 4. Deciphering the Nature of the Higgs Sector*, (2017), arXiv: [1610.07922 \[hep-ph\]](#).
- [50] P. Nason, *A new method for combining NLO QCD with shower Monte Carlo algorithms*, [JHEP **11** \(2004\) 040](#), arXiv: [hep-ph/0409146](#).
- [51] S. Frixione, P. Nason, and C. Oleari, *Matching NLO QCD computations with parton shower simulations: the POWHEG method*, [JHEP **11** \(2007\) 070](#), arXiv: [0709.2092 \[hep-ph\]](#).

- [52] S. Alioli, P. Nason, C. Oleari, and E. Re, *A general framework for implementing NLO calculations in shower Monte Carlo programs: the POWHEG BOX*, *JHEP* **06** (2010) 043, arXiv: [1002.2581 \[hep-ph\]](#).
- [53] H. B. Hartanto, B. Jäger, L. Reina, and D. Wackerroth, *Higgs boson production in association with top quarks in the POWHEG BOX*, *Phys. Rev. D* **91** (2015) 094003, arXiv: [1501.04498 \[hep-ph\]](#).
- [54] M. Beneke, P. Falgari, S. Klein, and C. Schwinn, *Hadronic top-quark pair production with NNLL threshold resummation*, *Nucl. Phys. B* **855** (2012) 695, arXiv: [1109.1536 \[hep-ph\]](#).
- [55] M. Cacciari, M. Czakon, M. Mangano, A. Mitov, and P. Nason, *Top-pair production at hadron colliders with next-to-next-to-leading logarithmic soft-gluon resummation*, *Phys. Lett. B* **710** (2012) 612, arXiv: [1111.5869 \[hep-ph\]](#).
- [56] P. Bärnreuther, M. Czakon, and A. Mitov, *Percent-Level-Precision Physics at the Tevatron: Next-to-Next-to-Leading Order QCD Corrections to $q\bar{q} \rightarrow t\bar{t} + X$* , *Phys. Rev. Lett.* **109** (2012) 132001, arXiv: [1204.5201 \[hep-ph\]](#).
- [57] M. Czakon and A. Mitov, *NNLO corrections to top-pair production at hadron colliders: the all-fermionic scattering channels*, *JHEP* **12** (2012) 054, arXiv: [1207.0236 \[hep-ph\]](#).
- [58] M. Czakon and A. Mitov, *NNLO corrections to top pair production at hadron colliders: the quark-gluon reaction*, *JHEP* **01** (2013) 080, arXiv: [1210.6832 \[hep-ph\]](#).
- [59] M. Czakon, P. Fiedler, and A. Mitov, *Total Top-Quark Pair-Production Cross Section at Hadron Colliders Through $O(\alpha_S^4)$* , *Phys. Rev. Lett.* **110** (2013) 252004, arXiv: [1303.6254 \[hep-ph\]](#).
- [60] M. Czakon and A. Mitov, *Top++: A program for the calculation of the top-pair cross-section at hadron colliders*, *Comput. Phys. Commun.* **185** (2014) 2930, arXiv: [1112.5675 \[hep-ph\]](#).
- [61] ATLAS Collaboration, *Studies on top-quark Monte Carlo modelling for Top2016*, ATL-PHYS-PUB-2016-020, 2016, URL: <https://cds.cern.ch/record/2216168>.
- [62] S. Frixione, E. Laenen, P. Motylinski, C. White, and B. R. Webber, *Single-top hadroproduction in association with a W boson*, *JHEP* **07** (2008) 029, arXiv: [0805.3067 \[hep-ph\]](#).
- [63] N. Kidonakis, *Two-loop soft anomalous dimensions for single top quark associated production with a W^- or H^-* , *Phys. Rev. D* **82** (2010) 054018, arXiv: [1005.4451 \[hep-ph\]](#).
- [64] M. Aliev et al., *HATHOR – HAdronic Top and Heavy quarks crOss section calculator*, *Comput. Phys. Commun.* **182** (2011) 1034, arXiv: [1007.1327 \[hep-ph\]](#).
- [65] P. Kant et al., *HatHor for single top-quark production: Updated predictions and uncertainty estimates for single top-quark production in hadronic collisions*, *Comput. Phys. Commun.* **191** (2015) 74, arXiv: [1406.4403 \[hep-ph\]](#).
- [66] ATLAS Collaboration, *Measurement of the Z/γ^* boson transverse momentum distribution in pp collisions at $\sqrt{s} = 7$ TeV with the ATLAS detector*, *JHEP* **09** (2014) 145, arXiv: [1406.3660 \[hep-ex\]](#).

- [67] ATLAS Collaboration, *Vertex Reconstruction Performance of the ATLAS Detector at $\sqrt{s} = 13$ TeV*, ATL-PHYS-PUB-2015-026, 2015, URL: <https://cds.cern.ch/record/2037717>.
- [68] ATLAS Collaboration, *Electron and photon performance measurements with the ATLAS detector using the 2015–2017 LHC proton–proton collision data*, *JINST* **14** (2019) P12006, arXiv: [1908.00005](https://arxiv.org/abs/1908.00005) [hep-ex].
- [69] ATLAS Collaboration, *Muon reconstruction and identification efficiency in ATLAS using the full Run 2 pp collision data set at $\sqrt{s} = 13$ TeV*, *Eur. Phys. J. C* **81** (2021) 578, arXiv: [2012.00578](https://arxiv.org/abs/2012.00578) [hep-ex].
- [70] ATLAS Collaboration, *Tools for estimating fake/non-prompt lepton backgrounds with the ATLAS detector at the LHC*, *JINST* **18** (2023) T11004, arXiv: [2211.16178](https://arxiv.org/abs/2211.16178) [hep-ex].
- [71] ATLAS Collaboration, *Evidence for the associated production of the Higgs boson and a top quark pair with the ATLAS detector*, *Phys. Rev. D* **97** (2018) 072003, arXiv: [1712.08891](https://arxiv.org/abs/1712.08891) [hep-ex].
- [72] ATLAS Collaboration, *Jet reconstruction and performance using particle flow with the ATLAS Detector*, *Eur. Phys. J. C* **77** (2017) 466, arXiv: [1703.10485](https://arxiv.org/abs/1703.10485) [hep-ex].
- [73] M. Cacciari, G. P. Salam, and G. Soyez, *The anti- k_t jet clustering algorithm*, *JHEP* **04** (2008) 063, arXiv: [0802.1189](https://arxiv.org/abs/0802.1189) [hep-ph].
- [74] M. Cacciari, G. P. Salam, and G. Soyez, *FastJet user Manual*, *Eur. Phys. J. C* **72** (2012) 1896, arXiv: [1111.6097](https://arxiv.org/abs/1111.6097) [hep-ph].
- [75] ATLAS Collaboration, *Jet energy scale and resolution measured in proton–proton collisions at $\sqrt{s} = 13$ TeV with the ATLAS detector*, *Eur. Phys. J. C* **81** (2021) 689, arXiv: [2007.02645](https://arxiv.org/abs/2007.02645) [hep-ex].
- [76] ATLAS Collaboration, *The performance of missing transverse momentum reconstruction and its significance with the ATLAS detector using 140fb^{-1} of $\sqrt{s} = 13$ TeV pp collisions*, (2024), arXiv: [2402.05858](https://arxiv.org/abs/2402.05858) [hep-ex].
- [77] ATLAS Collaboration, *ATLAS flavour-tagging algorithms for the LHC Run 2 pp collision dataset*, *Eur. Phys. J. C* **83** (2023) 681, arXiv: [2211.16345](https://arxiv.org/abs/2211.16345) [physics.data-an].
- [78] F. Chollet et al., *Keras*, 2015, URL: <https://keras.io>.
- [79] *TensorFlow: Large-Scale Machine Learning on Heterogeneous Systems*, Software available from tensorflow.org, 2015, URL: <https://www.tensorflow.org/>.
- [80] D. P. Kingma and J. Ba, *Adam: A Method for Stochastic Optimization*, 2017, arXiv: [1412.6980](https://arxiv.org/abs/1412.6980) [cs.LG].
- [81] ATLAS Collaboration, *Measurement of the total and differential cross-sections of $t\bar{t}W$ production in pp collisions at $\sqrt{s} = 13$ TeV with the ATLAS detector*, *JHEP* **05** (2024) 131, arXiv: [2401.05299](https://arxiv.org/abs/2401.05299) [hep-ex].
- [82] G. Avoni et al., *The new LUCID-2 detector for luminosity measurement and monitoring in ATLAS*, *JINST* **13** (2018) P07017.
- [83] ATLAS Collaboration, *Measurement of the Inelastic Proton–Proton Cross Section at $\sqrt{s} = 13$ TeV with the ATLAS Detector at the LHC*, *Phys. Rev. Lett.* **117** (2016) 182002, arXiv: [1606.02625](https://arxiv.org/abs/1606.02625) [hep-ex].

- [84] ATLAS Collaboration, *Electron and photon efficiencies in LHC Run 2 with the ATLAS experiment*, *JHEP* **05** (2023) 162, arXiv: [2308.13362 \[hep-ex\]](#).
- [85] ATLAS Collaboration, *Studies of the muon momentum calibration and performance of the ATLAS detector with pp collisions at $\sqrt{s} = 13$ TeV*, *Eur. Phys. J. C* **83** (2023) 686, arXiv: [2212.07338 \[hep-ex\]](#).
- [86] ATLAS Collaboration, *Performance of pile-up mitigation techniques for jets in pp collisions at $\sqrt{s} = 8$ TeV using the ATLAS detector*, *Eur. Phys. J. C* **76** (2016) 581, arXiv: [1510.03823 \[hep-ex\]](#).
- [87] ATLAS Collaboration, *ATLAS b -jet identification performance and efficiency measurement with $t\bar{t}$ events in pp collisions at $\sqrt{s} = 13$ TeV*, *Eur. Phys. J. C* **79** (2019) 970, arXiv: [1907.05120 \[hep-ex\]](#).
- [88] ATLAS Collaboration, *Measurement of the c -jet mistagging efficiency in $t\bar{t}$ events using pp collision data at $\sqrt{s} = 13$ TeV collected with the ATLAS detector*, *Eur. Phys. J. C* **82** (2022) 95, arXiv: [2109.10627 \[hep-ex\]](#).
- [89] ATLAS Collaboration, *Calibration of the light-flavour jet mistagging efficiency of the b -tagging algorithms with Z +jets events using 139fb^{-1} of ATLAS proton–proton collision data at $\sqrt{s} = 13$ TeV*, *Eur. Phys. J. C* **83** (2023) 728, arXiv: [2301.06319 \[hep-ex\]](#).
- [90] M. K. F. Febres Cordero and L. Reina, *Top-quark pair production in association with a W^\pm gauge boson in the POWHEG-BOX*, *Phys. Rev. D* **103** (2021) 094014, arXiv: [2101.11808 \[hep-ph\]](#).
- [91] R. Frederix, D. Pagani, and M. Zaro, *Large NLO corrections in $t\bar{t}W^\pm$ and $t\bar{t}t\bar{t}$ hadroproduction from supposedly subleading EW contributions*, *JHEP* **02** (2018) 031, arXiv: [1711.02116 \[hep-ph\]](#).
- [92] ATLAS Collaboration, *Observation of the associated production of a top quark and a Z boson in pp collisions at $\sqrt{s} = 13$ TeV with the ATLAS detector*, *JHEP* **07** (2020) 124, arXiv: [2002.07546 \[hep-ex\]](#).
- [93] ATLAS Collaboration, *Evidence for $t\bar{t}t\bar{t}$ production in the multilepton final state in proton–proton collisions at $\sqrt{s} = 13\text{TeV}$ with the ATLAS detector*, *Eur. Phys. J. C* **80** (2020) 1085, arXiv: [2007.14858 \[hep-ex\]](#).
- [94] S. Dulat et al., *New parton distribution functions from a global analysis of quantum chromodynamics*, *Phys. Rev. D* **93** (2016) 033006, arXiv: [1506.07443 \[hep-ph\]](#).
- [95] W. Verkerke and D. Kirkby, *The RooFit toolkit for data modeling*, 2003, arXiv: [physics/0306116 \[physics.data-an\]](#).
- [96] K. Cranmer, G. Lewis, L. Moneta, A. Shibata, and W. Verkerke, *HistFactory: A tool for creating statistical models for use with RooFit and RooStats*, *CERN-OPEN-2012-016* (2012).
- [97] G. Cowan, K. Cranmer, E. Gross, and O. Vitells, *Asymptotic formulae for likelihood-based tests of new physics*, *Eur. Phys. J. C* **71** (2011) 1554, arXiv: [1007.1727 \[physics.data-an\]](#), Erratum: *Eur. Phys. J. C* **73** (2013) 2501.

- [98] F. U. Bernlochner, D. C. Fry, S. B. Menary, and E. Persson, *Cover your bases: asymptotic distributions of the profile likelihood ratio when constraining effective field theories in high-energy physics*, *SciPost Phys. Core* **6** (2023) 013, arXiv: [2207.01350](https://arxiv.org/abs/2207.01350) [[physics.data-an](#)].
- [99] ATLAS Collaboration, *ATLAS Computing Acknowledgements*, ATL-SOFT-PUB-2023-001, 2023, URL: <https://cds.cern.ch/record/2869272>.

The ATLAS Collaboration

G. Aad ¹⁰⁵, E. Aakvaag ¹⁷, B. Abbott ¹²⁴, S. Abdelhameed ^{120a}, K. Abeling ⁵⁷, N.J. Abicht ⁵¹, S.H. Abidi ³⁰, M. Aboeela ⁴⁶, A. Aboulhorma ^{36e}, H. Abramowicz ¹⁵⁵, H. Abreu ¹⁵⁴, Y. Abulaiti ¹²¹, B.S. Acharya ^{71a,71b,k}, A. Ackermann ^{65a}, C. Adam Bourdarios ⁴, L. Adamczyk ^{88a}, S.V. Addepalli ¹⁴⁷, M.J. Addison ¹⁰⁴, J. Adelman ¹¹⁹, A. Adiguzel ^{22c}, T. Adye ¹³⁸, A.A. Affolder ¹⁴⁰, Y. Afik ⁴¹, M.N. Agaras ¹³, A. Aggarwal ¹⁰³, C. Agheorghiesei ^{28c}, F. Ahmadov ^{40,y}, S. Ahuja ⁹⁸, X. Ai ^{64e}, G. Aielli ^{78a,78b}, A. Aikot ¹⁶⁸, M. Ait Tamlihat ^{36e}, B. Aitbenkikh ^{36a}, M. Akbiyik ¹⁰³, T.P.A. Åkesson ¹⁰¹, A.V. Akimov ¹⁴⁹, D. Akiyama ¹⁷³, N.N. Akolkar ²⁵, S. Aktas ^{22a}, K. Al Houry ⁴³, G.L. Alberghi ^{24b}, J. Albert ¹⁷⁰, P. Albicocco ⁵⁵, G.L. Albouy ⁶², S. Alderweireldt ⁵⁴, Z.L. Alegria ¹²⁵, M. Aleksa ³⁷, I.N. Aleksandrov ⁴⁰, C. Alexa ^{28b}, T. Alexopoulos ¹⁰, F. Alfonsi ^{24b}, M. Algren ⁵⁸, M. Alhroob ¹⁷², B. Ali ¹³⁶, H.M.J. Ali ^{94,s}, S. Ali ³², S.W. Alibocus ⁹⁵, M. Aliev ^{34c}, G. Alimonti ^{73a}, W. Alkakh ⁵⁷, C. Allaire ⁶⁸, B.M.M. Allbrooke ¹⁵⁰, J.S. Allen ¹⁰⁴, J.F. Allen ⁵⁴, C.A. Allendes Flores ^{141f}, P.P. Allport ²¹, A. Aloisio ^{74a,74b}, F. Alonso ⁹³, C. Alpigiani ¹⁴², Z.M.K. Alsolami ⁹⁴, M. Alvarez Estevez ¹⁰², A. Alvarez Fernandez ¹⁰³, M. Alves Cardoso ⁵⁸, M.G. Alviggi ^{74a,74b}, M. Aly ¹⁰⁴, Y. Amaral Coutinho ^{85b}, A. Ambler ¹⁰⁷, C. Amelung ³⁷, M. Amerl ¹⁰⁴, C.G. Ames ¹¹², D. Amidei ¹⁰⁹, B. Amini ⁵⁶, K.J. Amirie ¹⁵⁹, S.P. Amor Dos Santos ^{134a}, K.R. Amos ¹⁶⁸, D. Amperiadou ¹⁵⁶, S. An ⁸⁶, V. Ananiev ¹²⁹, C. Anastopoulos ¹⁴³, T. Andeen ¹¹, J.K. Anders ³⁷, A.C. Anderson ⁶¹, S.Y. Andread ^{49a,49b}, A. Andreazza ^{73a,73b}, S. Angelidakis ⁹, A. Angerami ⁴³, A.V. Anisenkov ³⁹, A. Annovi ^{76a}, C. Antel ⁵⁸, E. Antipov ¹⁴⁹, M. Antonelli ⁵⁵, F. Anulli ^{77a}, M. Aoki ⁸⁶, T. Aoki ¹⁵⁷, M.A. Aparo ¹⁵⁰, L. Aperio Bella ⁵⁰, C. Appelt ¹⁵⁵, A. Apyan ²⁷, S.J. Arbiol Val ⁸⁹, C. Arcangeletti ⁵⁵, A.T.H. Arce ⁵³, J-F. Arguin ¹¹¹, S. Argyropoulos ¹⁵⁶, J.-H. Arling ⁵⁰, O. Arnaez ⁴, H. Arnold ¹⁴⁹, G. Artoni ^{77a,77b}, H. Asada ¹¹⁴, K. Asai ¹²², S. Asai ¹⁵⁷, N.A. Asbah ³⁷, R.A. Ashby Pickering ¹⁷², K. Assamagan ³⁰, R. Astalos ^{29a}, K.S.V. Astrand ¹⁰¹, S. Atashi ¹⁶³, R.J. Atkin ^{34a}, H. Atmani ^{36f}, P.A. Atlasiddha ¹³², K. Augsten ¹³⁶, A.D. Auriol ²¹, V.A. Austrup ¹⁰⁴, G. Avolio ³⁷, K. Axiotis ⁵⁸, G. Azuelos ^{111,ac}, D. Babal ^{29b}, H. Bachacou ¹³⁹, K. Bachas ^{156,o}, A. Bachi ³⁵, A. Badea ⁴¹, T.M. Baer ¹⁰⁹, P. Bagnaia ^{77a,77b}, M. Bahmani ¹⁹, D. Bahner ⁵⁶, K. Bai ¹²⁷, J.T. Baines ¹³⁸, L. Baines ⁹⁷, O.K. Baker ¹⁷⁷, E. Bakos ¹⁶, D. Bakshi Gupta ⁸, L.E. Balabram Filho ^{85b}, V. Balakrishnan ¹²⁴, R. Balasubramanian ⁴, E.M. Baldin ³⁹, P. Balek ^{88a}, E. Ballabene ^{24b,24a}, F. Balli ¹³⁹, L.M. Baltes ^{65a}, W.K. Balunas ³³, J. Balz ¹⁰³, I. Bamwidhi ^{120b}, E. Banas ⁸⁹, M. Bandieramonte ¹³³, A. Bandyopadhyay ²⁵, S. Bansal ²⁵, L. Barak ¹⁵⁵, M. Barakat ⁵⁰, E.L. Barberio ¹⁰⁸, D. Barberis ^{59b,59a}, M. Barbero ¹⁰⁵, M.Z. Barel ¹¹⁸, T. Barillari ¹¹³, M-S. Barisits ³⁷, T. Barklow ¹⁴⁷, P. Baron ¹²⁶, D.A. Baron Moreno ¹⁰⁴, A. Baroncelli ^{64a}, A.J. Barr ¹³⁰, J.D. Barr ⁹⁹, F. Barreiro ¹⁰², J. Barreiro Guimarães da Costa ¹⁴, M.G. Barros Teixeira ^{134a}, S. Barsov ³⁹, F. Bartels ^{65a}, R. Bartoldus ¹⁴⁷, A.E. Barton ⁹⁴, P. Bartos ^{29a}, A. Basan ¹⁰³, M. Baselga ⁵¹, A. Bassalat ^{68,b}, M.J. Basso ^{160a}, S. Bataju ⁴⁶, R. Bate ¹⁶⁹, R.L. Bates ⁶¹, S. Batlamous ¹⁰², B. Batool ¹⁴⁵, M. Battaglia ¹⁴⁰, D. Battulga ¹⁹, M. Bauc ^{77a,77b}, M. Bauer ⁸¹, P. Bauer ²⁵, L.T. Bazzano Hurrell ³¹, J.B. Beacham ⁵³, T. Beau ¹³¹, J.Y. Beauchamp ⁹³, P.H. Beauchemin ¹⁶², P. Bechtel ²⁵, H.P. Beck ^{20,n}, K. Becker ¹⁷², A.J. Beddall ⁸⁴, V.A. Bednyakov ⁴⁰, C.P. Bee ¹⁴⁹, L.J. Beemster ¹⁶, T.A. Beermann ³⁷, M. Begalli ^{85d}, M. Biegel ³⁰, A. Behera ¹⁴⁹, J.K. Behr ⁵⁰, J.F. Beirer ³⁷, F. Beisiegel ²⁵, M. Belfkir ^{120b}, G. Bella ¹⁵⁵, L. Bellagamba ^{24b}, A. Bellerive ³⁵, P. Bellos ²¹, K. Beloborodov ³⁹, D. Benchechroun ^{36a}, F. Bendebba ^{36a}, Y. Benhammou ¹⁵⁵, K.C. Benkendorfer ⁶³, L. Beresford ⁵⁰, M. Beretta ⁵⁵, E. Bergeas Kuutmann ¹⁶⁶, N. Berger ⁴,

B. Bergmann [id136](#), J. Beringer [id18a](#), G. Bernardi [id5](#), C. Bernius [id147](#), F.U. Bernlochner [id25](#),
 F. Bernon [id37](#), A. Berrocal Guardia [id13](#), T. Berry [id98](#), P. Berta [id137](#), A. Berthold [id52](#), S. Bethke [id113](#),
 A. Betti [id77a,77b](#), A.J. Bevan [id97](#), N.K. Bhalla [id56](#), S. Bhatta [id149](#), D.S. Bhattacharya [id171](#),
 P. Bhattarai [id147](#), Z.M. Bhatti [id121](#), K.D. Bhide [id56](#), V.S. Bhopatkar [id125](#), R.M. Bianchi [id133](#),
 G. Bianco [id24b,24a](#), O. Biebel [id112](#), M. Biglietti [id79a](#), C.S. Billingsley [id46](#), Y. Bimgdi [id36f](#), M. Bindi [id57](#),
 A. Bingul [id22b](#), C. Bini [id77a,77b](#), G.A. Bird [id33](#), M. Birman [id174](#), M. Biros [id137](#), S. Biryukov [id150](#),
 T. Bisanz [id51](#), E. Bisceglie [id45b,45a](#), J.P. Biswal [id138](#), D. Biswas [id145](#), I. Bloch [id50](#), A. Blue [id61](#),
 U. Blumenschein [id97](#), J. Blumenthal [id103](#), V.S. Bobrovnikov [id39](#), M. Boehler [id56](#), B. Boehm [id171](#),
 D. Bogavac [id37](#), A.G. Bogdanchikov [id39](#), L.S. Boggia [id131](#), C. Bohm [id49a](#), V. Boisvert [id98](#),
 P. Bokan [id37](#), T. Bold [id88a](#), M. Bomben [id5](#), M. Bona [id97](#), M. Boonekamp [id139](#), A.G. Borbély [id61](#),
 I.S. Bordulev [id39](#), G. Borissov [id94](#), D. Bortoletto [id130](#), D. Boscherini [id24b](#), M. Bosman [id13](#),
 K. Bouaouda [id36a](#), N. Bouchhar [id168](#), L. Boudet [id4](#), J. Boudreau [id133](#), E.V. Bouhova-Thacker [id94](#),
 D. Boumediene [id42](#), R. Bouquet [id59b,59a](#), A. Boveia [id123](#), J. Boyd [id37](#), D. Boye [id30](#), I.R. Boyko [id40](#),
 L. Bozianu [id58](#), J. Bracik [id21](#), N. Brahimi [id4](#), G. Brandt [id176](#), O. Brandt [id33](#), B. Brau [id106](#),
 J.E. Brau [id127](#), R. Brenner [id174](#), L. Brenner [id118](#), R. Brenner [id166](#), S. Bressler [id174](#), G. Brianti [id80a,80b](#),
 D. Britton [id61](#), D. Britzger [id113](#), I. Brock [id25](#), R. Brock [id110](#), G. Brooijmans [id43](#), A.J. Brooks [id70](#),
 E.M. Brooks [id160b](#), E. Brost [id30](#), L.M. Brown [id170](#), L.E. Bruce [id63](#), T.L. Bruckler [id130](#),
 P.A. Bruckman de Renstrom [id89](#), B. Brüers [id50](#), A. Bruni [id24b](#), G. Bruni [id24b](#), D. Brunner [id49a,49b](#),
 M. Bruschi [id24b](#), N. Bruscino [id77a,77b](#), T. Buanes [id17](#), Q. Buat [id142](#), D. Buchin [id113](#), A.G. Buckley [id61](#),
 O. Bulekov [id39](#), B.A. Bullard [id147](#), S. Burdin [id95](#), C.D. Burgard [id51](#), A.M. Burger [id37](#),
 B. Burghgrave [id8](#), O. Burlayenko [id56](#), J. Burleson [id167](#), J.T.P. Burr [id33](#), J.C. Burzynski [id146](#),
 E.L. Busch [id43](#), V. Büscher [id103](#), P.J. Bussey [id61](#), J.M. Butler [id26](#), C.M. Buttar [id61](#),
 J.M. Butterworth [id99](#), W. Buttinger [id138](#), C.J. Buxo Vazquez [id110](#), A.R. Buzykaev [id39](#),
 S. Cabrera Urbán [id168](#), L. Cadamuro [id68](#), D. Caforio [id60](#), H. Cai [id133](#), Y. Cai [id14,115c](#), Y. Cai [id115a](#),
 V.M.M. Cairo [id37](#), O. Cakir [id3a](#), N. Calace [id37](#), P. Calafiura [id18a](#), G. Calderini [id131](#), P. Calfayan [id35](#),
 G. Callea [id61](#), L.P. Caloba [id85b](#), D. Calvet [id42](#), S. Calvet [id42](#), R. Camacho Toro [id131](#), S. Camarda [id37](#),
 D. Camarero Munoz [id27](#), P. Camarri [id78a,78b](#), M.T. Camerlingo [id74a,74b](#), D. Cameron [id37](#),
 C. Camincher [id170](#), M. Campanelli [id99](#), A. Camplani [id44](#), V. Canale [id74a,74b](#), A.C. Canbay [id3a](#),
 E. Canonero [id98](#), J. Cantero [id168](#), Y. Cao [id167](#), F. Capocasa [id27](#), M. Capua [id45b,45a](#), A. Carbone [id73a,73b](#),
 R. Cardarelli [id78a](#), J.C.J. Cardenas [id8](#), M.P. Cardiff [id27](#), G. Carducci [id45b,45a](#), T. Carli [id37](#),
 G. Carlino [id74a](#), J.I. Carlotto [id13](#), B.T. Carlson [id133,p](#), E.M. Carlson [id170,160a](#), J. Carmignani [id95](#),
 L. Carminati [id73a,73b](#), A. Carnelli [id139](#), M. Carnesale [id37](#), S. Caron [id117](#), E. Carquin [id141f](#),
 I.B. Carr [id108](#), S. Carrá [id73a](#), G. Carratta [id24b,24a](#), A.M. Carroll [id127](#), M.P. Casado [id13,h](#), M. Caspar [id50](#),
 F.L. Castillo [id4](#), L. Castillo Garcia [id13](#), V. Castillo Gimenez [id168](#), N.F. Castro [id134a,134e](#),
 A. Catinaccio [id37](#), J.R. Catmore [id129](#), T. Cavaliere [id4](#), V. Cavaliere [id30](#), N. Cavalli [id24a](#),
 L.J. Caviedes Betancourt [id23b](#), Y.C. Cekmecelioglu [id50](#), E. Celebi [id84](#), S. Cella [id37](#), V. Cepaitis [id58](#),
 K. Cerny [id126](#), A.S. Cerqueira [id85a](#), A. Cerri [id150](#), L. Cerrito [id78a,78b](#), F. Cerutti [id18a](#), B. Cervato [id145](#),
 A. Cervelli [id24b](#), G. Cesarini [id55](#), S.A. Cetin [id84](#), P.M. Chabrilat [id131](#), D. Chakraborty [id119](#),
 J. Chan [id18a](#), W.Y. Chan [id157](#), J.D. Chapman [id33](#), E. Chapon [id139](#), B. Chargeishvili [id153b](#),
 D.G. Charlton [id21](#), M. Chatterjee [id20](#), C. Chauhan [id137](#), Y. Che [id115a](#), S. Chekanov [id6](#),
 S.V. Chekulaev [id160a](#), G.A. Chelkov [id40,a](#), A. Chen [id109](#), B. Chen [id155](#), B. Chen [id170](#), H. Chen [id115a](#),
 H. Chen [id30](#), J. Chen [id64c](#), J. Chen [id146](#), M. Chen [id130](#), S. Chen [id90](#), S.J. Chen [id115a](#), X. Chen [id64c](#),
 X. Chen [id15,ab](#), Y. Chen [id64a](#), C.L. Cheng [id175](#), H.C. Cheng [id66a](#), S. Cheong [id147](#), A. Cheplakov [id40](#),
 E. Cheremushkina [id50](#), E. Cherepanova [id118](#), R. Cherkaoui El Moursli [id36e](#), E. Cheu [id7](#), K. Cheung [id67](#),
 L. Chevalier [id139](#), V. Chiarella [id55](#), G. Chiarelli [id76a](#), N. Chiedde [id105](#), G. Chiodini [id72a](#),
 A.S. Chisholm [id21](#), A. Chitan [id28b](#), M. Chitishvili [id168](#), M.V. Chizhov [id40,q](#), K. Choi [id11](#), Y. Chou [id142](#),
 E.Y.S. Chow [id117](#), K.L. Chu [id174](#), M.C. Chu [id66a](#), X. Chu [id14,115c](#), Z. Chubinidze [id55](#), J. Chudoba [id135](#),

J.J. Chwastowski [ID89](#), D. Cieri [ID113](#), K.M. Ciesla [ID88a](#), V. Cindro [ID96](#), A. Ciocio [ID18a](#), F. Cirotto [ID74a,74b](#), Z.H. Citron [ID174](#), M. Citterio [ID73a](#), D.A. Ciubotaru^{28b}, A. Clark [ID58](#), P.J. Clark [ID54](#), N. Clarke Hall [ID99](#), C. Clarry [ID159](#), J.M. Clavijo Columbie [ID50](#), S.E. Clawson [ID50](#), C. Clement [ID49a,49b](#), Y. Coadou [ID105](#), M. Cobal [ID71a,71c](#), A. Coccaro [ID59b](#), R.F. Coelho Barrue [ID134a](#), R. Coelho Lopes De Sa [ID106](#), S. Coelli [ID73a](#), L.S. Colangeli [ID159](#), B. Cole [ID43](#), J. Collot [ID62](#), P. Conde Muiño [ID134a,134g](#), M.P. Connell [ID34c](#), S.H. Connell [ID34c](#), E.I. Conroy [ID130](#), F. Conventi [ID74a,ad](#), H.G. Cooke [ID21](#), A.M. Cooper-Sarkar [ID130](#), F.A. Corchia [ID24b,24a](#), A. Cordeiro Oudot Choi [ID131](#), L.D. Corpe [ID42](#), M. Corradi [ID77a,77b](#), F. Corriveau [ID107,x](#), A. Cortes-Gonzalez [ID19](#), M.J. Costa [ID168](#), F. Costanza [ID4](#), D. Costanzo [ID143](#), B.M. Cote [ID123](#), J. Couthures [ID4](#), G. Cowan [ID98](#), K. Cranmer [ID175](#), L. Cremer [ID51](#), D. Cremonini [ID24b,24a](#), S. Crépe-Renaudin [ID62](#), F. Crescioli [ID131](#), M. Cristinziani [ID145](#), M. Cristoforetti [ID80a,80b](#), V. Croft [ID118](#), J.E. Crosby [ID125](#), G. Crosetti [ID45b,45a](#), A. Cueto [ID102](#), H. Cui [ID99](#), Z. Cui [ID7](#), W.R. Cunningham [ID61](#), F. Curcio [ID168](#), J.R. Curran [ID54](#), P. Czodrowski [ID37](#), M.J. Da Cunha Sargedas De Sousa [ID59b,59a](#), J.V. Da Fonseca Pinto [ID85b](#), C. Da Via [ID104](#), W. Dabrowski [ID88a](#), T. Dado [ID37](#), S. Dahbi [ID152](#), T. Dai [ID109](#), D. Dal Santo [ID20](#), C. Dallapiccola [ID106](#), M. Dam [ID44](#), G. D'amen [ID30](#), V. D'Amico [ID112](#), J. Damp [ID103](#), J.R. Dandoy [ID35](#), D. Dannheim [ID37](#), M. Danninger [ID146](#), V. Dao [ID149](#), G. Darbo [ID59b](#), S.J. Das [ID30](#), F. Dattola [ID50](#), S. D'Auria [ID73a,73b](#), A. D'Avanzo [ID74a,74b](#), C. David [ID34a](#), T. Davidek [ID137](#), I. Dawson [ID97](#), H.A. Day-hall [ID136](#), K. De [ID8](#), C. De Almeida Rossi [ID159](#), R. De Asmundis [ID74a](#), N. De Biase [ID50](#), S. De Castro [ID24b,24a](#), N. De Groot [ID117](#), P. de Jong [ID118](#), H. De la Torre [ID119](#), A. De Maria [ID115a](#), A. De Salvo [ID77a](#), U. De Sanctis [ID78a,78b](#), F. De Santis [ID72a,72b](#), A. De Santo [ID150](#), J.B. De Vivie De Regie [ID62](#), J. Debec [ID96](#), D.V. Dedovich⁴⁰, J. Degens [ID95](#), A.M. Deiana [ID46](#), F. Del Corso [ID24b,24a](#), J. Del Peso [ID102](#), L. Delagrangé [ID131](#), F. Deliot [ID139](#), C.M. Delitzsch [ID51](#), M. Della Pietra [ID74a,74b](#), D. Della Volpe [ID58](#), A. Dell'Acqua [ID37](#), L. Dell'Asta [ID73a,73b](#), M. Delmastro [ID4](#), C.C. Delogu [ID103](#), P.A. Delsart [ID62](#), S. Demers [ID177](#), M. Demichev [ID40](#), S.P. Denisov [ID39](#), L. D'Eramo [ID42](#), D. Derendarz [ID89](#), F. Derue [ID131](#), P. Dervan [ID95](#), K. Desch [ID25](#), C. Deutsch [ID25](#), F.A. Di Bello [ID59b,59a](#), A. Di Ciaccio [ID78a,78b](#), L. Di Ciaccio [ID4](#), A. Di Domenico [ID77a,77b](#), C. Di Donato [ID74a,74b](#), A. Di Girolamo [ID37](#), G. Di Gregorio [ID37](#), A. Di Luca [ID80a,80b](#), B. Di Micco [ID79a,79b](#), R. Di Nardo [ID79a,79b](#), K.F. Di Petrillo [ID41](#), M. Diamantopoulou [ID35](#), F.A. Dias [ID118](#), T. Dias Do Vale [ID146](#), M.A. Diaz [ID141a,141b](#), A.R. Didenko⁴⁰, M. Didenko [ID168](#), E.B. Diehl [ID109](#), S. Díez Cornell [ID50](#), C. Díez Pardos [ID145](#), C. Dimitriadi [ID166](#), A. Dimitrievska [ID21](#), J. Dingfelder [ID25](#), T. Dingley [ID130](#), I-M. Dinu [ID28b](#), S.J. Dittmeier [ID65b](#), F. Dittus [ID37](#), M. Divisek [ID137](#), B. Dixit [ID95](#), F. Djama [ID105](#), T. Djobava [ID153b](#), C. Doglioni [ID104,101](#), A. Dohnalova [ID29a](#), Z. Dolezal [ID137](#), K. Domijan [ID88a](#), K.M. Dona [ID41](#), M. Donadelli [ID85d](#), B. Dong [ID110](#), J. Donini [ID42](#), A. D'Onofrio [ID74a,74b](#), M. D'Onofrio [ID95](#), J. Dopke [ID138](#), A. Doria [ID74a](#), N. Dos Santos Fernandes [ID134a](#), P. Dougan [ID104](#), M.T. Dova [ID93](#), A.T. Doyle [ID61](#), M.A. Draguet [ID130](#), M.P. Drescher [ID57](#), E. Dreyer [ID174](#), I. Drivas-koulouris [ID10](#), M. Drnevich [ID121](#), M. Drozdova [ID58](#), D. Du [ID64a](#), T.A. du Pree [ID118](#), F. Dubinin [ID39](#), M. Dubovsky [ID29a](#), E. Duchovni [ID174](#), G. Duckeck [ID112](#), O.A. Ducu [ID28b](#), D. Duda [ID54](#), A. Dudarev [ID37](#), E.R. Duden [ID27](#), M. D'uffizi [ID104](#), L. Duflot [ID68](#), M. Dührssen [ID37](#), I. Duminica [ID28g](#), A.E. Dumitriu [ID28b](#), M. Dunford [ID65a](#), S. Dungs [ID51](#), K. Dunne [ID49a,49b](#), A. Duperrin [ID105](#), H. Duran Yildiz [ID3a](#), M. Düren [ID60](#), A. Durglishvili [ID153b](#), B.L. Dwyer [ID119](#), G.I. Dyckes [ID18a](#), M. Dyndal [ID88a](#), B.S. Dziedzic [ID37](#), Z.O. Earnshaw [ID150](#), G.H. Eberwein [ID130](#), B. Eckerova [ID29a](#), S. Eggebrecht [ID57](#), E. Egidio Purcino De Souza [ID85e](#), L.F. Ehrke [ID58](#), G. Eigen [ID17](#), K. Einsweiler [ID18a](#), T. Ekelof [ID166](#), P.A. Ekman [ID101](#), S. El Farkh [ID36b](#), Y. El Ghazali [ID64a](#), H. El Jarrari [ID37](#), A. El Moussaouy [ID36a](#), V. Ellajosyula [ID166](#), M. Ellert [ID166](#), F. Ellinghaus [ID176](#), N. Ellis [ID37](#), J. Elmsheuser [ID30](#), M. Elsayy [ID120a](#), M. Elsing [ID37](#), D. Emelianov [ID138](#), Y. Enari [ID86](#), I. Ene [ID18a](#), S. Epari [ID13](#), P.A. Erland [ID89](#), D. Ernani Martins Neto [ID89](#), M. Errenst [ID176](#), M. Escalier [ID68](#), C. Escobar [ID168](#), E. Etzion [ID155](#), G. Evans [ID134a](#), H. Evans [ID70](#), L.S. Evans [ID98](#), A. Ezhilov [ID39](#), S. Ezzarqtouni [ID36a](#), F. Fabbri [ID24b,24a](#),

L. Fabbri ^{24b,24a}, G. Facini ⁹⁹, V. Fadeyev ¹⁴⁰, R.M. Fakhruddinov ³⁹, D. Fakoudis ¹⁰³,
 S. Falciano ^{77a}, L.F. Falda Ulhoa Coelho ^{134a}, F. Fallavollita ¹¹³, G. Falsetti ^{45b,45a}, J. Faltova ¹³⁷,
 C. Fan ¹⁶⁷, K.Y. Fan ^{66b}, Y. Fan ¹⁴, Y. Fang ^{14,115c}, M. Fanti ^{73a,73b}, M. Faraj ^{71a,71b},
 Z. Farazpay ¹⁰⁰, A. Farbin ⁸, A. Farilla ^{79a}, T. Farooque ¹¹⁰, J.N. Farr ¹⁷⁷,
 S.M. Farrington ^{138,54}, F. Fassi ^{36e}, D. Fassouliotis ⁹, M. Faucci Giannelli ^{78a,78b}, W.J. Fawcett ³³,
 L. Fayard ⁶⁸, P. Federic ¹³⁷, P. Federicova ¹³⁵, O.L. Fedin ^{39,a}, M. Feickert ¹⁷⁵, L. Feligioni ¹⁰⁵,
 D.E. Fellers ¹²⁷, C. Feng ^{64b}, Z. Feng ¹¹⁸, M.J. Fenton ¹⁶³, L. Ferencz ⁵⁰, R.A.M. Ferguson ⁹⁴,
 P. Fernandez Martinez ¹³, M.J.V. Fernoux ¹⁰⁵, J. Ferrando ⁹⁴, A. Ferrari ¹⁶⁶, P. Ferrari ^{118,117},
 R. Ferrari ^{75a}, D. Ferrere ⁵⁸, C. Ferretti ¹⁰⁹, M.P. Fewell ¹, D. Fiacco ^{77a,77b}, F. Fiedler ¹⁰³,
 P. Fiedler ¹³⁶, S. Filimonov ³⁹, A. Filipčič ⁹⁶, E.K. Filmer ^{160a}, F. Filthaut ¹¹⁷,
 M.C.N. Fiolhais ^{134a,134c,c}, L. Fiorini ¹⁶⁸, W.C. Fisher ¹¹⁰, T. Fitschen ¹⁰⁴, P.M. Fitzhugh ¹³⁹,
 I. Fleck ¹⁴⁵, P. Fleischmann ¹⁰⁹, T. Flick ¹⁷⁶, M. Flores ^{34d,z}, L.R. Flores Castillo ^{66a},
 L. Flores Sanz De Acedo ³⁷, F.M. Follega ^{80a,80b}, N. Fomin ³³, J.H. Foo ¹⁵⁹, A. Formica ¹³⁹,
 A.C. Forti ¹⁰⁴, E. Fortin ³⁷, A.W. Fortman ^{18a}, M.G. Foti ^{18a}, L. Fountas ^{9,i}, D. Fournier ⁶⁸,
 H. Fox ⁹⁴, P. Francavilla ^{76a,76b}, S. Francescato ⁶³, S. Franchellucci ⁵⁸, M. Franchini ^{24b,24a},
 S. Franchino ^{65a}, D. Francis ³⁷, L. Franco ¹¹⁷, V. Franco Lima ³⁷, L. Franconi ⁵⁰, M. Franklin ⁶³,
 G. Frattari ²⁷, Y.Y. Frid ¹⁵⁵, J. Friend ⁶¹, N. Fritzsche ³⁷, A. Froch ⁵⁸, D. Froidevaux ³⁷,
 J.A. Frost ¹³⁰, Y. Fu ^{64a}, S. Fuenzalida Garrido ^{141f}, M. Fujimoto ¹⁰⁵, K.Y. Fung ^{66a},
 E. Furtado De Simas Filho ^{85e}, M. Furukawa ¹⁵⁷, J. Fuster ¹⁶⁸, A. Gaa ⁵⁷, A. Gabrielli ^{24b,24a},
 A. Gabrielli ¹⁵⁹, P. Gadow ³⁷, G. Gagliardi ^{59b,59a}, L.G. Gagnon ^{18a}, S. Gaid ¹⁶⁵,
 S. Galantzan ¹⁵⁵, J. Gallagher ¹, E.J. Gallas ¹³⁰, A.L. Gallen ¹⁶⁶, B.J. Gallop ¹³⁸, K.K. Gan ¹²³,
 S. Ganguly ¹⁵⁷, Y. Gao ⁵⁴, F.M. Garay Walls ^{141a,141b}, B. Garcia ³⁰, C. García ¹⁶⁸,
 A. Garcia Alonso ¹¹⁸, A.G. Garcia Caffaro ¹⁷⁷, J.E. García Navarro ¹⁶⁸, M. Garcia-Sciveres ^{18a},
 G.L. Gardner ¹³², R.W. Gardner ⁴¹, N. Garelli ¹⁶², R.B. Garg ¹⁴⁷, J.M. Gargan ⁵⁴, C.A. Garner ¹⁵⁹,
 C.M. Garvey ^{34a}, V.K. Gassmann ¹⁶², G. Gaudio ^{75a}, V. Gautam ¹³, P. Gauzzi ^{77a,77b},
 J. Gavranovic ⁹⁶, I.L. Gavrilenko ³⁹, A. Gavriluk ³⁹, C. Gay ¹⁶⁹, G. Gaycken ¹²⁷,
 E.N. Gazis ¹⁰, A.A. Geanta ^{28b}, A. Gekow ¹²³, C. Gemme ^{59b}, M.H. Genest ⁶², A.D. Gentry ¹¹⁶,
 S. George ⁹⁸, W.F. George ²¹, T. Gerialis ⁴⁸, A.A. Gerwin ¹²⁴, P. Gessinger-Befurt ³⁷,
 M.E. Geyik ¹⁷⁶, M. Ghani ¹⁷², K. Ghorbanian ⁹⁷, A. Ghosal ¹⁴⁵, A. Ghosh ¹⁶³, A. Ghosh ⁷,
 B. Giacobbe ^{24b}, S. Giagu ^{77a,77b}, T. Giani ¹¹⁸, A. Giannini ^{64a}, S.M. Gibson ⁹⁸, M. Gignac ¹⁴⁰,
 D.T. Gil ^{88b}, A.K. Gilbert ^{88a}, B.J. Gilbert ⁴³, D. Gillberg ³⁵, G. Gilles ¹¹⁸, L. Ginabat ¹³¹,
 D.M. Gingrich ^{2,ac}, M.P. Giordani ^{71a,71c}, P.F. Giraud ¹³⁹, G. Giugliarelli ^{71a,71c}, D. Giugni ^{73a},
 F. Giuli ^{78a,78b}, I. Kialas ^{9,i}, L.K. Gladilin ³⁹, C. Glasman ¹⁰², G.R. Gledhill ¹²⁷, G. Glemža ⁵⁰,
 M. Glisic ¹²⁷, I. Gnesi ^{45b}, Y. Go ³⁰, M. Goblirsch-Kolb ³⁷, B. Gocke ⁵¹, D. Godin ¹¹¹,
 B. Gokturk ^{22a}, S. Goldfarb ¹⁰⁸, T. Golling ⁵⁸, M.G.D. Gololo ^{34g}, D. Golubkov ³⁹,
 J.P. Gombas ¹¹⁰, A. Gomes ^{134a,134b}, G. Gomes Da Silva ¹⁴⁵, A.J. Gomez Delegido ¹⁶⁸,
 R. Gonçalves ^{134a}, L. Gonella ²¹, A. Gongadze ^{153c}, F. Gonnella ²¹, J.L. Gonski ¹⁴⁷,
 R.Y. González Andana ⁵⁴, S. González de la Hoz ¹⁶⁸, R. Gonzalez Lopez ⁹⁵,
 C. Gonzalez Renteria ^{18a}, M.V. Gonzalez Rodrigues ⁵⁰, R. Gonzalez Suarez ¹⁶⁶,
 S. Gonzalez-Sevilla ⁵⁸, L. Goossens ³⁷, B. Gorini ³⁷, E. Gorini ^{72a,72b}, A. Gorišek ⁹⁶,
 T.C. Gosart ¹³², A.T. Goshaw ⁵³, M.I. Gostkin ⁴⁰, S. Goswami ¹²⁵, C.A. Gottardo ³⁷,
 S.A. Gotz ¹¹², M. Gouighri ^{36b}, V. Goumarre ⁵⁰, A.G. Goussiou ¹⁴², N. Govender ^{34c},
 R.P. Grabarczyk ¹³⁰, I. Grabowska-Bold ^{88a}, K. Graham ³⁵, E. Gramstad ¹²⁹,
 S. Grancagnolo ^{72a,72b}, C.M. Grant ^{1,139}, P.M. Gravila ^{28f}, F.G. Gravili ^{72a,72b}, H.M. Gray ^{18a},
 M. Greco ^{72a,72b}, M.J. Green ¹, C. Grefe ²⁵, A.S. Grefsrud ¹⁷, I.M. Gregor ⁵⁰, K.T. Greif ¹⁶³,
 P. Grenier ¹⁴⁷, S.G. Grewe ¹¹³, A.A. Grillo ¹⁴⁰, K. Grimm ³², S. Grinstein ^{13,t}, J.-F. Grivaz ⁶⁸,
 E. Gross ¹⁷⁴, J. Grosse-Knetter ⁵⁷, L. Guan ¹⁰⁹, J.G.R. Guerrero Rojas ¹⁶⁸, G. Guerrieri ³⁷,

R. Gugel ¹⁰³, J.A.M. Guhit ¹⁰⁹, A. Guida ¹⁹, E. Guilloton ¹⁷², S. Guindon ³⁷, F. Guo ^{14,115c}, J. Guo ^{64c}, L. Guo ⁵⁰, L. Guo ¹⁴, Y. Guo ¹⁰⁹, A. Gupta ⁵¹, R. Gupta ¹³³, S. Gurbuz ²⁵, S.S. Gurdasani ⁵⁶, G. Gustavino ^{77a,77b}, P. Gutierrez ¹²⁴, L.F. Gutierrez Zagazeta ¹³², M. Gutsche ⁵², C. Gutschow ⁹⁹, C. Gwenlan ¹³⁰, C.B. Gwilliam ⁹⁵, E.S. Haaland ¹²⁹, A. Haas ¹²¹, M. Habedank ⁶¹, C. Haber ^{18a}, H.K. Hadavand ⁸, A. Hadeef ⁵², A.I. Hagan ⁹⁴, J.J. Hahn ¹⁴⁵, E.H. Haines ⁹⁹, M. Haleem ¹⁷¹, J. Haley ¹²⁵, G.D. Hallowell ¹⁰⁵, L. Halser ²⁰, K. Hamano ¹⁷⁰, M. Hamer ²⁵, E.J. Hampshire ⁹⁸, J. Han ^{64b}, L. Han ^{115a}, L. Han ^{64a}, S. Han ^{18a}, Y.F. Han ¹⁵⁹, K. Hanagaki ⁸⁶, M. Hance ¹⁴⁰, D.A. Hangal ⁴³, H. Hanif ¹⁴⁶, M.D. Hank ¹³², J.B. Hansen ⁴⁴, P.H. Hansen ⁴⁴, D. Harada ⁵⁸, T. Harenberg ¹⁷⁶, S. Harkusha ¹⁷⁸, M.L. Harris ¹⁰⁶, Y.T. Harris ²⁵, J. Harrison ¹³, N.M. Harrison ¹²³, P.F. Harrison ¹⁷², N.M. Hartman ¹¹³, N.M. Hartmann ¹¹², R.Z. Hasan ^{98,138}, Y. Hasegawa ¹⁴⁴, F. Haslbeck ¹³⁰, S. Hassan ¹⁷, R. Hauser ¹¹⁰, C.M. Hawkes ²¹, R.J. Hawkins ³⁷, Y. Hayashi ¹⁵⁷, D. Hayden ¹¹⁰, C. Hayes ¹⁰⁹, R.L. Hayes ¹¹⁸, C.P. Hays ¹³⁰, J.M. Hays ⁹⁷, H.S. Hayward ⁹⁵, F. He ^{64a}, M. He ^{14,115c}, Y. He ⁵⁰, Y. He ⁹⁹, N.B. Heatley ⁹⁷, V. Hedberg ¹⁰¹, A.L. Heggelund ¹²⁹, N.D. Hehir ^{97,*}, C. Heidegger ⁵⁶, K.K. Heidegger ⁵⁶, J. Heilman ³⁵, S. Heim ⁵⁰, T. Heim ^{18a}, J.G. Heinlein ¹³², J.J. Heinrich ¹²⁷, L. Heinrich ^{113,aa}, J. Hejbal ¹³⁵, A. Held ¹⁷⁵, S. Hellesund ¹⁷, C.M. Helling ¹⁶⁹, S. Hellman ^{49a,49b}, R.C.W. Henderson ⁹⁴, L. Henkelmann ³³, A.M. Henriques Correia ³⁷, H. Herde ¹⁰¹, Y. Hernández Jiménez ¹⁴⁹, L.M. Herrmann ²⁵, T. Herrmann ⁵², G. Herten ⁵⁶, R. Hertenberger ¹¹², L. Hervas ³⁷, M.E. Hesping ¹⁰³, N.P. Hessey ^{160a}, J. Hessler ¹¹³, M. Hidaoui ^{36b}, N. Hidic ¹³⁷, E. Hill ¹⁵⁹, S.J. Hillier ²¹, J.R. Hinds ¹¹⁰, F. Hinterkeuser ²⁵, M. Hirose ¹²⁸, S. Hirose ¹⁶¹, D. Hirschbuehl ¹⁷⁶, T.G. Hitchings ¹⁰⁴, B. Hiti ⁹⁶, J. Hobbs ¹⁴⁹, R. Hobincu ^{28e}, N. Hod ¹⁷⁴, M.C. Hodgkinson ¹⁴³, B.H. Hodgkinson ¹³⁰, A. Hoecker ³⁷, D.D. Hofer ¹⁰⁹, J. Hofer ¹⁶⁸, T. Holm ²⁵, M. Holzbock ³⁷, L.B.A.H. Hommels ³³, B.P. Honan ¹⁰⁴, J.J. Hong ⁷⁰, J. Hong ^{64c}, T.M. Hong ¹³³, B.H. Hooberman ¹⁶⁷, W.H. Hopkins ⁶, M.C. Hoppesch ¹⁶⁷, Y. Horii ¹¹⁴, M.E. Horstmann ¹¹³, S. Hou ¹⁵², M.R. Housenga ¹⁶⁷, A.S. Howard ⁹⁶, J. Howarth ⁶¹, J. Hoya ⁶, M. Hrabovsky ¹²⁶, A. Hrynevich ⁵⁰, T. Hryn'ova ⁴, P.J. Hsu ⁶⁷, S.-C. Hsu ¹⁴², T. Hsu ⁶⁸, M. Hu ^{18a}, Q. Hu ^{64a}, S. Huang ³³, X. Huang ^{14,115c}, Y. Huang ¹⁴³, Y. Huang ¹⁰³, Y. Huang ¹⁴, Z. Huang ¹⁰⁴, Z. Hubacek ¹³⁶, M. Huebner ²⁵, F. Huegging ²⁵, T.B. Huffman ¹³⁰, M. Hufnagel Maranha De Faria ^{85a}, C.A. Hugli ⁵⁰, M. Huhtinen ³⁷, S.K. Huiberts ¹⁷, R. Hulsken ¹⁰⁷, N. Huseynov ^{12,f}, J. Huston ¹¹⁰, J. Huth ⁶³, R. Hyneman ¹⁴⁷, G. Iacobucci ⁵⁸, G. Iakovidis ³⁰, L. Iconomidou-Fayard ⁶⁸, J.P. Iddon ³⁷, P. Iengo ^{74a,74b}, R. Iguchi ¹⁵⁷, Y. Iiyama ¹⁵⁷, T. Iizawa ¹³⁰, Y. Ikegami ⁸⁶, D. Iliadis ¹⁵⁶, N. Ilic ¹⁵⁹, H. Imam ^{85c}, G. Inacio Goncalves ^{85d}, T. Ingebretsen Carlson ^{49a,49b}, J.M. Inglis ⁹⁷, G. Introzzi ^{75a,75b}, M. Iodice ^{79a}, V. Ippolito ^{77a,77b}, R.K. Irwin ⁹⁵, M. Ishino ¹⁵⁷, W. Islam ¹⁷⁵, C. Issever ¹⁹, S. Istin ^{22a,ag}, H. Ito ¹⁷³, R. Iuppa ^{80a,80b}, A. Ivina ¹⁷⁴, J.M. Izen ⁴⁷, V. Izzo ^{74a}, P. Jacka ¹³⁵, P. Jackson ¹, C.S. Jagfeld ¹¹², G. Jain ^{160a}, P. Jain ⁵⁰, K. Jakobs ⁵⁶, T. Jakoubek ¹⁷⁴, J. Jamieson ⁶¹, W. Jang ¹⁵⁷, M. Javurkova ¹⁰⁶, P. Jawahar ¹⁰⁴, L. Jeanty ¹²⁷, J. Jejelava ^{153a}, P. Jenni ^{56,e}, C.E. Jessiman ³⁵, C. Jia ^{64b}, H. Jia ¹⁶⁹, J. Jia ¹⁴⁹, X. Jia ^{14,115c}, Z. Jia ^{115a}, C. Jiang ⁵⁴, S. Jiggins ⁵⁰, J. Jimenez Pena ¹³, S. Jin ^{115a}, A. Jinaru ^{28b}, O. Jinnouchi ¹⁵⁸, P. Johansson ¹⁴³, K.A. Johns ⁷, J.W. Johnson ¹⁴⁰, F.A. Jolly ⁵⁰, D.M. Jones ¹⁵⁰, E. Jones ⁵⁰, K.S. Jones ⁸, P. Jones ³³, R.W.L. Jones ⁹⁴, T.J. Jones ⁹⁵, H.L. Joos ^{57,37}, R. Joshi ¹²³, J. Jovicevic ¹⁶, X. Ju ^{18a}, J.J. Junggeburth ³⁷, T. Junkermann ^{65a}, A. Juste Rozas ^{13,t}, M.K. Juzek ⁸⁹, S. Kabana ^{141e}, A. Kaczmarska ⁸⁹, M. Kado ¹¹³, H. Kagan ¹²³, M. Kagan ¹⁴⁷, A. Kahn ¹³², C. Kahra ¹⁰³, T. Kaji ¹⁵⁷, E. Kajomovitz ¹⁵⁴, N. Kakati ¹⁷⁴, I. Kalaitzidou ⁵⁶, C.W. Kalderon ³⁰, N.J. Kang ¹⁴⁰, D. Kar ^{34g}, K. Karava ¹³⁰, M.J. Kareem ^{160b}, E. Karentzos ²⁵, O. Karkout ¹¹⁸, S.N. Karpov ⁴⁰, Z.M. Karpova ⁴⁰, V. Kartvelishvili ⁹⁴, A.N. Karyukhin ³⁹,

E. Kasimi ¹⁵⁶, J. Katzy ⁵⁰, S. Kaur ³⁵, K. Kawade ¹⁴⁴, M.P. Kawale ¹²⁴, C. Kawamoto ⁹⁰,
 T. Kawamoto ^{64a}, E.F. Kay ³⁷, F.I. Kaya ¹⁶², S. Kazakos ¹¹⁰, V.F. Kazanin ³⁹, Y. Ke ¹⁴⁹,
 J.M. Keaveney ^{34a}, R. Keeler ¹⁷⁰, G.V. Kehris ⁶³, J.S. Keller ³⁵, J.J. Kempster ¹⁵⁰, O. Kepka ¹³⁵,
 J. Kerr ^{160b}, B.P. Kerridge ¹³⁸, S. Kersten ¹⁷⁶, B.P. Kerševan ⁹⁶, L. Keszeghova ^{29a},
 S. Kitabchi Haghghat ¹⁵⁹, R.A. Khan ¹³³, A. Khanov ¹²⁵, A.G. Kharlamov ³⁹, T. Kharlamova ³⁹,
 E.E. Khoda ¹⁴², M. Kholodenko ^{134a}, T.J. Khoo ¹⁹, G. Khoriauli ¹⁷¹, J. Khubua ^{153b,*},
 Y.A.R. Khwaira ¹³¹, B. Kibirige ^{34g}, D. Kim ⁶, D.W. Kim ^{49a,49b}, Y.K. Kim ⁴¹, N. Kimura ⁹⁹,
 M.K. Kingston ⁵⁷, A. Kirchhoff ⁵⁷, C. Kirfel ²⁵, F. Kirfel ²⁵, J. Kirk ¹³⁸, A.E. Kiryunin ¹¹³,
 S. Kita ¹⁶¹, C. Kitsaki ¹⁰, O. Kivernyk ²⁵, M. Klassen ¹⁶², C. Klein ³⁵, L. Klein ¹⁷¹,
 M.H. Klein ⁴⁶, S.B. Klein ⁵⁸, U. Klein ⁹⁵, A. Klimentov ³⁰, T. Klioutchnikova ³⁷, P. Kluit ¹¹⁸,
 S. Kluth ¹¹³, E. Kneringer ⁸¹, T.M. Knight ¹⁵⁹, A. Knue ⁵¹, D. Kobylanskii ¹⁷⁴, S.F. Koch ¹³⁰,
 M. Kocian ¹⁴⁷, P. Kodyš ¹³⁷, D.M. Koeck ¹²⁷, P.T. Koenig ²⁵, T. Koffas ³⁵, O. Kolay ⁵²,
 I. Koletsou ⁴, T. Komarek ⁸⁹, K. Köneke ⁵⁷, A.X.Y. Kong ¹, T. Kono ¹²², N. Konstantinidis ⁹⁹,
 P. Kontaxakis ⁵⁸, B. Konya ¹⁰¹, R. Kopeliansky ⁴³, S. Koperny ^{88a}, K. Korcyl ⁸⁹,
 K. Kordas ^{156,d}, A. Korn ⁹⁹, S. Korn ⁵⁷, I. Korolkov ¹³, N. Korotkova ³⁹, B. Kortman ¹¹⁸,
 O. Kortner ¹¹³, S. Kortner ¹¹³, W.H. Kostecka ¹¹⁹, V.V. Kostyukhin ¹⁴⁵, A. Kotsokechagia ³⁷,
 A. Kotwal ⁵³, A. Koulouris ³⁷, A. Kourkoumeli-Charalampidi ^{75a,75b}, C. Kourkoumelis ⁹,
 E. Kourlitis ^{113,aa}, O. Kovanda ¹²⁷, R. Kowalewski ¹⁷⁰, W. Kozanecki ¹²⁷, A.S. Kozhin ³⁹,
 V.A. Kramarenko ³⁹, G. Kramberger ⁹⁶, P. Kramer ²⁵, M.W. Krasny ¹³¹, A. Krasznahorkay ³⁷,
 A.C. Kraus ¹¹⁹, J.W. Kraus ¹⁷⁶, J.A. Kremer ⁵⁰, T. Kresse ⁵², L. Kretschmann ¹⁷⁶,
 J. Kretschmar ⁹⁵, K. Kreul ¹⁹, P. Krieger ¹⁵⁹, K. Krizka ²¹, K. Kroeninger ⁵¹, H. Kroha ¹¹³,
 J. Kroll ¹³⁵, J. Kroll ¹³², K.S. Krowpman ¹¹⁰, U. Kruchonak ⁴⁰, H. Krüger ²⁵, N. Krumnack ⁸³,
 M.C. Kruse ⁵³, O. Kuchinskaia ³⁹, S. Kuday ^{3a}, S. Kuehn ³⁷, R. Kuesters ⁵⁶, T. Kuhl ⁵⁰,
 V. Kukhtin ⁴⁰, Y. Kulchitsky ⁴⁰, S. Kuleshov ^{141d,141b}, M. Kumar ^{34g}, N. Kumari ⁵⁰,
 P. Kumari ^{160b}, A. Kupco ¹³⁵, T. Kupfer ⁵¹, A. Kupich ³⁹, O. Kuprash ⁵⁶, H. Kurashige ⁸⁷,
 L.L. Kurchaninov ^{160a}, O. Kurdysh ⁵⁸, Y.A. Kurochkin ³⁸, A. Kurova ³⁹, M. Kuze ¹⁵⁸,
 A.K. Kvam ¹⁰⁶, J. Kvita ¹²⁶, T. Kwan ¹⁰⁷, N.G. Kyriacou ¹⁰⁹, L.A.O. Laatu ¹⁰⁵, C. Lacasta ¹⁶⁸,
 F. Lacava ^{77a,77b}, H. Lacker ¹⁹, D. Lacour ¹³¹, N.N. Lad ⁹⁹, E. Ladygin ⁴⁰, A. Lafarge ⁴²,
 B. Laforge ¹³¹, T. Lagouri ¹⁷⁷, F.Z. Lahbabi ^{36a}, S. Lai ⁵⁷, J.E. Lambert ¹⁷⁰, S. Lammers ⁷⁰,
 W. Lampl ⁷, C. Lampoudis ^{156,d}, G. Lamprinoudis ¹⁰³, A.N. Lancaster ¹¹⁹, E. Lançon ³⁰,
 U. Landgraf ⁵⁶, M.P.J. Landon ⁹⁷, V.S. Lang ⁵⁶, O.K.B. Langrekken ¹²⁹, A.J. Lankford ¹⁶³,
 F. Lanni ³⁷, K. Lantzsch ²⁵, A. Lanza ^{75a}, M. Lanzac Berrocal ¹⁶⁸, J.F. Laporte ¹³⁹, T. Lari ^{73a},
 F. Lasagni Manghi ^{24b}, M. Lassnig ³⁷, V. Latonova ¹³⁵, S.D. Lawlor ¹⁴³, Z. Lawrence ¹⁰⁴,
 R. Lazaridou ¹⁷², M. Lazzaroni ^{73a,73b}, B. Le ¹⁰⁴, H.D.M. Le ¹¹⁰, E.M. Le Boulicaut ¹⁷⁷,
 L.T. Le Pottier ^{18a}, B. Leban ^{24b,24a}, A. Lebedev ⁸³, M. LeBlanc ¹⁰⁴, F. Ledroit-Guillon ⁶²,
 S.C. Lee ¹⁵², S. Lee ^{49a,49b}, T.F. Lee ⁹⁵, L.L. Leeuw ^{34c}, M. Lefebvre ¹⁷⁰, C. Leggett ^{18a},
 G. Lehmann Miotto ³⁷, M. Leigh ⁵⁸, W.A. Leight ¹⁰⁶, W. Leinonen ¹¹⁷, A. Leisos ^{156,r},
 M.A.L. Leite ^{85c}, C.E. Leitgeb ¹⁹, R. Leitner ¹³⁷, K.J.C. Leney ⁴⁶, T. Lenz ²⁵, S. Leone ^{76a},
 C. Leonidopoulos ⁵⁴, A. Leopold ¹⁴⁸, R. Les ¹¹⁰, C.G. Lester ³³, M. Levchenko ³⁹,
 J. Levêque ⁴, L.J. Levinson ¹⁷⁴, G. Levrini ^{24b,24a}, M.P. Lewicki ⁸⁹, C. Lewis ¹⁴², D.J. Lewis ⁴,
 L. Lewitt ¹⁴³, A. Li ³⁰, B. Li ^{64b}, C. Li ^{64a}, C-Q. Li ¹¹³, H. Li ^{64a}, H. Li ^{64b}, H. Li ^{115a},
 H. Li ¹⁵, H. Li ^{64b}, J. Li ^{64c}, K. Li ¹⁴, L. Li ^{64c}, M. Li ^{14,115c}, S. Li ^{14,115c}, S. Li ^{64d,64c},
 T. Li ⁵, X. Li ¹⁰⁷, Z. Li ¹⁵⁷, Z. Li ^{14,115c}, Z. Li ^{64a}, S. Liang ^{14,115c}, Z. Liang ¹⁴,
 M. Liberatore ¹³⁹, B. Liberti ^{78a}, K. Lie ^{66c}, J. Lieber Marin ^{85e}, H. Lien ⁷⁰, H. Lin ¹⁰⁹,
 K. Lin ¹¹⁰, L. Linden ¹¹², R.E. Lindley ⁷, J.H. Lindon ², J. Ling ⁶³, E. Lipeles ¹³²,
 A. Lipniacka ¹⁷, A. Lister ¹⁶⁹, J.D. Little ⁷⁰, B. Liu ¹⁴, B.X. Liu ^{115b}, D. Liu ^{64d,64c},
 E.H.L. Liu ²¹, J.B. Liu ^{64a}, J.K.K. Liu ³³, K. Liu ^{64d}, K. Liu ^{64d,64c}, M. Liu ^{64a}, M.Y. Liu ^{64a},

P. Liu ¹⁴, Q. Liu ^{64d,142,64c}, X. Liu ^{64a}, X. Liu ^{64b}, Y. Liu ^{115b,115c}, Y.L. Liu ^{64b}, Y.W. Liu ^{64a},
 S.L. Lloyd ⁹⁷, E.M. Lobodzinska ⁵⁰, P. Loch ⁷, E. Lodhi ¹⁵⁹, T. Lohse ¹⁹, K. Lohwasser ¹⁴³,
 E. Loiacono ⁵⁰, J.D. Lomas ²¹, J.D. Long ⁴³, I. Longarini ¹⁶³, R. Longo ¹⁶⁷, I. Lopez Paz ⁶⁹,
 A. Lopez Solis ⁵⁰, N.A. Lopez-canelas ⁷, N. Lorenzo Martinez ⁴, A.M. Lory ¹¹², M. Losada ^{120a},
 G. Löschke Centeno ¹⁵⁰, O. Loseva ³⁹, X. Lou ^{49a,49b}, X. Lou ^{14,115c}, A. Lounis ⁶⁸,
 P.A. Love ⁹⁴, G. Lu ^{14,115c}, M. Lu ⁶⁸, S. Lu ¹³², Y.J. Lu ¹⁵², H.J. Lubatti ¹⁴², C. Luci ^{77a,77b},
 F.L. Lucio Alves ^{115a}, F. Luehring ⁷⁰, O. Lukianchuk ⁶⁸, B.S. Lunday ¹³², O. Lundberg ¹⁴⁸,
 B. Lund-Jensen ^{148,*}, N.A. Luongo ⁶, M.S. Lutz ³⁷, A.B. Lux ²⁶, D. Lynn ³⁰, R. Lysak ¹³⁵,
 E. Lytken ¹⁰¹, V. Lyubushkin ⁴⁰, T. Lyubushkina ⁴⁰, M.M. Lyukova ¹⁴⁹, M.Firdaus M. Soberi ⁵⁴,
 H. Ma ³⁰, K. Ma ^{64a}, L.L. Ma ^{64b}, W. Ma ^{64a}, Y. Ma ¹²⁵, J.C. MacDonald ¹⁰³,
 P.C. Machado De Abreu Farias ^{85e}, R. Madar ⁴², T. Madula ⁹⁹, J. Maeda ⁸⁷, T. Maeno ³⁰,
 P.T. Mafa ^{34c}, H. Maguire ¹⁴³, V. Maiboroda ¹³⁹, A. Maio ^{134a,134b,134d}, K. Maj ^{88a},
 O. Majersky ⁵⁰, S. Majewski ¹²⁷, N. Makovec ⁶⁸, V. Maksimovic ¹⁶, B. Malaescu ¹³¹,
 Pa. Malecki ⁸⁹, V.P. Maleev ³⁹, F. Malek ^{62,m}, M. Mali ⁹⁶, D. Malito ⁹⁸, U. Mallik ^{82,*},
 S. Maltezos ¹⁰, S. Malyukov ⁴⁰, J. Mamuzic ¹³, G. Mancini ⁵⁵, M.N. Mancini ²⁷, G. Manco ^{75a,75b},
 J.P. Mandalia ⁹⁷, S.S. Mandarry ¹⁵⁰, I. Mandić ⁹⁶, L. Manhaes de Andrade Filho ^{85a},
 I.M. Maniatis ¹⁷⁴, J. Manjarres Ramos ⁹², D.C. Mankad ¹⁷⁴, A. Mann ¹¹², S. Manzoni ³⁷,
 L. Mao ^{64c}, X. Mapekula ^{34c}, A. Marantis ^{156,r}, G. Marchiori ⁵, M. Marcisovsky ¹³⁵,
 C. Marcon ^{73a}, M. Marinescu ²¹, S. Marium ⁵⁰, M. Marjanovic ¹²⁴, A. Markhoos ⁵⁶,
 M. Markovitch ⁶⁸, M.K. Maroun ¹⁰⁶, E.J. Marshall ⁹⁴, Z. Marshall ^{18a}, S. Marti-Garcia ¹⁶⁸,
 J. Martin ⁹⁹, T.A. Martin ¹³⁸, V.J. Martin ⁵⁴, B. Martin dit Latour ¹⁷, L. Martinelli ^{77a,77b},
 M. Martinez ^{13,t}, P. Martinez Agullo ¹⁶⁸, V.I. Martinez Outschoorn ¹⁰⁶, P. Martinez Suarez ¹³,
 S. Martin-Haugh ¹³⁸, G. Martinovicova ¹³⁷, V.S. Martoiu ^{28b}, A.C. Martyniuk ⁹⁹, A. Marzin ³⁷,
 D. Mascione ^{80a,80b}, L. Masetti ¹⁰³, J. Masik ¹⁰⁴, A.L. Maslennikov ³⁹, S.L. Mason ⁴³,
 P. Massarotti ^{74a,74b}, P. Mastrandrea ^{76a,76b}, A. Mastroberardino ^{45b,45a}, T. Masubuchi ¹²⁸,
 T.T. Mathew ¹²⁷, T. Mathisen ¹⁶⁶, J. Matousek ¹³⁷, D.M. Mattern ⁵¹, J. Maurer ^{28b},
 T. Maurin ⁶¹, A.J. Maury ⁶⁸, B. Maček ⁹⁶, D.A. Maximov ³⁹, A.E. May ¹⁰⁴, R. Mazini ^{34g},
 I. Maznas ¹¹⁹, M. Mazza ¹¹⁰, S.M. Mazza ¹⁴⁰, E. Mazzeo ^{73a,73b}, J.P. Mc Gowan ¹⁷⁰,
 S.P. Mc Kee ¹⁰⁹, C.A. Mc Lean ⁶, C.C. McCracken ¹⁶⁹, E.F. McDonald ¹⁰⁸, A.E. McDougall ¹¹⁸,
 L.F. Mcelhinney ⁹⁴, J.A. Mcfayden ¹⁵⁰, R.P. McGovern ¹³², R.P. Mckenzie ^{34g},
 T.C. McLachlan ⁵⁰, D.J. McLaughlin ⁹⁹, S.J. McMahon ¹³⁸, C.M. Mcpartland ⁹⁵,
 R.A. McPherson ^{170,x}, S. Mehlhase ¹¹², A. Mehta ⁹⁵, D. Melini ¹⁶⁸, B.R. Mellado Garcia ^{34g},
 A.H. Melo ⁵⁷, F. Meloni ⁵⁰, A.M. Mendes Jacques Da Costa ¹⁰⁴, H.Y. Meng ¹⁵⁹, L. Meng ⁹⁴,
 S. Menke ¹¹³, M. Mentink ³⁷, E. Meoni ^{45b,45a}, G. Mercado ¹¹⁹, S. Merianos ¹⁵⁶,
 C. Merlassino ^{71a,71c}, L. Merola ^{74a,74b}, C. Meroni ^{73a,73b}, J. Metcalfe ⁶, A.S. Mete ⁶,
 E. Meuser ¹⁰³, C. Meyer ⁷⁰, J.P. Meyer ¹³⁹, R.P. Middleton ¹³⁸, L. Mijović ⁵⁴,
 G. Mikenberg ¹⁷⁴, M. Mikestikova ¹³⁵, M. Mikuž ⁹⁶, H. Mildner ¹⁰³, A. Milic ³⁷,
 D.W. Miller ⁴¹, E.H. Miller ¹⁴⁷, L.S. Miller ³⁵, A. Milov ¹⁷⁴, D.A. Milstead ^{49a,49b}, T. Min ^{115a},
 A.A. Minaenko ³⁹, I.A. Minashvili ^{153b}, A.I. Mincer ¹²¹, B. Mindur ^{88a}, M. Mineev ⁴⁰,
 Y. Mino ⁹⁰, L.M. Mir ¹³, M. Miralles Lopez ⁶¹, M. Mironova ^{18a}, M.C. Missio ¹¹⁷, A. Mitra ¹⁷²,
 V.A. Mitsou ¹⁶⁸, Y. Mitsumori ¹¹⁴, O. Miu ¹⁵⁹, P.S. Miyagawa ⁹⁷, T. Mkrtchyan ^{65a},
 M. Mlinarevic ⁹⁹, T. Mlinarevic ⁹⁹, M. Mlynarikova ³⁷, S. Mobius ²⁰, P. Mogg ¹¹²,
 M.H. Mohamed Farook ¹¹⁶, A.F. Mohammed ^{14,115c}, S. Mohapatra ⁴³, G. Mokgatitwane ^{34g},
 L. Moleri ¹⁷⁴, B. Mondal ¹⁴⁵, S. Mondal ¹³⁶, K. Mönig ⁵⁰, E. Monnier ¹⁰⁵,
 L. Monsonis Romero ¹⁶⁸, J. Montejo Berlingen ¹³, A. Montella ^{49a,49b}, M. Montella ¹²³,
 F. Montekali ^{79a,79b}, F. Monticelli ⁹³, S. Monzani ^{71a,71c}, A. Morancho Tarda ⁴⁴, N. Morange ⁶⁸,
 A.L. Moreira De Carvalho ⁵⁰, M. Moreno Llácer ¹⁶⁸, C. Moreno Martinez ⁵⁸, J.M. Moreno Perez ^{23b},

P. Morettini ^{59b}, S. Morgenstern ³⁷, M. Morii ⁶³, M. Morinaga ¹⁵⁷, M. Moritsu ⁹¹,
 F. Morodei ^{77a,77b}, P. Moschovakos ³⁷, B. Moser ¹³⁰, M. Mosidze ^{153b}, T. Moskalets ⁴⁶,
 P. Moskvitina ¹¹⁷, J. Moss ^{32j}, P. Moszkowicz ^{88a}, A. Moussa ^{36d}, Y. Moyal ¹⁷⁴,
 E.J.W. Moyse ¹⁰⁶, O. Mtintsilana ^{34g}, S. Muanza ¹⁰⁵, J. Mueller ¹³³, D. Muenstermann ⁹⁴,
 R. Müller ³⁷, G.A. Mullier ¹⁶⁶, A.J. Mullin ³³, J.J. Mullin ¹³², A.E. Mulski ⁶³, D.P. Mungo ¹⁵⁹,
 D. Munoz Perez ¹⁶⁸, F.J. Munoz Sanchez ¹⁰⁴, M. Murin ¹⁰⁴, W.J. Murray ^{172,138}, M. Muškinja ⁹⁶,
 C. Mwewa ³⁰, A.G. Myagkov ^{39,a}, A.J. Myers ⁸, G. Myers ¹⁰⁹, M. Myska ¹³⁶, B.P. Nachman ^{18a},
 K. Nagai ¹³⁰, K. Nagano ⁸⁶, R. Nagasaka ¹⁵⁷, J.L. Nagle ^{30,ae}, E. Nagy ¹⁰⁵, A.M. Nairz ³⁷,
 Y. Nakahama ⁸⁶, K. Nakamura ⁸⁶, K. Nakkalil ⁵, H. Nanjo ¹²⁸, E.A. Narayanan ⁴⁶,
 Y. Narukawa ¹⁵⁷, I. Naryshkin ³⁹, L. Nasella ^{73a,73b}, S. Nasri ^{120b}, C. Nass ²⁵, G. Navarro ^{23a},
 J. Navarro-Gonzalez ¹⁶⁸, R. Nayak ¹⁵⁵, A. Nayaz ¹⁹, P.Y. Nechaeva ³⁹, S. Nechaeva ^{24b,24a},
 F. Nechansky ¹³⁵, L. Nedic ¹³⁰, T.J. Neep ²¹, A. Negri ^{75a,75b}, M. Negrini ^{24b}, C. Nellist ¹¹⁸,
 C. Nelson ¹⁰⁷, K. Nelson ¹⁰⁹, S. Nemecek ¹³⁵, M. Nessi ^{37,g}, M.S. Neubauer ¹⁶⁷,
 F. Neuhaus ¹⁰³, J. Neundorf ⁵⁰, J. Newell ⁹⁵, P.R. Newman ²¹, C.W. Ng ¹³³, Y.W.Y. Ng ⁵⁰,
 B. Ngair ^{120a}, H.D.N. Nguyen ¹¹¹, R.B. Nickerson ¹³⁰, R. Nicolaidou ¹³⁹, J. Nielsen ¹⁴⁰,
 M. Niemeyer ⁵⁷, J. Niermann ³⁷, N. Nikiforou ³⁷, V. Nikolaenko ^{39,a}, I. Nikolic-Audit ¹³¹,
 K. Nikolopoulos ²¹, P. Nilsson ³⁰, I. Ninca ⁵⁰, G. Ninio ¹⁵⁵, A. Nisati ^{77a}, N. Nishu ²,
 R. Nisius ¹¹³, N. Nitika ^{71a,71c}, J-E. Nitschke ⁵², E.K. Nkadimeng ^{34g}, T. Nobe ¹⁵⁷,
 T. Nommensen ¹⁵¹, M.B. Norfolk ¹⁴³, B.J. Norman ³⁵, M. Noury ^{36a}, J. Novak ⁹⁶, T. Novak ⁹⁶,
 L. Novotny ¹³⁶, R. Novotny ¹¹⁶, L. Nozka ¹²⁶, K. Ntekas ¹⁶³, N.M.J. Nunes De Moura Junior ^{85b},
 J. Ocariz ¹³¹, A. Ochi ⁸⁷, I. Ochoa ^{134a}, S. Oerdek ^{50,u}, J.T. Offermann ⁴¹, A. Ogrodnik ¹³⁷,
 A. Oh ¹⁰⁴, C.C. Ohm ¹⁴⁸, H. Oide ⁸⁶, R. Oishi ¹⁵⁷, M.L. Ojeda ³⁷, Y. Okumura ¹⁵⁷,
 L.F. Oleiro Seabra ^{134a}, I. Oleksiyuk ⁵⁸, S.A. Olivares Pino ^{141d}, G. Oliveira Correa ¹³,
 D. Oliveira Damazio ³⁰, J.L. Oliver ¹⁶³, Ö.O. Öncel ⁵⁶, A.P. O'Neill ²⁰, A. Onofre ^{134a,134e},
 P.U.E. Onyisi ¹¹, M.J. Oreglia ⁴¹, D. Orestano ^{79a,79b}, N. Orlando ¹³, R.S. Orr ¹⁵⁹,
 L.M. Osojnak ¹³², Y. Osumi ¹¹⁴, G. Otero y Garzon ³¹, H. Otono ⁹¹, P.S. Ott ^{65a}, G.J. Ottino ^{18a},
 M. Ouchrif ^{36d}, F. Ould-Saada ¹²⁹, T. Ovsianikova ¹⁴², M. Owen ⁶¹, R.E. Owen ¹³⁸,
 V.E. Ozcan ^{22a}, F. Ozturk ⁸⁹, N. Ozturk ⁸, S. Ozturk ⁸⁴, H.A. Pacey ¹³⁰, A. Pacheco Pages ¹³,
 C. Padilla Aranda ¹³, G. Padovano ^{77a,77b}, S. Pagan Griso ^{18a}, G. Palacino ⁷⁰, A. Palazzo ^{72a,72b},
 J. Pampel ²⁵, J. Pan ¹⁷⁷, T. Pan ^{66a}, D.K. Panchal ¹¹, C.E. Pandini ¹¹⁸,
 J.G. Panduro Vazquez ¹³⁸, H.D. Pandya ¹, H. Pang ¹⁵, P. Pani ⁵⁰, G. Panizzo ^{71a,71c},
 L. Panwar ¹³¹, L. Paolozzi ⁵⁸, S. Parajuli ¹⁶⁷, A. Paramonov ⁶, C. Paraskevopoulos ⁵⁵,
 D. Paredes Hernandez ^{66b}, A. Pareti ^{75a,75b}, K.R. Park ⁴³, T.H. Park ¹⁵⁹, M.A. Parker ³³,
 F. Parodi ^{59b,59a}, V.A. Parrish ⁵⁴, J.A. Parsons ⁴³, U. Parzefall ⁵⁶, B. Pascual Dias ¹¹¹,
 L. Pascual Dominguez ¹⁰², E. Pasqualucci ^{77a}, S. Passaggio ^{59b}, F. Pastore ⁹⁸, P. Patel ⁸⁹,
 U.M. Patel ⁵³, J.R. Pater ¹⁰⁴, T. Pauly ³⁷, F. Pauwels ¹³⁷, C.I. Pazos ¹⁶², M. Pedersen ¹²⁹,
 R. Pedro ^{134a}, S.V. Peleganchuk ³⁹, O. Penc ³⁷, E.A. Pender ⁵⁴, S. Peng ¹⁵, G.D. Penn ¹⁷⁷,
 K.E. Pensi ¹¹², M. Penzin ³⁹, B.S. Peralva ^{85d}, A.P. Pereira Peixoto ¹⁴², L. Pereira Sanchez ¹⁴⁷,
 D.V. Perepelitsa ^{30,ae}, G. Perera ¹⁰⁶, E. Perez Codina ^{160a}, M. Perganti ¹⁰, H. Pernegger ³⁷,
 S. Perrella ^{77a,77b}, O. Perrin ⁴², K. Peters ⁵⁰, R.F.Y. Peters ¹⁰⁴, B.A. Petersen ³⁷,
 T.C. Petersen ⁴⁴, E. Petit ¹⁰⁵, V. Petousis ¹³⁶, C. Petridou ^{156,d}, T. Petru ¹³⁷, A. Petrukhin ¹⁴⁵,
 M. Pettee ^{18a}, A. Petukhov ⁸⁴, K. Petukhova ³⁷, R. Pezoa ^{141f}, L. Pezzotti ³⁷, G. Pezzullo ¹⁷⁷,
 A.J. Pflieger ³⁷, T.M. Pham ¹⁷⁵, T. Pham ¹⁰⁸, P.W. Phillips ¹³⁸, G. Piacquadio ¹⁴⁹, E. Pianori ^{18a},
 F. Piazza ¹²⁷, R. Piegaia ³¹, D. Pietreanu ^{28b}, A.D. Pilkington ¹⁰⁴, M. Pinamonti ^{71a,71c},
 J.L. Pinfeld ², B.C. Pinheiro Pereira ^{134a}, J. Pinol Bel ¹³, A.E. Pinto Pinoargote ^{139,139},
 L. Pintucci ^{71a,71c}, K.M. Piper ¹⁵⁰, A. Pirttikoski ⁵⁸, D.A. Pizzi ³⁵, L. Pizzimento ^{66b},
 A. Pizzini ¹¹⁸, M.-A. Pleier ³⁰, V. Pleskot ¹³⁷, E. Plotnikova ⁴⁰, G. Poddar ⁹⁷, R. Poettgen ¹⁰¹,

L. Poggioli ¹³¹, S. Polacek ¹³⁷, G. Polesello ^{75a}, A. Poley ^{146,160a}, A. Polini ^{24b}, C.S. Pollard ¹⁷²,
 Z.B. Pollock ¹²³, E. Pompa Pacchi ¹²⁴, N.I. Pond ⁹⁹, D. Ponomarenko ⁷⁰, L. Pontecorvo ³⁷,
 S. Popa ^{28a}, G.A. Popeneciu ^{28d}, A. Poreba ³⁷, D.M. Portillo Quintero ^{160a}, S. Pospisil ¹³⁶,
 M.A. Postill ¹⁴³, P. Postolache ^{28c}, K. Potamianos ¹⁷², P.A. Potepa ^{88a}, I.N. Potrap ⁴⁰,
 C.J. Potter ³³, H. Potti ¹⁵¹, J. Poveda ¹⁶⁸, M.E. Pozo Astigarraga ³⁷, A. Prades Ibanez ^{78a,78b},
 J. Pretel ¹⁷⁰, D. Price ¹⁰⁴, M. Primavera ^{72a}, L. Primomo ^{71a,71c}, M.A. Principe Martin ¹⁰²,
 R. Privara ¹²⁶, T. Procter ⁶¹, M.L. Proffitt ¹⁴², N. Proklova ¹³², K. Prokofiev ^{66c}, G. Proto ¹¹³,
 J. Proudfoot ⁶, M. Przybycien ^{88a}, W.W. Przygoda ^{88b}, A. Psallidas ⁴⁸, J.E. Puddefoot ¹⁴³,
 D. Pudzha ⁵⁶, D. Pyatiizbyantseva ³⁹, J. Qian ¹⁰⁹, R. Qian ¹¹⁰, D. Qichen ¹⁰⁴, Y. Qin ¹³,
 T. Qiu ⁵⁴, A. Quadt ⁵⁷, M. Queitsch-Maitland ¹⁰⁴, G. Quetant ⁵⁸, R.P. Quinn ¹⁶⁹,
 G. Rabanal Bolanos ⁶³, D. Rafanoharana ⁵⁶, F. Raffaelli ^{78a,78b}, F. Ragusa ^{73a,73b}, J.L. Rainbolt ⁴¹,
 J.A. Raine ⁵⁸, S. Rajagopalan ³⁰, E. Ramakoti ³⁹, L. Rambelli ^{59b,59a}, I.A. Ramirez-Berend ³⁵,
 K. Ran ^{50,115c}, D.S. Rankin ¹³², N.P. Rapheeha ^{34g}, H. Rasheed ^{28b}, V. Raskina ¹³¹,
 D.F. Rassloff ^{65a}, A. Rastogi ^{18a}, S. Rave ¹⁰³, S. Ravera ^{59b,59a}, B. Ravina ⁵⁷, I. Ravinovich ¹⁷⁴,
 M. Raymond ³⁷, A.L. Read ¹²⁹, N.P. Readioff ¹⁴³, D.M. Rebuzzi ^{75a,75b}, G. Redlinger ³⁰,
 A.S. Reed ¹¹³, K. Reeves ²⁷, J.A. Reidelsturz ¹⁷⁶, D. Reikher ¹²⁷, A. Rej ⁵¹, C. Rembser ³⁷,
 M. Renda ^{28b}, F. Renner ⁵⁰, A.G. Rennie ¹⁶³, A.L. Rescia ⁵⁰, S. Resconi ^{73a},
 M. Ressegotti ^{59b,59a}, S. Rettie ³⁷, J.G. Reyes Rivera ¹¹⁰, E. Reynolds ^{18a}, O.L. Rezanova ³⁹,
 P. Reznicek ¹³⁷, H. Riani ^{36d}, N. Ribaric ⁵³, E. Ricci ^{80a,80b}, R. Richter ¹¹³, S. Richter ^{49a,49b},
 E. Richter-Was ^{88b}, M. Ridel ¹³¹, S. Ridouani ^{36d}, P. Rieck ¹²¹, P. Riedler ³⁷, E.M. Riefel ^{49a,49b},
 J.O. Rieger ¹¹⁸, M. Rijssenbeek ¹⁴⁹, M. Rimoldi ³⁷, L. Rinaldi ^{24b,24a}, P. Rincke ^{57,166},
 T.T. Rinn ³⁰, M.P. Rinnagel ¹¹², G. Ripellino ¹⁶⁶, I. Riu ¹³, J.C. Rivera Vergara ¹⁷⁰,
 F. Rizatdinova ¹²⁵, E. Rizvi ⁹⁷, B.R. Roberts ^{18a}, S.S. Roberts ¹⁴⁰, S.H. Robertson ^{107,x},
 D. Robinson ³³, M. Robles Manzano ¹⁰³, A. Robson ⁶¹, A. Rocchi ^{78a,78b}, C. Roda ^{76a,76b},
 S. Rodriguez Bosca ³⁷, Y. Rodriguez Garcia ^{23a}, A.M. Rodríguez Vera ¹¹⁹, S. Roe ³⁷,
 J.T. Roemer ³⁷, A.R. Roepe-Gier ¹⁴⁰, O. Röhne ¹²⁹, R.A. Rojas ¹⁰⁶, C.P.A. Roland ¹³¹,
 J. Roloff ³⁰, A. Romaniouk ⁸¹, E. Romano ^{75a,75b}, M. Romano ^{24b}, A.C. Romero Hernandez ¹⁶⁷,
 N. Rompotis ⁹⁵, L. Roos ¹³¹, S. Rosati ^{77a}, B.J. Rosser ⁴¹, E. Rossi ¹³⁰, E. Rossi ^{74a,74b},
 L.P. Rossi ⁶³, L. Rossini ⁵⁶, R. Rosten ¹²³, M. Rotaru ^{28b}, B. Rottler ⁵⁶, C. Rougier ⁹²,
 D. Rousseau ⁶⁸, D. Rouso ⁵⁰, A. Roy ¹⁶⁷, S. Roy-Garand ¹⁵⁹, A. Rozanov ¹⁰⁵,
 Z.M.A. Rozario ⁶¹, Y. Rozen ¹⁵⁴, A. Rubio Jimenez ¹⁶⁸, V.H. Ruelas Rivera ¹⁹, T.A. Ruggeri ¹,
 A. Ruggiero ¹³⁰, A. Ruiz-Martinez ¹⁶⁸, A. Rummler ³⁷, Z. Rurikova ⁵⁶, N.A. Rusakovich ⁴⁰,
 H.L. Russell ¹⁷⁰, G. Russo ^{77a,77b}, J.P. Rutherford ⁷, S. Rutherford Colmenares ³³, M. Rybar ¹³⁷,
 E.B. Rye ¹²⁹, A. Ryzhov ⁴⁶, J.A. Sabater Iglesias ⁵⁸, H.F.W. Sadrozinski ¹⁴⁰, F. Safai Tehrani ^{77a},
 B. Safarzadeh Samani ¹³⁸, S. Saha ¹, M. Sahinsoy ⁸⁴, A. Saibel ¹⁶⁸, M. Saimpert ¹³⁹,
 M. Saito ¹⁵⁷, T. Saito ¹⁵⁷, A. Sala ^{73a,73b}, D. Salamani ³⁷, A. Salnikov ¹⁴⁷, J. Salt ¹⁶⁸,
 A. Salvador Salas ¹⁵⁵, D. Salvatore ^{45b,45a}, F. Salvatore ¹⁵⁰, A. Salzburger ³⁷, D. Sammel ⁵⁶,
 E. Sampson ⁹⁴, D. Sampsonidis ^{156,d}, D. Sampsonidou ¹²⁷, J. Sánchez ¹⁶⁸,
 V. Sanchez Sebastian ¹⁶⁸, H. Sandaker ¹²⁹, C.O. Sander ⁵⁰, J.A. Sandesara ¹⁰⁶, M. Sandhoff ¹⁷⁶,
 C. Sandoval ^{23b}, L. Sanfilippo ^{65a}, D.P.C. Sankey ¹³⁸, T. Sano ⁹⁰, A. Sansoni ⁵⁵, L. Santi ^{37,77b},
 C. Santoni ⁴², H. Santos ^{134a,134b}, A. Santra ¹⁷⁴, E. Sanzani ^{24b,24a}, K.A. Saoucha ¹⁶⁵,
 J.G. Saraiva ^{134a,134d}, J. Sardain ⁷, O. Sasaki ⁸⁶, K. Sato ¹⁶¹, C. Sauer ³⁷, E. Sauvan ⁴,
 P. Savard ^{159,ac}, R. Sawada ¹⁵⁷, C. Sawyer ¹³⁸, L. Sawyer ¹⁰⁰, C. Sbarra ^{24b}, A. Sbrizzi ^{24b,24a},
 T. Scanlon ⁹⁹, J. Schaarschmidt ¹⁴², U. Schäfer ¹⁰³, A.C. Schaffer ^{68,46}, D. Schaile ¹¹²,
 R.D. Schamberger ¹⁴⁹, C. Scharf ¹⁹, M.M. Schefer ²⁰, V.A. Schegelsky ³⁹, D. Scheirich ¹³⁷,
 M. Schernau ^{141e}, C. Scheulen ⁵⁸, C. Schiavi ^{59b,59a}, M. Schioppa ^{45b,45a}, B. Schlag ^{147,1},
 S. Schlenker ³⁷, J. Schmeing ¹⁷⁶, M.A. Schmidt ¹⁷⁶, K. Schmieden ¹⁰³, C. Schmitt ¹⁰³,

N. Schmitt ¹⁰³, S. Schmitt ⁵⁰, L. Schoeffel ¹³⁹, A. Schoening ^{65b}, P.G. Scholer ³⁵, E. Schopf ¹³⁰,
 M. Schott ²⁵, J. Schovancova ³⁷, S. Schramm ⁵⁸, T. Schroer ⁵⁸, H-C. Schultz-Coulon ^{65a},
 M. Schumacher ⁵⁶, B.A. Schumm ¹⁴⁰, Ph. Schune ¹³⁹, A.J. Schuy ¹⁴², H.R. Schwartz ¹⁴⁰,
 A. Schwartzman ¹⁴⁷, T.A. Schwarz ¹⁰⁹, Ph. Schwemling ¹³⁹, R. Schwienhorst ¹¹⁰,
 F.G. Sciacca ²⁰, A. Sciandra ³⁰, G. Sciolla ²⁷, F. Scuri ^{76a}, C.D. Sebastiani ⁹⁵, K. Sedlaczek ¹¹⁹,
 S.C. Seidel ¹¹⁶, A. Seiden ¹⁴⁰, B.D. Seidlitz ⁴³, C. Seitz ⁵⁰, J.M. Seixas ^{85b}, G. Sekhniaidze ^{74a},
 L. Selem ⁶², N. Semprini-Cesari ^{24b,24a}, A. Semushin ^{178,39}, D. Sengupta ⁵⁸, V. Senthilkumar ¹⁶⁸,
 L. Serin ⁶⁸, M. Sessa ^{78a,78b}, H. Severini ¹²⁴, F. Sforza ^{59b,59a}, A. Sfyrta ⁵⁸, Q. Sha ¹⁴,
 E. Shabalina ⁵⁷, A.H. Shah ³³, R. Shaheen ¹⁴⁸, J.D. Shahinian ¹³², D. Shaked Renous ¹⁷⁴,
 L.Y. Shan ¹⁴, M. Shapiro ^{18a}, A. Sharma ³⁷, A.S. Sharma ¹⁶⁹, P. Sharma ³⁰, P.B. Shatalov ³⁹,
 K. Shaw ¹⁵⁰, S.M. Shaw ¹⁰⁴, Q. Shen ^{64c}, D.J. Sheppard ¹⁴⁶, P. Sherwood ⁹⁹, L. Shi ⁹⁹,
 X. Shi ¹⁴, S. Shimizu ⁸⁶, C.O. Shimmin ¹⁷⁷, I.P.J. Shipsey ¹³⁰, S. Shirabe ⁹¹, M. Shiyakova ^{40,v},
 M.J. Shochet ⁴¹, D.R. Shope ¹²⁹, B. Shrestha ¹²⁴, S. Shrestha ^{123,af}, I. Shreyber ³⁹,
 M.J. Shroff ¹⁷⁰, P. Sicho ¹³⁵, A.M. Sickles ¹⁶⁷, E. Sideras Haddad ^{34g,164}, A.C. Sidley ¹¹⁸,
 A. Sidoti ^{24b}, F. Siegert ⁵², Dj. Sijacki ¹⁶, F. Sili ⁹³, J.M. Silva ⁵⁴, I. Silva Ferreira ^{85b},
 M.V. Silva Oliveira ³⁰, S.B. Silverstein ^{49a}, S. Simion ⁶⁸, R. Simoniello ³⁷, E.L. Simpson ¹⁰⁴,
 H. Simpson ¹⁵⁰, L.R. Simpson ¹⁰⁹, S. Simsek ⁸⁴, S. Sindhu ⁵⁷, P. Sinervo ¹⁵⁹, S. Singh ³⁰,
 S. Sinha ⁵⁰, S. Sinha ¹⁰⁴, M. Sioli ^{24b,24a}, I. Siral ³⁷, E. Sitnikova ⁵⁰, J. Sjölin ^{49a,49b},
 A. Skaf ⁵⁷, E. Skorda ²¹, P. Skubic ¹²⁴, M. Slawinska ⁸⁹, I. Slazyk ¹⁷, V. Smakhtin ¹⁷⁴,
 B.H. Smart ¹³⁸, S. Yu. Smirnov ³⁹, Y. Smirnov ³⁹, L.N. Smirnova ^{39,a}, O. Smirnova ¹⁰¹,
 A.C. Smith ⁴³, D.R. Smith ¹⁶³, E.A. Smith ⁴¹, J.L. Smith ¹⁰⁴, R. Smith ¹⁴⁷, H. Smitmanns ¹⁰³,
 M. Smizanska ⁹⁴, K. Smolek ¹³⁶, A.A. Snesarev ³⁹, H.L. Snoek ¹¹⁸, S. Snyder ³⁰,
 R. Sobie ^{170,x}, A. Soffer ¹⁵⁵, C.A. Solans Sanchez ³⁷, E. Yu. Soldatov ³⁹, U. Soldevila ¹⁶⁸,
 A.A. Solodkov ³⁹, S. Solomon ²⁷, A. Soloshenko ⁴⁰, K. Solovieva ⁵⁶, O.V. Solovyanov ⁴²,
 P. Sommer ⁵², A. Sonay ¹³, W.Y. Song ^{160b}, A. Sopczak ¹³⁶, A.L. Sopio ⁵⁴, F. Sopkova ^{29b},
 J.D. Sorenson ¹¹⁶, I.R. Sotarriva Alvarez ¹⁵⁸, V. Sothilingam ^{65a}, O.J. Soto Sandoval ^{141c,141b},
 S. Sottocornola ⁷⁰, R. Soualah ¹⁶⁵, Z. Soumami ^{36e}, D. South ⁵⁰, N. Soybelman ¹⁷⁴,
 S. Spagnolo ^{72a,72b}, M. Spalla ¹¹³, D. Sperlich ⁵⁶, G. Spigo ³⁷, B. Spisso ^{74a,74b}, D.P. Spiteri ⁶¹,
 M. Spousta ¹³⁷, E.J. Staats ³⁵, R. Stamen ^{65a}, A. Stampekis ²¹, E. Stanecka ⁸⁹,
 W. Stanek-Maslouska ⁵⁰, M.V. Stange ⁵², B. Stanislaus ^{18a}, M.M. Stanitzki ⁵⁰, B. Stapf ⁵⁰,
 E.A. Starchenko ³⁹, G.H. Stark ¹⁴⁰, J. Stark ⁹², P. Staroba ¹³⁵, P. Starovoitov ^{65a}, S. Stärz ¹⁰⁷,
 R. Staszewski ⁸⁹, G. Stavropoulos ⁴⁸, A. Steff ³⁷, P. Steinberg ³⁰, B. Stelzer ^{146,160a},
 H.J. Stelzer ¹³³, O. Stelzer-Chilton ^{160a}, H. Stenzel ⁶⁰, T.J. Stevenson ¹⁵⁰, G.A. Stewart ³⁷,
 J.R. Stewart ¹²⁵, M.C. Stockton ³⁷, G. Stoicea ^{28b}, M. Stolarski ^{134a}, S. Stonjek ¹¹³,
 A. Straessner ⁵², J. Strandberg ¹⁴⁸, S. Strandberg ^{49a,49b}, M. Stratmann ¹⁷⁶, M. Strauss ¹²⁴,
 T. Streblor ¹⁰⁵, P. Strizenec ^{29b}, R. Ströhmer ¹⁷¹, D.M. Strom ¹²⁷, R. Stroynowski ⁴⁶,
 A. Strubig ^{49a,49b}, S.A. Stucci ³⁰, B. Stugu ¹⁷, J. Stupak ¹²⁴, N.A. Styles ⁵⁰, D. Su ¹⁴⁷,
 S. Su ^{64a}, W. Su ^{64d}, X. Su ^{64a}, D. Suchy ^{29a}, K. Sugizaki ¹⁵⁷, V.V. Sulin ³⁹, M.J. Sullivan ⁹⁵,
 D.M.S. Sultan ¹³⁰, L. Sultanaliyeva ³⁹, S. Sultansoy ^{3b}, T. Sumida ⁹⁰, S. Sun ¹⁷⁵, W. Sun ¹⁴,
 O. Sunneborn Gudnadottir ¹⁶⁶, N. Sur ¹⁰⁵, M.R. Sutton ¹⁵⁰, H. Suzuki ¹⁶¹, M. Svatos ¹³⁵,
 M. Swiatlowski ^{160a}, T. Swirski ¹⁷¹, I. Sykora ^{29a}, M. Sykora ¹³⁷, T. Sykora ¹³⁷, D. Ta ¹⁰³,
 K. Tackmann ^{50,u}, A. Taffard ¹⁶³, R. Tafirout ^{160a}, J.S. Tafoya Vargas ⁶⁸, Y. Takubo ⁸⁶,
 M. Talby ¹⁰⁵, A.A. Talyshev ³⁹, K.C. Tam ^{66b}, N.M. Tamir ¹⁵⁵, A. Tanaka ¹⁵⁷, J. Tanaka ¹⁵⁷,
 R. Tanaka ⁶⁸, M. Tanasini ¹⁴⁹, Z. Tao ¹⁶⁹, S. Tapia Araya ^{141f}, S. Tapprogge ¹⁰³,
 A. Tarek Abouelfadl Mohamed ¹¹⁰, S. Tarem ¹⁵⁴, K. Tariq ¹⁴, G. Tarna ^{28b}, G.F. Tartarelli ^{73a},
 M.J. Tartarin ⁹², P. Tas ¹³⁷, M. Tasevsky ¹³⁵, E. Tassi ^{45b,45a}, A.C. Tate ¹⁶⁷, G. Tateno ¹⁵⁷,
 Y. Tayalati ^{36e,w}, G.N. Taylor ¹⁰⁸, W. Taylor ^{160b}, P. Teixeira-Dias ⁹⁸, J.J. Teoh ¹⁵⁹,

K. Terashi ¹⁵⁷, J. Terron ¹⁰², S. Terzo ¹³, M. Testa ⁵⁵, R.J. Teuscher ^{159,x}, A. Thaler ⁸¹,
 O. Theiner ⁵⁸, T. Thevenaux-Pelzer ¹⁰⁵, O. Thielmann ¹⁷⁶, D.W. Thomas ⁹⁸, J.P. Thomas ²¹,
 E.A. Thompson ^{18a}, P.D. Thompson ²¹, E. Thomson ¹³², R.E. Thornberry ⁴⁶, C. Tian ^{64a},
 Y. Tian ⁵⁸, V. Tikhomirov ^{39,a}, Yu.A. Tikhonov ³⁹, S. Timoshenko ³⁹, D. Timoshyn ¹³⁷,
 E.X.L. Ting ¹, P. Tipton ¹⁷⁷, A. Tishelman-Charny ³⁰, S.H. Tlou ^{34g}, K. Todome ¹⁵⁸,
 S. Todorova-Nova ¹³⁷, S. Todt ⁵², L. Toffolin ^{71a,71c}, M. Togawa ⁸⁶, J. Tojo ⁹¹, S. Tokár ^{29a},
 K. Tokushuku ⁸⁶, O. Toldaiev ⁷⁰, G. Tolkachev ¹⁰⁵, M. Tomoto ^{86,114}, L. Tompkins ^{147,1},
 E. Torrence ¹²⁷, H. Torres ⁹², E. Torró Pastor ¹⁶⁸, M. Toscani ³¹, C. Toscirì ⁴¹, M. Tost ¹¹,
 D.R. Tovey ¹⁴³, I.S. Trandafir ^{28b}, T. Trefzger ¹⁷¹, A. Tricoli ³⁰, I.M. Trigger ^{160a},
 S. Trincaz-Duvoid ¹³¹, D.A. Trischuk ²⁷, B. Trocmé ⁶², A. Tropina ⁴⁰, L. Truong ^{34c},
 M. Trzebinski ⁸⁹, A. Trzuppek ⁸⁹, F. Tsai ¹⁴⁹, M. Tsai ¹⁰⁹, A. Tsiamis ¹⁵⁶, P.V. Tsiarehka ⁴⁰,
 S. Tsigaridas ^{160a}, A. Tsigotis ^{156,r}, V. Tsiskaridze ¹⁵⁹, E.G. Tskhadadze ^{153a}, M. Tsopoulou ¹⁵⁶,
 Y. Tsujikawa ⁹⁰, I.I. Tsukerman ³⁹, V. Tsulaia ^{18a}, S. Tsuno ⁸⁶, K. Tsurì ¹²², D. Tsybychev ¹⁴⁹,
 Y. Tu ^{66b}, A. Tudorache ^{28b}, V. Tudorache ^{28b}, A.N. Tuna ⁶³, S. Turchikhin ^{59b,59a},
 I. Turk Cakir ^{3a}, R. Turra ^{73a}, T. Turtuvshin ⁴⁰, P.M. Tuts ⁴³, S. Tzamarias ^{156,d}, E. Tzovara ¹⁰³,
 F. Ukegawa ¹⁶¹, P.A. Ulloa Poblete ^{141c,141b}, E.N. Umaka ³⁰, G. Unal ³⁷, A. Undrus ³⁰,
 G. Unel ¹⁶³, J. Urban ^{29b}, P. Urrejola ^{141a}, G. Usai ⁸, R. Ushioda ¹⁵⁸, M. Usman ¹¹¹,
 F. Ustuner ⁵⁴, Z. Uysal ⁸⁴, V. Vacek ¹³⁶, B. Vachon ¹⁰⁷, T. Vafeiadis ³⁷, A. Vaitkus ⁹⁹,
 C. Valderanis ¹¹², E. Valdes Santurio ^{49a,49b}, M. Valente ^{160a}, S. Valentinetti ^{24b,24a}, A. Valero ¹⁶⁸,
 E. Valiente Moreno ¹⁶⁸, A. Vallier ⁹², J.A. Valls Ferrer ¹⁶⁸, D.R. Van Arneman ¹¹⁸,
 T.R. Van Daalen ¹⁴², A. Van Der Graaf ⁵¹, P. Van Gemmeren ⁶, M. Van Rijnbach ³⁷,
 S. Van Stroud ⁹⁹, I. Van Vulpen ¹¹⁸, P. Vana ¹³⁷, M. Vanadia ^{78a,78b}, U.M. Vande Voorde ¹⁴⁸,
 W. Vandelli ³⁷, E.R. Vandewall ¹²⁵, D. Vannicola ¹⁵⁵, L. Vannoli ⁵⁵, R. Vari ^{77a}, E.W. Varnes ⁷,
 C. Varni ^{18b}, D. Varouchas ⁶⁸, L. Varriale ¹⁶⁸, K.E. Varvell ¹⁵¹, M.E. Vasile ^{28b}, L. Vaslin ⁸⁶,
 A. Vasyukov ⁴⁰, L.M. Vaughan ¹²⁵, R. Vavricka ¹⁰³, T. Vazquez Schroeder ³⁷, J. Veatch ³²,
 V. Vecchio ¹⁰⁴, M.J. Veen ¹⁰⁶, I. Veliscek ³⁰, L.M. Veloce ¹⁵⁹, F. Veloso ^{134a,134c},
 S. Veneziano ^{77a}, A. Ventura ^{72a,72b}, S. Ventura Gonzalez ¹³⁹, A. Verbytskyi ¹¹³,
 M. Verducci ^{76a,76b}, C. Vergis ⁹⁷, M. Verissimo De Araujo ^{85b}, W. Verkerke ¹¹⁸,
 J.C. Vermeulen ¹¹⁸, C. Vernieri ¹⁴⁷, M. Vessella ¹⁶³, M.C. Vetterli ^{146,ac}, A. Vgenopoulos ¹⁰³,
 N. Viaux Maira ^{141f}, T. Vickey ¹⁴³, O.E. Vickey Boeriu ¹⁴³, G.H.A. Viehhauser ¹³⁰, L. Vignani ^{65b},
 M. Vigl ¹¹³, M. Villa ^{24b,24a}, M. Villaplana Perez ¹⁶⁸, E.M. Villhauer ⁵⁴, E. Vilucchi ⁵⁵,
 M.G. Vincter ³⁵, A. Visibile ¹¹⁸, C. Vittori ³⁷, I. Vivarelli ^{24b,24a}, E. Voevodina ¹¹³, F. Vogel ¹¹²,
 J.C. Voigt ⁵², P. Vokac ¹³⁶, Yu. Volkotrub ^{88b}, E. Von Toerne ²⁵, A. Vorlander ¹⁷⁶,
 B. Vormwald ³⁷, V. Vorobel ¹³⁷, K. Vorobev ³⁹, M. Vos ¹⁶⁸, K. Voss ¹⁴⁵, M. Vozak ¹¹⁸,
 L. Vozdecky ¹²⁴, N. Vranjes ¹⁶, M. Vranjes Milosavljevic ¹⁶, M. Vreeswijk ¹¹⁸, N.K. Vu ^{64d},
 R. Vuillermet ³⁷, O. Vujinovic ¹⁰³, I. Vukotic ⁴¹, I.K. Vyas ³⁵, S. Wada ¹⁶¹, C. Wagner ¹⁴⁷,
 J.M. Wagner ^{18a}, W. Wagner ¹⁷⁶, S. Wahdan ¹⁷⁶, H. Wahlberg ⁹³, C.H. Waits ¹²⁴, J. Walder ¹³⁸,
 R. Walker ¹¹², W. Walkowiak ¹⁴⁵, A. Wall ¹³², E.J. Wallin ¹⁰¹, T. Wamorkar ⁶, A.Z. Wang ¹⁴⁰,
 C. Wang ¹⁰³, C. Wang ¹¹, H. Wang ^{18a}, J. Wang ^{66c}, P. Wang ¹⁰⁴, P. Wang ⁹⁹, R. Wang ⁶³,
 R. Wang ⁶, S.M. Wang ¹⁵², S. Wang ¹⁴, T. Wang ^{64a}, W.T. Wang ⁸², W. Wang ¹⁴,
 X. Wang ¹⁶⁷, X. Wang ^{64c}, Y. Wang ^{64d}, Y. Wang ^{115a}, Y. Wang ^{64a}, Z. Wang ¹⁰⁹,
 Z. Wang ^{64d,53,64c}, Z. Wang ¹⁰⁹, A. Warburton ¹⁰⁷, R.J. Ward ²¹, N. Warrack ⁶¹,
 S. Waterhouse ⁹⁸, A.T. Watson ²¹, H. Watson ⁵⁴, M.F. Watson ²¹, E. Watton ^{61,138}, G. Watts ¹⁴²,
 B.M. Waugh ⁹⁹, J.M. Webb ⁵⁶, C. Weber ³⁰, H.A. Weber ¹⁹, M.S. Weber ²⁰, S.M. Weber ^{65a},
 C. Wei ^{64a}, Y. Wei ⁵⁶, A.R. Weidberg ¹³⁰, E.J. Weik ¹²¹, J. Weingarten ⁵¹, C. Weiser ⁵⁶,
 C.J. Wells ⁵⁰, T. Wenaus ³⁰, B. Wendland ⁵¹, T. Wengler ³⁷, N.S. Wenke ¹¹³, N. Wermes ²⁵,
 M. Wessels ^{65a}, A.M. Wharton ⁹⁴, A.S. White ⁶³, A. White ⁸, M.J. White ¹, D. Whiteson ¹⁶³,

L. Wickremasinghe ¹²⁸, W. Wiedenmann ¹⁷⁵, M. Wielers ¹³⁸, C. Wigglesworth ⁴⁴, D.J. Wilbern ¹²⁴, H.G. Wilkens ³⁷, J.J.H. Wilkinson ³³, D.M. Williams ⁴³, H.H. Williams ¹³², S. Williams ³³, S. Willocq ¹⁰⁶, B.J. Wilson ¹⁰⁴, D.J. Wilson ¹⁰⁴, P.J. Windischhofer ⁴¹, F.I. Winkel ³¹, F. Winklmeier ¹²⁷, B.T. Winter ⁵⁶, J.K. Winter ¹⁰⁴, M. Wittgen ¹⁴⁷, M. Wobisch ¹⁰⁰, T. Wojtkowski ⁶², Z. Wolffs ¹¹⁸, J. Wollrath ³⁷, M.W. Wolter ⁸⁹, H. Wolters ^{134a,134c}, M.C. Wong ¹⁴⁰, E.L. Woodward ⁴³, S.D. Worm ⁵⁰, B.K. Wosiek ⁸⁹, K.W. Woźniak ⁸⁹, S. Wozniowski ⁵⁷, K. Wraight ⁶¹, C. Wu ²¹, M. Wu ^{115b}, M. Wu ¹¹⁷, S.L. Wu ¹⁷⁵, X. Wu ⁵⁸, X. Wu ^{64a}, Y. Wu ^{64a}, Z. Wu ⁴, J. Wuerzinger ^{113,aa}, T.R. Wyatt ¹⁰⁴, B.M. Wynne ⁵⁴, S. Xella ⁴⁴, L. Xia ^{115a}, M. Xia ¹⁵, M. Xie ^{64a}, A. Xiong ¹²⁷, J. Xiong ^{18a}, D. Xu ¹⁴, H. Xu ^{64a}, L. Xu ^{64a}, R. Xu ¹³², T. Xu ¹⁰⁹, Y. Xu ¹⁴², Z. Xu ⁵⁴, Z. Xu ^{115a}, B. Yabsley ¹⁵¹, S. Yacoob ^{34a}, Y. Yamaguchi ⁸⁶, E. Yamashita ¹⁵⁷, H. Yamauchi ¹⁶¹, T. Yamazaki ^{18a}, Y. Yamazaki ⁸⁷, S. Yan ⁶¹, Z. Yan ¹⁰⁶, H.J. Yang ^{64c,64d}, H.T. Yang ^{64a}, S. Yang ^{64a}, T. Yang ^{66c}, X. Yang ³⁷, X. Yang ¹⁴, Y. Yang ⁴⁶, Y. Yang ^{64a}, W-M. Yao ^{18a}, H. Ye ⁵⁷, J. Ye ¹⁴, S. Ye ³⁰, X. Ye ^{64a}, Y. Yeh ⁹⁹, I. Yeletsikh ⁴⁰, B. Yeo ^{18b}, M.R. Yexley ⁹⁹, T.P. Yildirim ¹³⁰, P. Yin ⁴³, K. Yorita ¹⁷³, S. Younas ^{28b}, C.J.S. Young ³⁷, C. Young ¹⁴⁷, C. Yu ^{14,115c}, Y. Yu ^{64a}, J. Yuan ^{14,115c}, M. Yuan ¹⁰⁹, R. Yuan ^{64d,64c}, L. Yue ⁹⁹, M. Zaazoua ^{64a}, B. Zabinski ⁸⁹, I. Zahir ^{36a}, E. Zaid ⁵⁴, Z.K. Zak ⁸⁹, T. Zakareishvili ¹⁶⁸, S. Zambito ⁵⁸, J.A. Zamora Saa ^{141d,141b}, J. Zang ¹⁵⁷, D. Zanzi ⁵⁶, R. Zanzottera ^{73a,73b}, O. Zaplatilek ¹³⁶, C. Zeitnitz ¹⁷⁶, H. Zeng ¹⁴, J.C. Zeng ¹⁶⁷, D.T. Zenger Jr ²⁷, O. Zenin ³⁹, T. Ženiš ^{29a}, S. Zenz ⁹⁷, S. Zerradi ^{36a}, D. Zerwas ⁶⁸, M. Zhai ^{14,115c}, D.F. Zhang ¹⁴³, J. Zhang ^{64b}, J. Zhang ⁶, K. Zhang ^{14,115c}, L. Zhang ^{64a}, L. Zhang ^{115a}, P. Zhang ^{14,115c}, R. Zhang ¹⁷⁵, S. Zhang ¹⁰⁹, S. Zhang ⁹², T. Zhang ¹⁵⁷, X. Zhang ^{64c}, Y. Zhang ¹⁴², Y. Zhang ⁹⁹, Y. Zhang ^{115a}, Z. Zhang ^{18a}, Z. Zhang ^{64b}, Z. Zhang ⁶⁸, H. Zhao ¹⁴², T. Zhao ^{64b}, Y. Zhao ¹⁴⁰, Z. Zhao ^{64a}, Z. Zhao ^{64a}, A. Zhemchugov ⁴⁰, J. Zheng ^{115a}, K. Zheng ¹⁶⁷, X. Zheng ^{64a}, Z. Zheng ¹⁴⁷, D. Zhong ¹⁶⁷, B. Zhou ¹⁰⁹, H. Zhou ⁷, N. Zhou ^{64c}, Y. Zhou ¹⁵, Y. Zhou ^{115a}, Y. Zhou ⁷, C.G. Zhu ^{64b}, J. Zhu ¹⁰⁹, X. Zhu ^{64d}, Y. Zhu ^{64c}, Y. Zhu ^{64a}, X. Zhuang ¹⁴, K. Zhukov ⁷⁰, N.I. Zimine ⁴⁰, J. Zinsser ^{65b}, M. Ziolkowski ¹⁴⁵, L. Živković ¹⁶, A. Zoccoli ^{24b,24a}, K. Zoch ⁶³, T.G. Zorbas ¹⁴³, O. Zormpa ⁴⁸, W. Zou ⁴³, L. Zwalinski ³⁷.

¹Department of Physics, University of Adelaide, Adelaide; Australia.

²Department of Physics, University of Alberta, Edmonton AB; Canada.

³(^a)Department of Physics, Ankara University, Ankara; (^b)Division of Physics, TOBB University of Economics and Technology, Ankara; Türkiye.

⁴LAPP, Université Savoie Mont Blanc, CNRS/IN2P3, Annecy; France.

⁵APC, Université Paris Cité, CNRS/IN2P3, Paris; France.

⁶High Energy Physics Division, Argonne National Laboratory, Argonne IL; United States of America.

⁷Department of Physics, University of Arizona, Tucson AZ; United States of America.

⁸Department of Physics, University of Texas at Arlington, Arlington TX; United States of America.

⁹Physics Department, National and Kapodistrian University of Athens, Athens; Greece.

¹⁰Physics Department, National Technical University of Athens, Zografou; Greece.

¹¹Department of Physics, University of Texas at Austin, Austin TX; United States of America.

¹²Institute of Physics, Azerbaijan Academy of Sciences, Baku; Azerbaijan.

¹³Institut de Física d'Altes Energies (IFAE), Barcelona Institute of Science and Technology, Barcelona; Spain.

¹⁴Institute of High Energy Physics, Chinese Academy of Sciences, Beijing; China.

¹⁵Physics Department, Tsinghua University, Beijing; China.

¹⁶Institute of Physics, University of Belgrade, Belgrade; Serbia.

- ¹⁷Department for Physics and Technology, University of Bergen, Bergen; Norway.
- ¹⁸(^a)Physics Division, Lawrence Berkeley National Laboratory, Berkeley CA; (^b)University of California, Berkeley CA; United States of America.
- ¹⁹Institut für Physik, Humboldt Universität zu Berlin, Berlin; Germany.
- ²⁰Albert Einstein Center for Fundamental Physics and Laboratory for High Energy Physics, University of Bern, Bern; Switzerland.
- ²¹School of Physics and Astronomy, University of Birmingham, Birmingham; United Kingdom.
- ²²(^a)Department of Physics, Bogazici University, Istanbul; (^b)Department of Physics Engineering, Gaziantep University, Gaziantep; (^c)Department of Physics, Istanbul University, Istanbul; Türkiye.
- ²³(^a)Facultad de Ciencias y Centro de Investigaciones, Universidad Antonio Nariño, Bogotá; (^b)Departamento de Física, Universidad Nacional de Colombia, Bogotá; Colombia.
- ²⁴(^a)Dipartimento di Fisica e Astronomia A. Righi, Università di Bologna, Bologna; (^b)INFN Sezione di Bologna; Italy.
- ²⁵Physikalisches Institut, Universität Bonn, Bonn; Germany.
- ²⁶Department of Physics, Boston University, Boston MA; United States of America.
- ²⁷Department of Physics, Brandeis University, Waltham MA; United States of America.
- ²⁸(^a)Transilvania University of Brasov, Brasov; (^b)Horia Hulubei National Institute of Physics and Nuclear Engineering, Bucharest; (^c)Department of Physics, Alexandru Ioan Cuza University of Iasi, Iasi; (^d)National Institute for Research and Development of Isotopic and Molecular Technologies, Physics Department, Cluj-Napoca; (^e)National University of Science and Technology Politehnica, Bucharest; (^f)West University in Timisoara, Timisoara; (^g)Faculty of Physics, University of Bucharest, Bucharest; Romania.
- ²⁹(^a)Faculty of Mathematics, Physics and Informatics, Comenius University, Bratislava; (^b)Department of Subnuclear Physics, Institute of Experimental Physics of the Slovak Academy of Sciences, Kosice; Slovak Republic.
- ³⁰Physics Department, Brookhaven National Laboratory, Upton NY; United States of America.
- ³¹Universidad de Buenos Aires, Facultad de Ciencias Exactas y Naturales, Departamento de Física, y CONICET, Instituto de Física de Buenos Aires (IFIBA), Buenos Aires; Argentina.
- ³²California State University, CA; United States of America.
- ³³Cavendish Laboratory, University of Cambridge, Cambridge; United Kingdom.
- ³⁴(^a)Department of Physics, University of Cape Town, Cape Town; (^b)iThemba Labs, Western Cape; (^c)Department of Mechanical Engineering Science, University of Johannesburg, Johannesburg; (^d)National Institute of Physics, University of the Philippines Diliman (Philippines); (^e)University of South Africa, Department of Physics, Pretoria; (^f)University of Zululand, KwaDlangezwa; (^g)School of Physics, University of the Witwatersrand, Johannesburg; South Africa.
- ³⁵Department of Physics, Carleton University, Ottawa ON; Canada.
- ³⁶(^a)Faculté des Sciences Ain Chock, Université Hassan II de Casablanca; (^b)Faculté des Sciences, Université Ibn-Tofail, Kénitra; (^c)Faculté des Sciences Semlalia, Université Cadi Ayyad, LPHEA-Marrakech; (^d)LPMR, Faculté des Sciences, Université Mohamed Premier, Oujda; (^e)Faculté des sciences, Université Mohammed V, Rabat; (^f)Institute of Applied Physics, Mohammed VI Polytechnic University, Ben Guerir; Morocco.
- ³⁷CERN, Geneva; Switzerland.
- ³⁸Affiliated with an institute formerly covered by a cooperation agreement with CERN.
- ³⁹Affiliated with an institute covered by a cooperation agreement with CERN.
- ⁴⁰Affiliated with an international laboratory covered by a cooperation agreement with CERN.
- ⁴¹Enrico Fermi Institute, University of Chicago, Chicago IL; United States of America.
- ⁴²LPC, Université Clermont Auvergne, CNRS/IN2P3, Clermont-Ferrand; France.
- ⁴³Nevis Laboratory, Columbia University, Irvington NY; United States of America.

- ⁴⁴Niels Bohr Institute, University of Copenhagen, Copenhagen; Denmark.
- ⁴⁵(^a)Dipartimento di Fisica, Università della Calabria, Rende; (^b)INFN Gruppo Collegato di Cosenza, Laboratori Nazionali di Frascati; Italy.
- ⁴⁶Physics Department, Southern Methodist University, Dallas TX; United States of America.
- ⁴⁷Physics Department, University of Texas at Dallas, Richardson TX; United States of America.
- ⁴⁸National Centre for Scientific Research "Demokritos", Agia Paraskevi; Greece.
- ⁴⁹(^a)Department of Physics, Stockholm University; (^b)Oskar Klein Centre, Stockholm; Sweden.
- ⁵⁰Deutsches Elektronen-Synchrotron DESY, Hamburg and Zeuthen; Germany.
- ⁵¹Fakultät Physik, Technische Universität Dortmund, Dortmund; Germany.
- ⁵²Institut für Kern- und Teilchenphysik, Technische Universität Dresden, Dresden; Germany.
- ⁵³Department of Physics, Duke University, Durham NC; United States of America.
- ⁵⁴SUPA - School of Physics and Astronomy, University of Edinburgh, Edinburgh; United Kingdom.
- ⁵⁵INFN e Laboratori Nazionali di Frascati, Frascati; Italy.
- ⁵⁶Physikalisches Institut, Albert-Ludwigs-Universität Freiburg, Freiburg; Germany.
- ⁵⁷II. Physikalisches Institut, Georg-August-Universität Göttingen, Göttingen; Germany.
- ⁵⁸Département de Physique Nucléaire et Corpusculaire, Université de Genève, Genève; Switzerland.
- ⁵⁹(^a)Dipartimento di Fisica, Università di Genova, Genova; (^b)INFN Sezione di Genova; Italy.
- ⁶⁰II. Physikalisches Institut, Justus-Liebig-Universität Giessen, Giessen; Germany.
- ⁶¹SUPA - School of Physics and Astronomy, University of Glasgow, Glasgow; United Kingdom.
- ⁶²LPSC, Université Grenoble Alpes, CNRS/IN2P3, Grenoble INP, Grenoble; France.
- ⁶³Laboratory for Particle Physics and Cosmology, Harvard University, Cambridge MA; United States of America.
- ⁶⁴(^a)Department of Modern Physics and State Key Laboratory of Particle Detection and Electronics, University of Science and Technology of China, Hefei; (^b)Institute of Frontier and Interdisciplinary Science and Key Laboratory of Particle Physics and Particle Irradiation (MOE), Shandong University, Qingdao; (^c)School of Physics and Astronomy, Shanghai Jiao Tong University, Key Laboratory for Particle Astrophysics and Cosmology (MOE), SKLPPC, Shanghai; (^d)Tsung-Dao Lee Institute, Shanghai; (^e)School of Physics and Microelectronics, Zhengzhou University; China.
- ⁶⁵(^a)Kirchhoff-Institut für Physik, Ruprecht-Karls-Universität Heidelberg, Heidelberg; (^b)Physikalisches Institut, Ruprecht-Karls-Universität Heidelberg, Heidelberg; Germany.
- ⁶⁶(^a)Department of Physics, Chinese University of Hong Kong, Shatin, N.T., Hong Kong; (^b)Department of Physics, University of Hong Kong, Hong Kong; (^c)Department of Physics and Institute for Advanced Study, Hong Kong University of Science and Technology, Clear Water Bay, Kowloon, Hong Kong; China.
- ⁶⁷Department of Physics, National Tsing Hua University, Hsinchu; Taiwan.
- ⁶⁸IJCLab, Université Paris-Saclay, CNRS/IN2P3, 91405, Orsay; France.
- ⁶⁹Centro Nacional de Microelectrónica (IMB-CNM-CSIC), Barcelona; Spain.
- ⁷⁰Department of Physics, Indiana University, Bloomington IN; United States of America.
- ⁷¹(^a)INFN Gruppo Collegato di Udine, Sezione di Trieste, Udine; (^b)ICTP, Trieste; (^c)Dipartimento Politecnico di Ingegneria e Architettura, Università di Udine, Udine; Italy.
- ⁷²(^a)INFN Sezione di Lecce; (^b)Dipartimento di Matematica e Fisica, Università del Salento, Lecce; Italy.
- ⁷³(^a)INFN Sezione di Milano; (^b)Dipartimento di Fisica, Università di Milano, Milano; Italy.
- ⁷⁴(^a)INFN Sezione di Napoli; (^b)Dipartimento di Fisica, Università di Napoli, Napoli; Italy.
- ⁷⁵(^a)INFN Sezione di Pavia; (^b)Dipartimento di Fisica, Università di Pavia, Pavia; Italy.
- ⁷⁶(^a)INFN Sezione di Pisa; (^b)Dipartimento di Fisica E. Fermi, Università di Pisa, Pisa; Italy.
- ⁷⁷(^a)INFN Sezione di Roma; (^b)Dipartimento di Fisica, Sapienza Università di Roma, Roma; Italy.
- ⁷⁸(^a)INFN Sezione di Roma Tor Vergata; (^b)Dipartimento di Fisica, Università di Roma Tor Vergata, Roma; Italy.

- ^{79(a)}INFN Sezione di Roma Tre;^(b)Dipartimento di Matematica e Fisica, Università Roma Tre, Roma; Italy.
- ^{80(a)}INFN-TIFPA;^(b)Università degli Studi di Trento, Trento; Italy.
- ⁸¹Universität Innsbruck, Department of Astro and Particle Physics, Innsbruck; Austria.
- ⁸²University of Iowa, Iowa City IA; United States of America.
- ⁸³Department of Physics and Astronomy, Iowa State University, Ames IA; United States of America.
- ⁸⁴Istinye University, Sariyer, Istanbul; Türkiye.
- ^{85(a)}Departamento de Engenharia Elétrica, Universidade Federal de Juiz de Fora (UFJF), Juiz de Fora;^(b)Universidade Federal do Rio De Janeiro COPPE/EE/IF, Rio de Janeiro;^(c)Instituto de Física, Universidade de São Paulo, São Paulo;^(d)Rio de Janeiro State University, Rio de Janeiro;^(e)Federal University of Bahia, Bahia; Brazil.
- ⁸⁶KEK, High Energy Accelerator Research Organization, Tsukuba; Japan.
- ⁸⁷Graduate School of Science, Kobe University, Kobe; Japan.
- ^{88(a)}AGH University of Krakow, Faculty of Physics and Applied Computer Science, Krakow;^(b)Marian Smoluchowski Institute of Physics, Jagiellonian University, Krakow; Poland.
- ⁸⁹Institute of Nuclear Physics Polish Academy of Sciences, Krakow; Poland.
- ⁹⁰Faculty of Science, Kyoto University, Kyoto; Japan.
- ⁹¹Research Center for Advanced Particle Physics and Department of Physics, Kyushu University, Fukuoka ; Japan.
- ⁹²L2IT, Université de Toulouse, CNRS/IN2P3, UPS, Toulouse; France.
- ⁹³Instituto de Física La Plata, Universidad Nacional de La Plata and CONICET, La Plata; Argentina.
- ⁹⁴Physics Department, Lancaster University, Lancaster; United Kingdom.
- ⁹⁵Oliver Lodge Laboratory, University of Liverpool, Liverpool; United Kingdom.
- ⁹⁶Department of Experimental Particle Physics, Jožef Stefan Institute and Department of Physics, University of Ljubljana, Ljubljana; Slovenia.
- ⁹⁷School of Physics and Astronomy, Queen Mary University of London, London; United Kingdom.
- ⁹⁸Department of Physics, Royal Holloway University of London, Egham; United Kingdom.
- ⁹⁹Department of Physics and Astronomy, University College London, London; United Kingdom.
- ¹⁰⁰Louisiana Tech University, Ruston LA; United States of America.
- ¹⁰¹Fysiska institutionen, Lunds universitet, Lund; Sweden.
- ¹⁰²Departamento de Física Teórica C-15 and CIAFF, Universidad Autónoma de Madrid, Madrid; Spain.
- ¹⁰³Institut für Physik, Universität Mainz, Mainz; Germany.
- ¹⁰⁴School of Physics and Astronomy, University of Manchester, Manchester; United Kingdom.
- ¹⁰⁵CPPM, Aix-Marseille Université, CNRS/IN2P3, Marseille; France.
- ¹⁰⁶Department of Physics, University of Massachusetts, Amherst MA; United States of America.
- ¹⁰⁷Department of Physics, McGill University, Montreal QC; Canada.
- ¹⁰⁸School of Physics, University of Melbourne, Victoria; Australia.
- ¹⁰⁹Department of Physics, University of Michigan, Ann Arbor MI; United States of America.
- ¹¹⁰Department of Physics and Astronomy, Michigan State University, East Lansing MI; United States of America.
- ¹¹¹Group of Particle Physics, University of Montreal, Montreal QC; Canada.
- ¹¹²Fakultät für Physik, Ludwig-Maximilians-Universität München, München; Germany.
- ¹¹³Max-Planck-Institut für Physik (Werner-Heisenberg-Institut), München; Germany.
- ¹¹⁴Graduate School of Science and Kobayashi-Maskawa Institute, Nagoya University, Nagoya; Japan.
- ^{115(a)}Department of Physics, Nanjing University, Nanjing;^(b)School of Science, Shenzhen Campus of Sun Yat-sen University;^(c)University of Chinese Academy of Science (UCAS), Beijing; China.
- ¹¹⁶Department of Physics and Astronomy, University of New Mexico, Albuquerque NM; United States of

America.

¹¹⁷Institute for Mathematics, Astrophysics and Particle Physics, Radboud University/Nikhef, Nijmegen; Netherlands.

¹¹⁸Nikhef National Institute for Subatomic Physics and University of Amsterdam, Amsterdam; Netherlands.

¹¹⁹Department of Physics, Northern Illinois University, DeKalb IL; United States of America.

¹²⁰(^a)New York University Abu Dhabi, Abu Dhabi;(^b)United Arab Emirates University, Al Ain; United Arab Emirates.

¹²¹Department of Physics, New York University, New York NY; United States of America.

¹²²Ochanomizu University, Otsuka, Bunkyo-ku, Tokyo; Japan.

¹²³Ohio State University, Columbus OH; United States of America.

¹²⁴Homer L. Dodge Department of Physics and Astronomy, University of Oklahoma, Norman OK; United States of America.

¹²⁵Department of Physics, Oklahoma State University, Stillwater OK; United States of America.

¹²⁶Palacký University, Joint Laboratory of Optics, Olomouc; Czech Republic.

¹²⁷Institute for Fundamental Science, University of Oregon, Eugene, OR; United States of America.

¹²⁸Graduate School of Science, Osaka University, Osaka; Japan.

¹²⁹Department of Physics, University of Oslo, Oslo; Norway.

¹³⁰Department of Physics, Oxford University, Oxford; United Kingdom.

¹³¹LPNHE, Sorbonne Université, Université Paris Cité, CNRS/IN2P3, Paris; France.

¹³²Department of Physics, University of Pennsylvania, Philadelphia PA; United States of America.

¹³³Department of Physics and Astronomy, University of Pittsburgh, Pittsburgh PA; United States of America.

¹³⁴(^a)Laboratório de Instrumentação e Física Experimental de Partículas - LIP, Lisboa;(^b)Departamento de Física, Faculdade de Ciências, Universidade de Lisboa, Lisboa;(^c)Departamento de Física, Universidade de Coimbra, Coimbra;(^d)Centro de Física Nuclear da Universidade de Lisboa, Lisboa;(^e)Departamento de Física, Universidade do Minho, Braga;(^f)Departamento de Física Teórica y del Cosmos, Universidad de Granada, Granada (Spain);(^g)Departamento de Física, Instituto Superior Técnico, Universidade de Lisboa, Lisboa; Portugal.

¹³⁵Institute of Physics of the Czech Academy of Sciences, Prague; Czech Republic.

¹³⁶Czech Technical University in Prague, Prague; Czech Republic.

¹³⁷Charles University, Faculty of Mathematics and Physics, Prague; Czech Republic.

¹³⁸Particle Physics Department, Rutherford Appleton Laboratory, Didcot; United Kingdom.

¹³⁹IRFU, CEA, Université Paris-Saclay, Gif-sur-Yvette; France.

¹⁴⁰Santa Cruz Institute for Particle Physics, University of California Santa Cruz, Santa Cruz CA; United States of America.

¹⁴¹(^a)Departamento de Física, Pontificia Universidad Católica de Chile, Santiago;(^b)Millennium Institute for Subatomic physics at high energy frontier (SAPHIR), Santiago;(^c)Instituto de Investigación Multidisciplinario en Ciencia y Tecnología, y Departamento de Física, Universidad de La Serena;(^d)Universidad Andres Bello, Department of Physics, Santiago;(^e)Instituto de Alta Investigación, Universidad de Tarapacá, Arica;(^f)Departamento de Física, Universidad Técnica Federico Santa María, Valparaíso; Chile.

¹⁴²Department of Physics, University of Washington, Seattle WA; United States of America.

¹⁴³Department of Physics and Astronomy, University of Sheffield, Sheffield; United Kingdom.

¹⁴⁴Department of Physics, Shinshu University, Nagano; Japan.

¹⁴⁵Department Physik, Universität Siegen, Siegen; Germany.

¹⁴⁶Department of Physics, Simon Fraser University, Burnaby BC; Canada.

- ¹⁴⁷SLAC National Accelerator Laboratory, Stanford CA; United States of America.
- ¹⁴⁸Department of Physics, Royal Institute of Technology, Stockholm; Sweden.
- ¹⁴⁹Departments of Physics and Astronomy, Stony Brook University, Stony Brook NY; United States of America.
- ¹⁵⁰Department of Physics and Astronomy, University of Sussex, Brighton; United Kingdom.
- ¹⁵¹School of Physics, University of Sydney, Sydney; Australia.
- ¹⁵²Institute of Physics, Academia Sinica, Taipei; Taiwan.
- ¹⁵³^(a)E. Andronikashvili Institute of Physics, Iv. Javakhishvili Tbilisi State University, Tbilisi; ^(b)High Energy Physics Institute, Tbilisi State University, Tbilisi; ^(c)University of Georgia, Tbilisi; Georgia.
- ¹⁵⁴Department of Physics, Technion, Israel Institute of Technology, Haifa; Israel.
- ¹⁵⁵Raymond and Beverly Sackler School of Physics and Astronomy, Tel Aviv University, Tel Aviv; Israel.
- ¹⁵⁶Department of Physics, Aristotle University of Thessaloniki, Thessaloniki; Greece.
- ¹⁵⁷International Center for Elementary Particle Physics and Department of Physics, University of Tokyo, Tokyo; Japan.
- ¹⁵⁸Department of Physics, Tokyo Institute of Technology, Tokyo; Japan.
- ¹⁵⁹Department of Physics, University of Toronto, Toronto ON; Canada.
- ¹⁶⁰^(a)TRIUMF, Vancouver BC; ^(b)Department of Physics and Astronomy, York University, Toronto ON; Canada.
- ¹⁶¹Division of Physics and Tomonaga Center for the History of the Universe, Faculty of Pure and Applied Sciences, University of Tsukuba, Tsukuba; Japan.
- ¹⁶²Department of Physics and Astronomy, Tufts University, Medford MA; United States of America.
- ¹⁶³Department of Physics and Astronomy, University of California Irvine, Irvine CA; United States of America.
- ¹⁶⁴University of West Attica, Athens; Greece.
- ¹⁶⁵University of Sharjah, Sharjah; United Arab Emirates.
- ¹⁶⁶Department of Physics and Astronomy, University of Uppsala, Uppsala; Sweden.
- ¹⁶⁷Department of Physics, University of Illinois, Urbana IL; United States of America.
- ¹⁶⁸Instituto de Física Corpuscular (IFIC), Centro Mixto Universidad de Valencia - CSIC, Valencia; Spain.
- ¹⁶⁹Department of Physics, University of British Columbia, Vancouver BC; Canada.
- ¹⁷⁰Department of Physics and Astronomy, University of Victoria, Victoria BC; Canada.
- ¹⁷¹Fakultät für Physik und Astronomie, Julius-Maximilians-Universität Würzburg, Würzburg; Germany.
- ¹⁷²Department of Physics, University of Warwick, Coventry; United Kingdom.
- ¹⁷³Waseda University, Tokyo; Japan.
- ¹⁷⁴Department of Particle Physics and Astrophysics, Weizmann Institute of Science, Rehovot; Israel.
- ¹⁷⁵Department of Physics, University of Wisconsin, Madison WI; United States of America.
- ¹⁷⁶Fakultät für Mathematik und Naturwissenschaften, Fachgruppe Physik, Bergische Universität Wuppertal, Wuppertal; Germany.
- ¹⁷⁷Department of Physics, Yale University, New Haven CT; United States of America.
- ¹⁷⁸Yerevan Physics Institute, Yerevan; Armenia.
- ^a Also Affiliated with an institute covered by a cooperation agreement with CERN.
- ^b Also at An-Najah National University, Nablus; Palestine.
- ^c Also at Borough of Manhattan Community College, City University of New York, New York NY; United States of America.
- ^d Also at Center for Interdisciplinary Research and Innovation (CIRI-AUTH), Thessaloniki; Greece.
- ^e Also at CERN, Geneva; Switzerland.
- ^f Also at CMD-AC UNEC Research Center, Azerbaijan State University of Economics (UNEC); Azerbaijan.

- ^g Also at Département de Physique Nucléaire et Corpusculaire, Université de Genève, Genève; Switzerland.
- ^h Also at Departament de Física de la Universitat Autònoma de Barcelona, Barcelona; Spain.
- ⁱ Also at Department of Financial and Management Engineering, University of the Aegean, Chios; Greece.
- ^j Also at Department of Physics, California State University, Sacramento; United States of America.
- ^k Also at Department of Physics, King's College London, London; United Kingdom.
- ^l Also at Department of Physics, Stanford University, Stanford CA; United States of America.
- ^m Also at Department of Physics, Stellenbosch University; South Africa.
- ⁿ Also at Department of Physics, University of Fribourg, Fribourg; Switzerland.
- ^o Also at Department of Physics, University of Thessaly; Greece.
- ^p Also at Department of Physics, Westmont College, Santa Barbara; United States of America.
- ^q Also at Faculty of Physics, Sofia University, 'St. Kliment Ohridski', Sofia; Bulgaria.
- ^r Also at Hellenic Open University, Patras; Greece.
- ^s Also at Imam Mohammad Ibn Saud Islamic University; Saudi Arabia.
- ^t Also at Institutio Catalana de Recerca i Estudis Avancats, ICREA, Barcelona; Spain.
- ^u Also at Institut für Experimentalphysik, Universität Hamburg, Hamburg; Germany.
- ^v Also at Institute for Nuclear Research and Nuclear Energy (INRNE) of the Bulgarian Academy of Sciences, Sofia; Bulgaria.
- ^w Also at Institute of Applied Physics, Mohammed VI Polytechnic University, Ben Guerir; Morocco.
- ^x Also at Institute of Particle Physics (IPP); Canada.
- ^y Also at Institute of Physics, Azerbaijan Academy of Sciences, Baku; Azerbaijan.
- ^z Also at National Institute of Physics, University of the Philippines Diliman (Philippines); Philippines.
- ^{aa} Also at Technical University of Munich, Munich; Germany.
- ^{ab} Also at The Collaborative Innovation Center of Quantum Matter (CICQM), Beijing; China.
- ^{ac} Also at TRIUMF, Vancouver BC; Canada.
- ^{ad} Also at Università di Napoli Parthenope, Napoli; Italy.
- ^{ae} Also at University of Colorado Boulder, Department of Physics, Colorado; United States of America.
- ^{af} Also at Washington College, Chestertown, MD; United States of America.
- ^{ag} Also at Yeditepe University, Physics Department, Istanbul; Türkiye.
- * Deceased